UNIVERSITÀ DEGLI STUDI
DI MILANO

DOTTORATO DI MEDICINA MOLECOLARE E TRASLAZIONALE

CICLO XXXII

Anno Accademico 2018/2019

TESI DI DOTTORATO DI RICERCA

MED26

Development of 3D *in vitro* model to study molecular mechanisms of spinal muscular atrophy

Dottorando:
Paola Rinchetti

Matricola:
R11617

TUTORE: Stefania Paola Corti

CO-TUTORE: Monica Nizzardo

COORDINATORE DEL DOTTORATO: prof. Michele SAMAJA

SOMMARIO

Background: l'atrofia muscolare spinale (SMA) è una malattia neurodegenerativa e la principale causa genetica di morte durante l'infanzia. La SMA è causata nella maggior parte dei casi (fino al 95%) da mutazioni del gene Survival Motor Neuron 1 (SMN1) che codifica per la proteina SMN, con conseguente paralisi muscolare progressiva dovuta alla degenerazione del secondo motoneurone. Una conoscenza più approfondita della biologia di SMN e del suo ruolo nei diversi organi/sistemi in modelli affidabili è molto importante per l'ottimizzazione dei trattamenti disponibili e lo sviluppo di approcci terapeutici. In particolare, può essere cruciale generare un modello umano in grado di ricapitolare la complessità del sistema nervoso centrale (SNC) e il suo sviluppo. Uno strumento promettente per studiare la patologia della SMA è costituito dagli organoidi, un modello tridimensionale (3D) ottenuto a partire da cellule staminali pluripotenti indotte (iPSC). Inoltre, questo stesso modello potrebbe essere utilizzato per identificare una nuova strategia terapeutica.

Razionale: In questo progetto abbiamo sfruttato la tecnologia degli organoidi del SNC, una nuova piattaforma 3D basata su cellule staminali che ha il potenziale per affrontare i limiti delle colture bidimensionali (2D) umane esistenti migliorando i test preclinici. Miriamo a dimostrare che questo approccio può ricapitolare parte della complessità della biologia dell'intero tessuto superando l'uso convenzionale dei motoneuroni derivati da iPSC 2D. Al giorno d'oggi, diverse strategie terapeutiche per la SMA sono state testate in studi clinici e due composti sono stati approvati dalla FDA. Tuttavia, tutti questi approcci sono completamente efficaci solo se somministrati nelle fasi pre-sintomatiche. La generazione di un nuovo modello per la SMA potrebbe portare a una migliore conoscenza dei

meccanismi alla base del disturbo durante lo sviluppo del sistema nervoso centrale e potrebbe contribuire a sviluppare opzioni terapeutiche nuove o combinate per i pazienti affetti.

Metodi: Abbiamo ottenuto iPSC da fibroblasti umani sia di soggetti sani che di pazienti SMA tipo 1 e, utilizzando due protocolli diversi che ricapitolano i passaggi dello sviluppo embrionale, abbiamo generato organoidi cerebrali 3D e sferoidi 3D simili al midollo spinale. Abbiamo effettuato analisi immunoistochimiche e molecolari per confermare il loro stato di differenziamento. Inoltre, per verificare la loro attività basale e la loro capacità di risposta agli stimoli, abbiamo eseguito analisi di calcium imaging ed elettrofisiologiche.

Risultati: gli organoidi del SNC derivati da soggetti sani e pazienti sono stati ottenuti con successo, come suggerito dai dati di espressione proteica e di qPCR. In particolare, gli organoidi cerebrali hanno dato origine a una formazione embrionale simile alla corteccia cerebrale contenente cellule progenitrici e sottotipi neurali più maturi. L'analisi elettrofisiologica ha dimostrato non solo la loro attività basale, ma anche la loro capacità di rispondere agli stimoli. Per quanto riguarda gli sferoidi simili al midollo spinale, abbiamo utilizzato un protocollo modificato per indurre la caudalizzazione e la ventralizzazione neurale. Questo modello ci ha fornito un potente strumento per studiare la patologia precoce dei motoneuroni e le cause della loro degenerazione. Come gli organoidi cerebrali, gli sferoidi simili al midollo spinale sono stati caratterizzati da immunoistochimica, analisi dell'espressione genica e dell’attività elettrofisiologica.

I risultati preliminari hanno suggerito che gli organoidi e gli sferoidi della SMA, rispetto ai controlli, presentavano non solo un'alterazione nell'espressione di alcuni marcatori, ma anche dell'attività elettrofisiologica.

Conclusione: abbiamo generato e caratterizzato con successo organoidi e sferoidi 3D SNC sani e SMA che hanno ricapitolato lo sviluppo umano del SNC e hanno mostrato caratteristiche correlate alla malattia. Questo modello può essere utilizzato come un innovativo sistema *in vitro* per studiare i meccanismi patogenetici, identificare target e testare potenziali strategie terapeutiche.

ABSTRACT

Background: Spinal muscular atrophy (SMA) is a neurodegenerative disease and the leading genetic cause of death during childhood. SMA is caused in the majority of the cases (up to 95%) by mutations in the Survival Motor Neuron 1 (SMN1) gene coding for the SMN protein, resulting in a progressive muscular paralysis due to lower motor neurons degeneration. A deeper knowledge of SMN biology and of its role in different organs/system in reliable models is very important for the optimization of available treatments and the development of complementary therapeutic approaches.

In particular, it can be crucial to generate a human model able to recapitulate the complexity of the central nervous system (CNS) and its development.

A promising tool to study SMA pathology is the three-dimensional (3D) organoid, obtained starting from induced pluripotent stem cell (iPSCs). Moreover, this model could be used to identify new therapeutic strategy.

Rationale: In this project, we exploited CNS organoid technology, which is a novel stem cell-based 3D platform that has the potential to address the limitations of human existing bi-dimensional (2D) cultures improving preclinical testing. We aim to demonstrate that this approach can recapitulate some of the complexity of whole-organism biology overcoming the conventional use of 2D iPSCs-derived motor neurons. Nowadays, several therapeutic strategies have been tested in clinical trials and two compounds have been approved by FDA. Nevertheless, all these approaches are completely efficacious only if administered at pre-symptomatic stages.

The generation of a new model for SMA could lead to a better knowledge of the mechanisms underlying the disorder during the development of the CNS and it might contribute to develop new or combined therapeutic options for affected patients.

Methods: We obtained iPSCs from human fibroblasts of both healthy subjects and SMA type 1 patients and, using two different protocols that recapitulate the embryonal developmental steps, we generated 3D brain organoids and 3D spinal cord-like spheroids. We performed immunohistochemical and molecular analysis to confirm their differentiation state. Moreover, to verify their basal activity and their capability to response to stimuli, we performed calcium imaging and electrophysiological analysis.

Results: CNS organoids derived from healthy subjects and patient have been successfully obtained, as suggested by the protein and gene expression data. In particular, brain organoids gave rise to an early cerebral cortex-like formation containing progenitor cells and more mature neural subtypes. Electrophysiological analysis demonstrated not only their basal activity, but also their ability to respond to stimuli. Concerning spinal cord-like spheroids, we used a modified protocol in order to induce neural caudalization and ventralization. This model gave us a powerful tool to investigate early motor neuron pathology and causes of degeneration. Like brain organoids, spinal cord-like spheroids have been characterized by immunohistochemistry, gene expression analysis and electrophysiological activity.

Preliminary results suggested that SMA organoids and spheroids, compared to the controls, exhibited not only an alteration in the proper markers expression, but also in the electrophysiological activity.

Conclusion: We successfully generated and characterized healthy and SMA CNS 3D organoids and spheroids that recapitulated human CNS development, showed disease-related features. This model can be used as an innovative *in vitro* system to study pathogenic mechanisms, identifying therapeutic targets and test potential therapeutic strategies.

TABLE OF CONTENT

1. RESEARCH INTEGRITY

I have no financial disclosure or conflicts of interest with the presented material in this project.

The study was conducted in accordance with the Declaration of Helsinki and followed ICH GCP guidelines.

All the subjects and the parents of the minors provided written informed consent for the collection, storage and analysis of the biological materials according to the disposition of the local ethics committees.

This study was approved by Institutional Ethic Committed.

2. AIM OF THE THESIS

Spinal Muscular Atrophy (SMA) is a monogenic inheritable neurodegenerative disorder, which impairs lower motor neurons in the spinal cord. It is caused by mutations of *Survival Motor Neuron 1* gene (*SMN1*) on chromosome 5q13, which lead to the depletion of functional SMN1 protein.

In humans is present a paralogous gene, *SMN2*, able to produce a small amount of the protein, but not sufficient to compensate *SMN1* depletion. Indeed, *SMN2* differs from *SMN1* only for a single nucleotide on exon 7, resulting in an alternative splicing with a production of a functional full-length protein only for the 10%. The disease severity depends on the numbers of SMN2 copies. Indeed, higher is the number of SMN2 copies, milder is the phenotype.

Nowadays, many innovative strategies have been developed and two have been approved for patients. The latter is based on antisense oligonucleotide (ASO) and gene therapy.

Spinraza, an ASO, was the first drug approved by FDA and EMA for SMA treatment in December 2016. This drug targets intronic splicing silencer N1 (*ISS-N1)*, which is a splicing sequence on *SMN2*, promoting the inclusion of the exon 7, resulting in a production of the full length SMN protein. Instead, gene therapy is based on non-integrating adeno-associated virus delivering of functional human wild-type *SMN1*. Up to now, results of both approved therapies are impressive, indeed data suggest a possible complete rescue of the

phenotype in SMA severe cases if the drug is administrated within few weeks after birth.

Although both therapies seem to be promising, there are still some concerns related to these treatments. For instance, the therapeutic window is very narrow and the treatment is not completely resolutive for all SMA types' patients. Moreover, the long-term side effects and the involvement of other organs during SMA pathogenesis is not clear. Besides, it is not yet defined the pathogenic mechanisms that trigger SMA. Thus, it is crucial to develop a new realistic and reliable model to study SMA.

One of the major discoveries during the recent years is the capability of stem cells to self-organize into 3D culture thanks to the proper induction pathways to generate different types of organs. These types of 3D *in vitro* cultures are also called organoids and they could offer new insight on physiological development, pathogenesis studies and drug testing.

We think that the development of an innovative human 3D *in vitro* model to study SMA, which has never been described in literature and is able to recapitulate both brain and spinal cord developmental hallmarks, can give the opportunity to a deeper comprehension of cellular and molecular mechanisms underlying disease onset.
With this study we aim:

- ⇒ To generate both control and SMA brain and ventral spinal cord like spheroids;

- ⇒ To characterize the obtained models through genetic and protein expression analyses at various developmental stages;
- ⇒ To assess the basal activity of central nervous system (CNS) control and SMA organoids and their ability to respond to exogenous stimuli;
- ⇒ To investigate pathological differences between controls and SMA CNS organoids.

This study will provide a protocol to develop, from control and SMA iPSCs, vital and functional brain organoids and spinal cord like spheroids. These models can represent not only a tool to study neurodevelopment, but also to investigate the pathogenesis of SMA. Once this model is validated, it will be useful for new drug testing and for the development of alternative strategies.

3. INTODUCTION

3.1 Spinal Muscular Atrophy

Motor neuron disorders (MNDs) involved a large group of diseases caused by degeneration of motor neurons (MNs) in brain stem and/or spinal cord and subsequent muscular atrophy.

Spinal Muscular Atrophy (SMA) is an MND, an inherited autosomal recessive neurodegenerative disease characterized by degeneration of anterior horn MNs (alpha MNs) in the lower spinal cord, resulting in a progressive symmetrical muscular weakness and atrophy. In particular, it is characterized by an acute phase, where a large amount of MNs degenerate and eventually die, and a later chronic phase.

The worldwide incidence of SMA is approximately 1-2 in 11.000, [1] and the prevalence is 1-2 per 100.000. The carrier frequency ranging from 1:91 in African Americans to 1:35 in Caucasians and 1:54 in United States [2,3] but could be slightly different based on the ethnic group [3,4]. Wednig and Hoffman in the early 1890s were the first to describe a mild phenotype of SMA, but only in early 1900s Beevor described for the first time a severe form of SMA and the involvement during the pathogenesis of the respiratory system due to intercostal muscle weakness [5,6].

This disorder is caused by loss (95% of SMA cases) or mutations (5% of SMA cases) of *Survival Motor Neuron* (*SMN*) gene on chromosome 5q, which encodes for SMN1 protein [7]. Moreover, it has

been found on the same chromosome a centromeric form of SMN1, called SMN2, which produce only 10% of the functional protein, because of the lacking the exon 7 in 90% of the transcript [7].

SMA pathology is a heterogeneous, with a broad phenotypic spectrum. It could be classified into five different types based on age of onset and maximum function (Table 1). Briefly, the most severe types are SMA 0 (Congenital SMA) and SMA type I (Werdnig-Hoffmann disease). Regarding SMA type 0, the onset is before birth (*in utero*) and death occurs immediately after or within two weeks from birth. In SMA type I, children never achieve the ability to sit independently and they present also fasciculations of the tongue; oculomotor and mimic muscle seem not to be involved, but cases of cardiogenesis defects have been reported [8]. Cognitive and sensory functions seem to not be compromised. Different studies reported abnormalities in the electromyogram (EMG), and histology showed serious atrophic muscle fibers. If not treated or unsupported, death usually occurs before reaching the second year of life [9]. SMA type II patients are able to sit but unable to walk independently and may survive into adulthood even though with shorter life expectancy. SMA type III and type IV are the mildest forms. In particular, SMA type III compared to SMA type II, patients are ambulant, even some of them can lose this ability over time, meanwhile SMA type IV is considered the “adult-onset” form of SMA, with onset after 30 and normal motor functions with only mild motor impairment, moreover life expectancy is preserved.

Although there is a broad phenotypic spectrum associated with SMN1 pathogenic variants spans a broad continuum without clear delineation of subtypes, we can generalize affirming that that in all SMA patients there is no expression of SMN1, but the severity of the disease is defined by SMN2 copy numbers.

Phenotype	Age of Onset	Life Span	Motor Milestones	SMN2 Copies
Healthy Carrier	/	Normal	Normal	0
SMA 0 (Congenital SMA)	Prenatal	<6 months	None achieved	1
SMA I (Werdnig-Hoffmann disease)	<6 months	Most often ≤2 years, but may live longer	Sit w/support only	2
SMA II (Dubowitz disease)	6-18 months	70% alive at age 25 years	Independent sitting when placed	3-4
SMA III (Kugelberg-Welander disease)	>18 months	Normal	Independent ambulation	3-4
SMA IV	Adulthood	Normal	Normal	4-8

Table 1. **Classification of SMA phenotype.**

SMA could be classified into 4 groups based on the severity of the disease and on the number of SMN2 copies carried from the patients [10].

3.2 SMN Gene And Protein

SMN1 is a telomeric gene composed by eight exons, called 1, 2a, 2b, 3, 4, 5, 6 and 7. This gene is located on chromosome 5 in a complex region (5q13.2) characterized by the duplication of a ca 500 kb element containing several genes [7].

SMN1 gene codifies for 294 amino acid RNA-binding protein (38 kDa) which is ubiquitously expressed in all body, with higher level in the spinal cord, brain, kidney and liver [7,11]. Immunohistological staining of SMN protein showed its localization in the nucleus, in the shape of foci, and diffuse staining in the cytoplasm [12]. The dot-like structure formed by SMN, similar and adjacent to coiled bodies (CBs or Cajal bodies), are called “Gemini of coiled bodies”, simplified as Gems [11]. Interesting, the number of gems is directly correlated to SMA phenotype and they respond to metabolic changes as coiled bodies, for this reason they are considered as dynamic nuclear structure [11,13].

SMN protein contains different domains, such as N-terminal-Gemin 2 domain, Tudor domain, basic/lysine-rich domain, C-terminal proline-rich domain and YG box (Fig. 1).

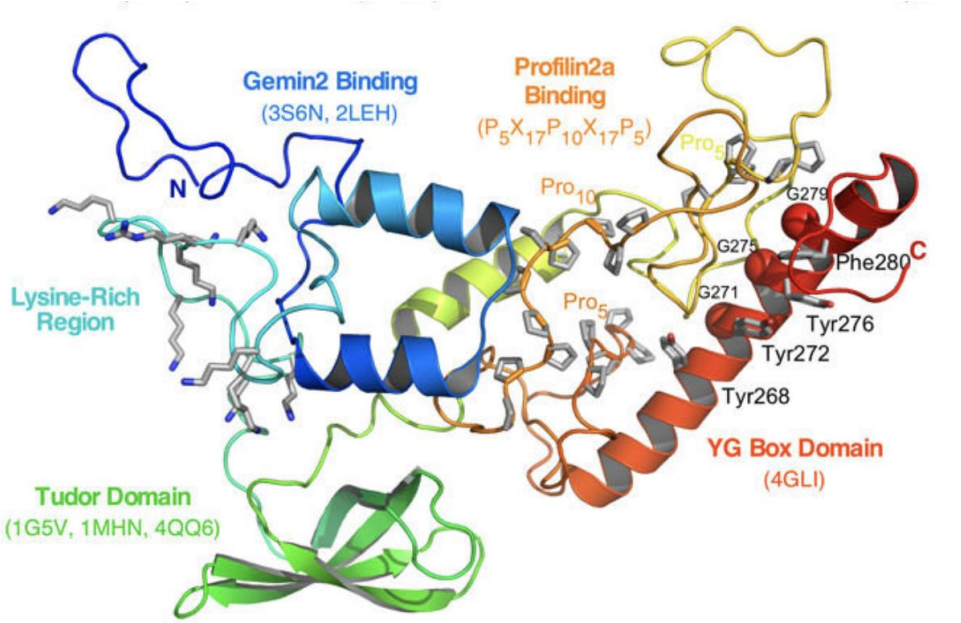

Fig. 1. SMN 3D structure.

SMN1 is composed by five domains: N-Termin al-Gemin 2 domain (blue), Tudor domain (green), basic-lysine-rich domain (light blue), YG box domain (red), and C-terminal proline-rich domain (yellow) [14].

In particular, the basic/lysin-rich region, encoded by exon 2, has been demonstrated to interact with SMN1-Interacting Protein 1 (SIP1), also known as Gemin2, RNAs and other protein such as p53, both *in vitro* and *in vivo* [15–17]. Tudor domain is another important region present on SMN1; it is a highly conserved motif codified by exon 3 that binds to the terminal glycine and symmetrical dimethylated arginine-rich tails of Sm ribonucleoproteins, facilitating the assembly of the spliceosomes [18–20]. Moreover, it is responsible for the interaction with other proteins, such as Histone 3, Fused-in-Sarcoma (FUS) and Fragile X Mental Retardation Protein (FMRP)

RNA polymerase II [21]. Mutations in this domain are often found in SMA patients [18–20].

The other domains of SMN1 are YG box (tyrosine-glycine-rich region, which interacts with zinc-finger protein (ZPR1), amphipathic helix protein SIN3A (transcription co-repressor) and Gemin3 [14], and the proline rich domain that interacts with Profilins, a family of protein involved in actin dynamics [22].

It has been reported that SMN1 protein, through YG domain, is able to oligomerize with itself and that the loss of exon 7 decreases the efficiency and stability of self-oligomerization [16,23]. (Fig. 2)

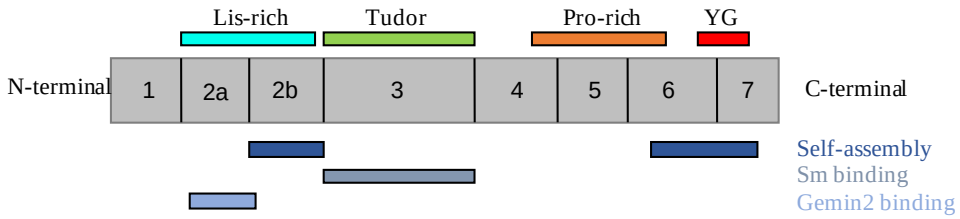

Fig. 2. Schematic representation of SMN1 binding domains.

SMN1 possess four domains which allowed the binding to other proteins or with itself. Lysine-rich domain, Proline-rich domain and YG box domain bind to other SMN1, Tudor domain allows the binding to Sm and Lysine-rich domain binds to Gemin2 protein.

SMN1 (also referred to as Gemin1) can also be recruited in a group of proteins called SMN complex [24–28]. This complex is composed by Gemin family, in particular from Gemin2 (formerly SIP1), Gemin3/DP103 (a DEAD-box RNA helicase), Gemin4, Gemin5/p175

(a WD repeat protein), Gemin6, Gemin7 and UNRIP (UNR-interacting protein) [29]. In the middle of the complex there are SMN, Gemin7 and Gemin8, while the other components are bound to the complex through different interactions [30] (Fig. 3).

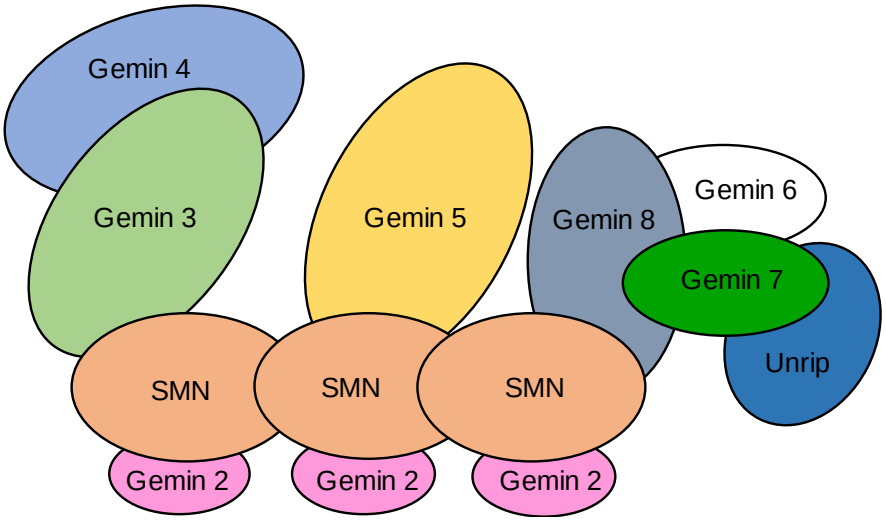

Fig. 3. Schematic representation of SMN complex.

SMN complex is composed by nine proteins, SMN, Gemin family from 2-7 and Unirip.

SMN1 plays a lot of different roles in cells, which are schematic represented in Fig. 4. We can divide them into five categories: RNA metabolism (pre-mRNA splicing, transcription through its interaction with CTD of pol II, translation and stress granule (SG) formation), Signal transduction, Intracellular trafficking (endocytosis, cytoskeleton), DNA recombination/repair and system-wide effects [14].

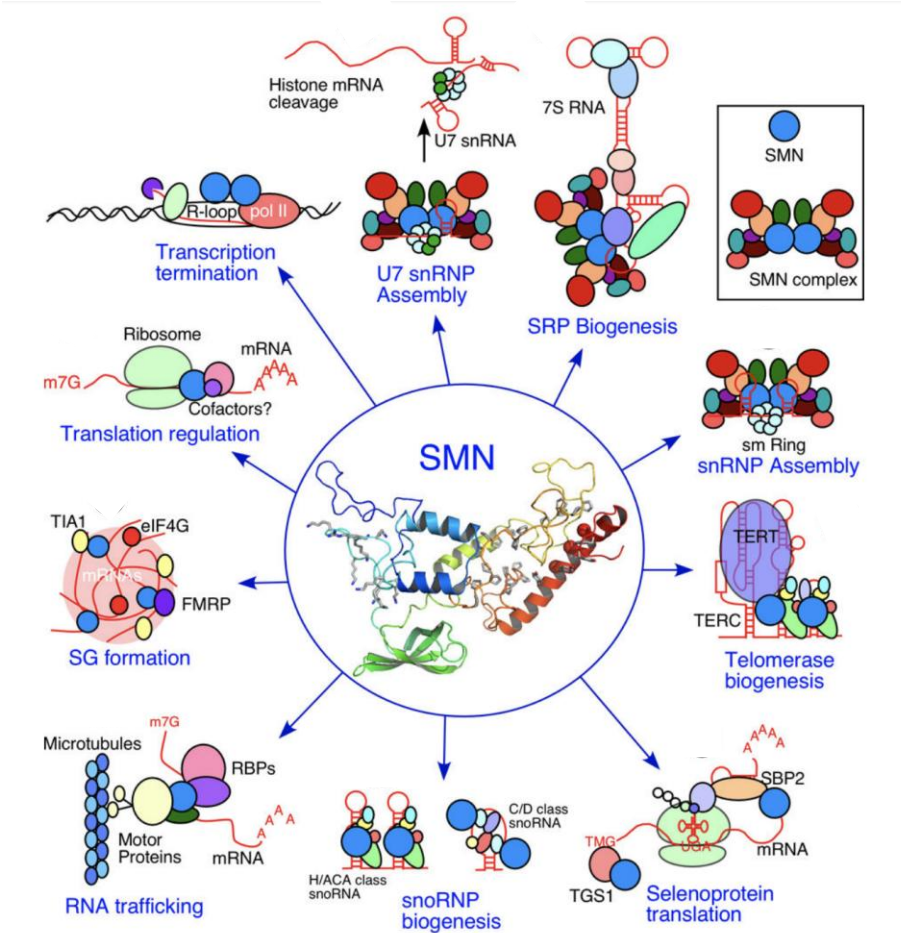

Fig. 4. Schematic representation of SMN roles.

It has been demonstrated that SMN is involved in different pathways, such as the regulation of mRNAs machinery and trafficking. It is also involved in Stress Granules (SGs) formation. [31]

In particular, regarding RNA metabolism, SMN complex not only is important for pre-mRNAs splicing, but it is also involved as a chaperon in maturation, assembly and function of spliceosomal small nuclear ribonucleoproteins (snRNPs) U1, U2, U4, and U5, which are the core component of spliceosomal complex [32–34]. Spliceosomal

snRNPs are U-rich snRNPs composed by seven Sm proteins (B/B′, D1, D2, D3, E, F, and G) that remove introns from pre-RNA. Their biogenesis is a multi-step process that begins in the nucleus, shifts into the cytoplasm and moves back to the nucleus. It starts with the transcription by RNA polymerase II (pol II) of pre-snRNAs that are co-transcriptionally processed at their ‘5-end, with the inclusion of 7-methyl guanosine (m7G) cap and cleaved at their 3’-end. Through an export complex, pre-snRNAs are transported in the cytoplasm where they are further processed by SMN complex and heptameric Sm ring. These bindings allowed the hypermethylation, the 3’-end trimming and subsequently snRNPs are moved all together into the nucleus; here the complex dissociates and SMN transiently localize in Cajal Bodies (CBs), where snRNAs undergo to fully maturation [14,35].

Another important role played by SMN is the trafficking of mRNAs along the axon and in the growth cone of primary MNs [36]. Indeed, it has been showed that SMN modulates the localization of β-actin within the growth cones [37]. In particular, SMN has been found to colocalized with profilin 2a, which is an actin-binding protein [38]. Moreover, SMN complex seems to interact also with candidate plasticity gene 15 (Cpg15). Indeed, it has been showed that the depletion of SMN causes Cpg15 and β-actin reduction in distal axons [39]. Furthermore, Rage and colleagues performed a genomewide study in MN-like cells (NSC-34) of SMN-associated RNAs. Results showed over 200 mRNAs associated with SMN, which 30% localized to the axon in a SMN-dependent manner [40]. Another evidence concerning SMN and mRNAs interaction in the axons, is provided by Fallini and colleagues; in fact, they present a potential non-canonical

function of SMN in axons through the binding of SMN Tudor domain to a neuronal-specific mRNA-binding protein, HuD, which has a role in neuronal development and plasticity [41]. Results showed that impairment in SMN expression caused the reduction of HuD protein level in the axons, and this decrease could impair the axonal localization and the interaction of mRNAs with mRNAs-binding proteins like HuD, KSRP, and hnRNP-R/Q resulting in a defective subcellular localization of transcripts likely necessary for MNs maintenance. They also demonstrated that SMN is required for axonal localization of poly(A) mRNA-containing granules. Although all these data suggest a possible involvement of SMN in mRNAs transport, it has not yet been demonstrated if mRNAs trafficking impairment is due to SMN deficiency, and whether the MN degeneration is caused by the damaged transport of specific transcripts.

Several are also the mechanisms which regulate SMN protein levels, such as posttranslational modifications (sumoylation, ubiquitination and phosphorylation), *SMN* mRNA stabilization, genomic and sequence integrity, transcription regulation, *trans*-regulatory splicing factors and subcellular localization. Moreover, also external factors could be involved in SMN expression regulation, such as oxidative stress, hypoxia and starvation [42].

On the same chromosome, is present a centromeric version of *SMN1* gene, *SMN2*, which shares more than 99% nucleotide identity; indeed, the sequence differs only in five nucleotides (two exonic and three intronic) [43]. Nevertheless, a single point mutation (840C→T

transition) in the last codon (exon 7) of *SMN2* modifies its splicing, resulting in a truncated and unstable form of SMN lacking 16 amino acids and carboxyl terminus. *SMN2* gene codifies for a SMN2 protein also called *SMNΔ7*. In most of the cases (90-95%) SMN2 protein is functionally defective, thus rapidly degrades (two-fold shorter half-life compared to the full length), although only 5-10% is a functional full-length (FL) protein [16] (Fig. 5).

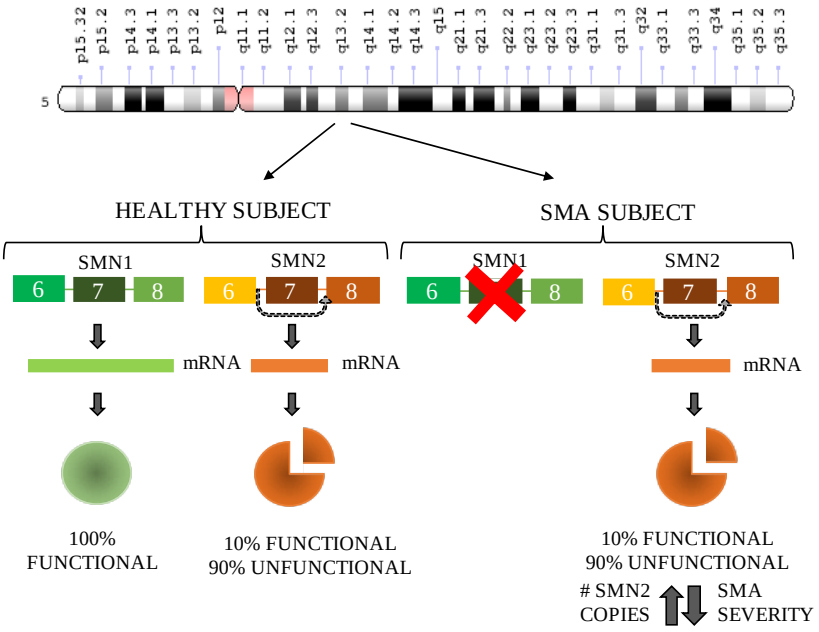

Fig. 5. Schematic representation of SMN1 and SMN2 in healthy and affected subjects.

Healthy subjects express 100% FL-SMN protein and 10% functional FL-SMN protein. SMA subjects have no more *SMN1* gene and SMN2 is only able to produce 10% of FL protein. There is an inverse correlation between the number of SMN2 copies and the severity of SMA, indeed, more copies of SMN2 a patient carries and less severe is the disorder.

As mentioned in the previous paragraph, SMA is cause by mutations in homozygosis of *SMN1* gene, resulting in the loss-of-function of SMN1 protein, and FL-SMN2 could partially compensate for SMN1 lacking. Indeed, several genotype/phenotype analyses confirmed a correlation between SMN2 copy numbers and SMA phenotype, thus higher is the copy number milder is the phenotype [44].

Nevertheless, in the most severe cases, SMN2 fails to rescue the cell phenotype [45].

Whereas, SMN1 and SMN2 proteins are express in the all body, it is unknown the reason why low levels of SMN1 in SMA patient lead to the specific MN degeneration.

3.3 Phenotype Modifiers

Phenotype or gene modifiers are genetic locus that could enhance or suppress the outcome of the primary disease-causing mutation, thus affecting different elements of the disease, such as the severity or the onset of the disease.

In literature are reported several genes considered as modifiers in SMA, among them there are: Actinin (ACTN), Transforming Growth Factor – β (TGF – β), Activating Transcription Factor 6 (ATF6), Fibroblast Growth Factor 2 (FGF2), Potassium Channel Calcium-Activated intermediate (KCNN3) [46], Ubiquitin-like modifier activating enzyme 1 (UBA1) [47], Phosphatase and tensin homolog (PTEN) [48].

Besides the genes listed above and *SMN2* (which could be considered as a gene modifier) the first identified as candidates were *H4F5*, *NAIP* and *p44*, which are located in proximity of *SMN* locus [49]. Although there is not a clear evidence that they are involved in modification of SMA patients phenotype, deletions in *H4F5* and *NAIP* were observed in almost 50% of SMA type I patients and they were more frequently mutated in SMA type I (68-90%) compared to SMA type II or type III (20-50%) [50–52].

Transcriptomic-wide differential expression analysis revealed *PLS3* as a gene modifier. PLS3, also called Plastin 3 or Plastin-T, is a sex-specific modifier (female, encoded on the X chromosome) and it is involved in formation and stabilization of actin bundle [53]. A study on siblings showed that female with SMN deletion and high level of PLS3 in the blood was unaffected, meanwhile male overexpressing

PLS3 was affected [54], suggesting that *PLS3* can selectively modify the phenotype independently from *SMN*. Furthermore, its role as a disease modifier has been demonstrating also in different models of SMA, such as zebrafish and mouse. In both cases its overexpression results showed an improvement in neurite and neuromuscular phenotype by stabilizing F actin-dependent processes [54,55].

Another gene modifier of SMA is *ZPR1* gene (Zinc Finger Protein 1). This protein was discovered through a study on lymphoblastoid cell lines from SMA patients and controls, whose aim was to identify the expression of SMN interacting proteins. Data showed elevated levels of *ZPR1* both in controls and in SMA mild affected subjects compare to SMA severe affected patients [56]. Indeed, ZPR1 in physiological conditions supported the accumulation of SMN in the nuclear bodies, and in SMA this interaction is disrupted [57]. In the SMA mouse model the decrease of ZPR1 levels led to an increase of disease severity with a decrease of the lifespan and its overexpression in human cell lines resulted in increased level of SMN protein and not the mRNA expression, indicating the role of ZPR1 in the stabilization of SMN-complex [58].

Insuline-like growth factor 1 (*IGF1*) is another candidate gene modifier in SMA. It is synthetized in the liver and it is involved in myoblast proliferation and myogenic differentiation both *in vitro* and *in vivo*. *In vivo* the overexpression of IGF1 led to an enlargement of myofibres and prolonged survival; moreover, the systemic administration of AAV1-*IGF1* in mice improved the motoneuronal and neuromuscular phenotype and it was also able to increase the

production of SMN in different organs, such as central nervous system (CNS) and heart [59].

A further gene modifier in SMA is neural calcium sensor neurocalcin delta (NCALD). This is a calcium-dependent negative regulator of endocytosis. It has been showed that its knockdown can ameliorate neuromuscular junction function and axonal outgrowth in different types of animal models, such as zebrafish and mice [60].

3.4 Pathogenesis

As mentioned in the previous paragraph, although SMN is expressed in the whole organism (with high level in the brain, spinal cord and kidney, low level in cardiac and skeletal muscle) only α-MNs in the ventral spinal cord are susceptible to its loss and underlying reasons are still unknown; moreover, SMN plays a role as a housekeeping gene, indeed *SMN* knockout in mice is embryonically lethal [61].

In literature, there are different studies on the possible explanation of selectively death. For instance, Ruggiu and collaborators, showed that *in vivo* α-MNs expressed lower levels of FL-*SMN2* mRNA compared to the other cells both in the dorsal spinal cord and in non-nervous system (skeletal muscle, kidney and skin), due to an inefficient inclusion of exon 7 selectively in MNs. Ruggiu and colleagues, also demonstrated that SMN deficiency causes a negative feedback pathway that results in further decrease of SMN in MNs [62].

Another group, Soler-Botija and collaborators, demonstrated that the level of expression of SMN2 in different organs not affected during the pathology, such as intestine, kidney and eyes, was the same in SMA and control samples [63]. Thus, it is possible that in SMA affected individuals, FL-SMN2 in non-affected tissue can compensate for the absence of SMN1, meanwhile in α-MNs, the low level of FL-SMN2 could favor the onset of the degeneration of these cells. Furthermore, SMA type I patients have around 100-fold decrease in SMN protein in the spinal cord compare to the control [7,13].

Another study, performed by Burlet and colleagues on SMA type I fetus, showed a drastic decrease of SMN in all tissue, leading to the observation that SMN protein in SMA subjects is significantly reduced prior the onset of the disease, while in normal fetus is strongly expressed [64]. Studies performed on MNs from fetal and post-natal tissue of SMA type I, described a reduction of MNs number and a different morphological appearance compared to the control [65,66]. Indeed, MNs in human fetus spinal cord around 15–25 weeks of gestation showed typical signs of apoptosis, heterotopic migration surrounded by astroglial cells and a reduction in number in MNs; moreover, MNs with DNA vulnerability were no longer detected in the post-natal period. All these results suggest that MNs start to degenerate during development and apoptosis might play a primary role in the MNs loss at early stages of the disease.

Furthermore, it has been demonstrated that in SMA fetus (around 12 and 15 weeks' gestational ages) B-cell lymphoma 2 (Bcl-2) and B-cell lymphoma extra-large (Bcl-X_l) (two antiapoptotic proteins) expression was downregulated in MNs, likely leading to the increase of neuronal death during SMA fetus development [67].

Unsurprisingly, there are differences also among SMA types, indeed, SMA type I individuals, have a higher decrease of SMN level and fewer gems compare to SMA type III patients [7,13]. Moreover, MNs from SMA type I patients die before those from SMA type II or type III individuals [68].

Another pathway that would be interesting to take in consideration for SMA pathogenesis, is the development of neuromuscular junctions

(NMJ). Indeed, it is not yet clear if the SMA type I phenotype derived from the degeneration of lower MNs or from the premature arrest of NMJ development. In literature are reported different studies demonstrating the premature loss of NMJs and defect in both pre and post-synaptic transmission. In fact, pre-synaptically, there is a defect in the organization of synaptic nerve terminals characterized by poor arborization, probably due to an accumulation of neurofilament (NF) protein in the nerves terminal; on the other hand, post-synaptic space present immature plaque-like acetylcholine receptors (AChR) cluster and embryonic form of the receptor. It has been showed also a decrease density of synaptic vesicles and a reduced quantum content [69–71]. Moreover, Kong and colleagues, demonstrated that NMJs in muscles (except for intercostal and paraspinal muscle, muscles particularly affected in SMA mice) remained innervated in late stages of the disease, although deeply altered in morphology and synaptic activity [70]. Significantly is the fact that NMJ impairment is not only present in the SMA mouse model but was also confirmed in muscle tissue of human patients. All these results suggest an impairment in NMJs maturation indicating that SMN is involved in assuring post-natal development of neuromuscular synapses.

SMN, besides the role in neuromuscular fetal development, has been found involved in myotubes maintenance. As a matter of fact, Martínez-Hernández and colleagues, analyzed the myotubes and skeletal muscle tissue from SMA type I fetus. Results showed a reduction in size of myotubes in all ages analyzed, a rearrangement in clusters close to larger and isolated myotubes. Interesting is the

fact that they did not find any differences in the SMA compared to the control in Terminal deoxynucleotidyl transferase dUTP nick end labelling (TUNEL) analysis and in Bcl-2 and Bcl-X1 expression level [72]. All these findings suggest that ventral horn MNs and skeletal muscles undergo different pathogenic pathway during development in SMA individuals.

According to disruption of the entire neuromuscular system, pathological findings suggested that axons are altered too. Studies performed on ventral root of SMA type I patients, demonstrated that they are atrophic; there is also a consistent loss of large myelinated fibers, glial extension on un-myelinated fibers, degeneration of un-myelinated axons in the proximal portion of anterior spinal roots and the fast anterograde axonal transport disruption [73–75]. Regarding fibres, SMA type I muscles display atrophy of the muscle fibres, both type I and type II, with immature aspect and central nuclei [72]. Moreover, there are evidence of denervation during embryogenesis [75].

Besides, probably due to a glia response triggered by the early MNs loss, it has been showed that the nerve roots display glial bundles, which consist in astrocytes processes and glial fibrillary acidic protein (GFAP) positive cells [76].

Other pathways that are impaired in SMN deficiency are neuromuscular transmission and synaptic transmission/synapse assembly. In fact, transcriptome analyses in SMN-deficient Drosophila, zebrafish and rodent models have showed two targets whose alternative splicing is directly affected by SMN deficiency:

stasimon (a transmembrane protein also called Tmem41b) and neurexin 2a [77–80]. Although during SMA pathogenesis the most affected cells are lower MNs, there are evidence reporting that in human SMA, regardless the severity of the phenotype or SMN2 copy numbers, in the ventral thalamus nuclei and dorsal root ganglia cells there are sign of neuronal ballooning and neurodegeneration [81–83].

In literature we can find also studies suggesting a non-cell autonomous pathway. For instance, Hua and collaborators, in their study, restored SMN level in central nervous system (CNS) and in peripheral tissue in the mouse model, using antisense oligonucleotides. Results showed that only the recovery of SMN in peripheral tissue rescued the phenotype in mild SMA mice, in addition in the severe SMA mice there is an extended survival with significant improvement in motor function and NMJs morphology [84]. These data might suggest that healthy peripheral tissue may provide neurotrophic factors which are necessary for MNs maintenance.

In conclusion, although SMA is a monogenic disease, it is important to develop a therapeutic strategy that consider all the different tissues involved in SMA pathogenesis.

3.5 Therapies

In recent years, important progresses have been done in new therapeutic treatment for SMA (Table 2). Indeed, there is not only a Food and Drug Administration (FDA)/ European Medicines Agency (EMA)-approved drug, but also a lot of promising advanced clinical trials.

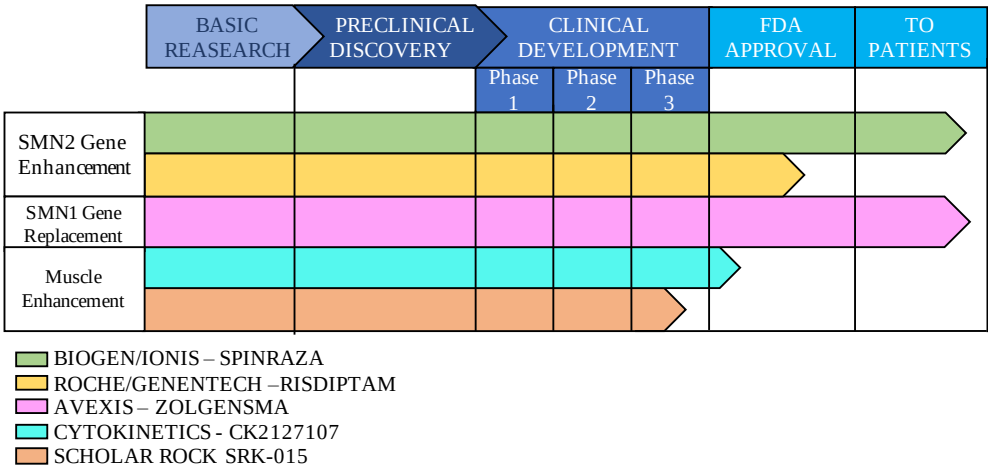

Table 2. Timeline showing the most promising drugs in clinical trials from Phase 1 to FDA approval. Updated June 2019.

Nowadays, the most promising mechanism to rescue the pathological and clinical phenotype consist of SMN protein level restoration. This can be achieved in different ways: through administration of functional *SMN1* gene, acting on SMN2 protein levels, and acting on peripheral tissues, such as skeletal muscle.

3.5.1 SMN2 Targeting Approaches

As mentioned above, SMN2 differs from SMN1 for only one base change and it is still present in all the patients. For this reason, it could be used as a target for therapy.

Compounds that have as target SMN2 can act with different mechanisms: through stabilization of SMN2 mRNA or protein, increasing of SMN2 transcription or enhancing exon 7 inclusion [85].

.

3.5.1.1 NUSINERSEN

In SMA patients, as previously describe, around 90% of SMN2 protein lack of exon 7, resulting in a non-functional and unstable protein; antisense oligonucleotides (ASOs) are synthetic, short and single-stranded oligodeoxynucleotides composed by phosphate backbone and sugar rings that can restore, reduce or modify protein expression. To switch the splicing of a mRNA, ASOs with a modified backbone chemistry are used. ASOs are engineered to specific binding to cis-acting splicing regulatory motif, promoting the exon 7 inclusion in SMN2 [86]. In particular, the inclusion of the exon 7 is modulated by two intronic splicing enhancers, both located on intron 7, and two intronic splicing silencer sequences (ISSs), in intron 6 and 7 (ISS-N1) [87]. Deletion in intron 7 of ISS-N1 leads to a significantly enhanced incorporation of exon 7 in SMN2 minigenes [88].

There are three different types of ASOs which are schematic represented in Fig.6:

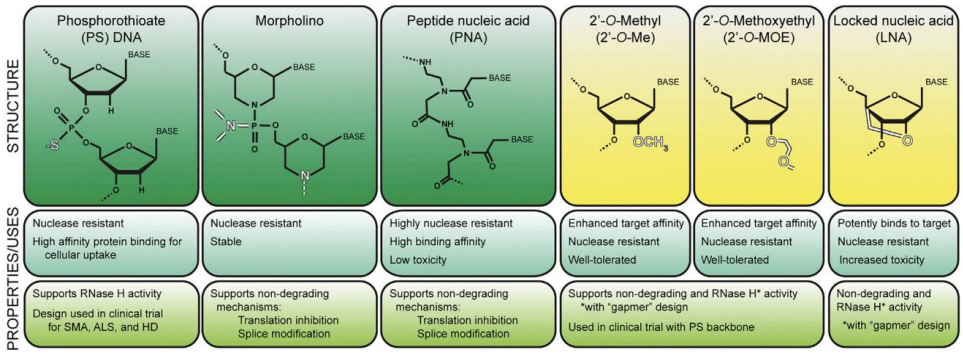

Fig. 6. Antisense oligonucleotide (ASO) structure, uses and properties. [89]**.**

Nusinersen, marked as Spinraza®, is the first FDA (FDA, 2016) and EMA-approved (EMA 2017) drug for SMA treatment. Its mechanism of action is based on ASOs;

Indeed, hybridization of Nusinersen to ISS-N1, causes rearrangements of the DNA structure masking site where splicing machinery binds (hnRNP A1/A2) promoting the inclusion of the exon 7 in SMN2, resulting in a production of FL-SMN protein [14] (Fig.7).

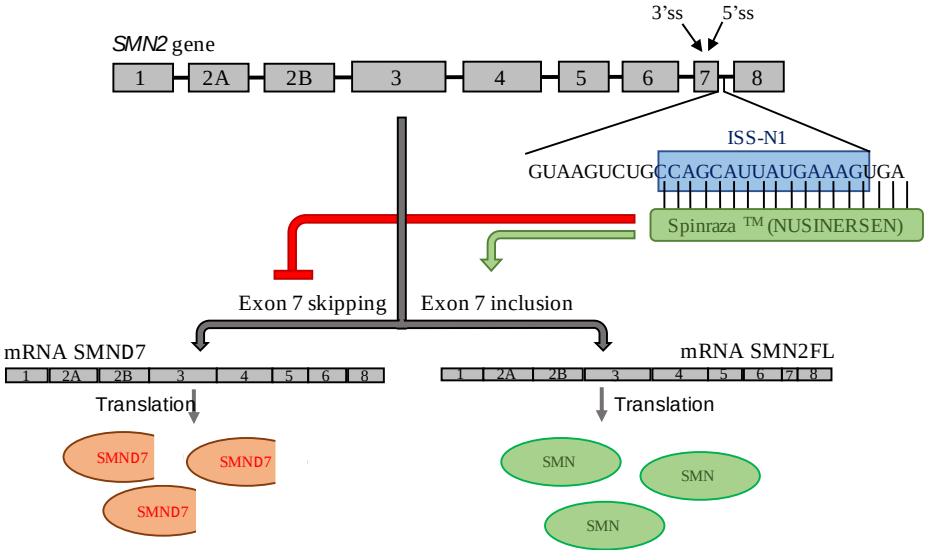

Fig. 7. Schematic representation of Nusinersen mechanism of action.

Nusinersen binds the ISS-N1 sequence on *SMN2* gene and modulate its splicing, leading to the production of a functional FL-SMN2 protein.

In particular, the most stable ASO, with a wide distribution and low toxicity, is Morpholino oligomers (MOs) [90]. It has been demonstrated that the delivery both *in vitro* and *in vivo* can increased not only the gems formation, but also FL-SMN2 protein [90,91]. Indeed, the delivery of MOs at post-natal day 0 (P0) intra-cerebro ventricularly (ICV) increased up to 5-fold the production of FL-SMN2 both in the spinal cord and in the brain [90]. Moreover, a single dose delivered after birth in SMAΔ7 mice, can not only ameliorate the phenotype but also increases the lifespan from 14 days up to 100 days. Unfortunately, the therapeutic window is very narrow, in fact the delay in the MOs administration causes the reduction of the improvements [90,92].

While the blood brain barrier (BBB) in neonatal mice is leaking and the ASOs could be delivered systematically, human BBB is more prominent, preventing systemic administration (subcutaneous or intravascular) which would require a higher dose potentially toxic for the liver and the kidney. For this reason, Nusinersen is delivered intrathecally [14]. The schedule of the treatment consists of four loading doses, the first to the third should be delivered at 14-days intervals, while the fourth dose should be administrated after 30 days. Once every 4 months a maintenance dose should be administrated lifelong (FDA, 2016).

3.5.1.2 RISDIPLAM or RG7916

Risdiplam, is a small molecule developed by Novartis Pharmaceutics and Hoffmann-La Roche. This compound is a pyridazine and showed affinity to exon 5 and exon 7, and it is able to modify their splicing pattern. It is an orally-administered medicine that can provide an increase of SMN-FL production both in the central nervous system and in peripheral organs. It has been showed that in SMA mouse model, it is able to increase the production of FL-SMN protein around 90% in the brain and around 70% in muscles [93].

Subsequently to problems of safety, compound RG7800 was change with compound RG7916 (RO7034067). Risdiplam is currently evaluated in 4 different trials with promising results: FIREFISH (NCT02913482) for SMA I, SUNFISH (NCT02908685) for SMA II and III and JEWELFISH (NCT03032172) for all types of SMA and RAINBOWFISH (NCT03779334) used in pre-symptomatic SMA [94].

3.5.2 SMN1 Gene Replacement

As previously mentioned, the presence of the BBB prevents the drugs crossing, making their delivery in the CNS very difficult. The discovery of Adeno-associated viruses (AAV) opened up a new field for the development of therapeutic strategy for the CNS; indeed, they can cross the BBB and, in particular the serotype 9, have a particular trophism for CNS and MNs [95,96].

It has been demonstrated that a single intravenous injection in neonatal mice of self-complementary AAV9 (scAAV9) can transduce around 60% of lumbar MNs and it is also able to penetrate in brain neurons, dorsal root ganglion, astrocytes both in the spinal cord and in the brain, in cardiac and skeletal muscle tissue. The persistence of the virus in these tissues was up to 5 months [96].

Another study demonstrated that the one-time injection on post-natal day 1 enhances the survival of SMA mice from 14 days up to 250 days [97]. Furthermore, they could also observe a phenotypical improvement of the mice, in particular better locomotor and righting abilities, weight gain and neuromuscular transmission [97]. Delay in the delivery of the virus, led to a mild improvement, with no changes at all after day 10 [97]. This strategy has been also tested on large animals, such as domestic cats (Felis catus), pigs (Sus scrofa) as well as non-human primates (cynomolgus macaques, Macaco fascicularis) [95,97–99].

AveXis took advantage of scAAV9 caring wild type *hSMN1* method to develop a new drug called Zolgensma, which was recently approved from FDA. This treatment consists in a single dose intravenous administration, which is enough to provide systemic delivery. Children that already had a titre of antibodies against the virus are excluded. Two of the main concerns are the efficacy decline, indeed, a repeated injection would not be feasible due to the formation of the antibodies against scAAV9 and the deficiency of SMN in peripheral tissue, which could reveal a previously hidden phenotype. In fact, AAV9 has a high affinity for post-mitotic cells such as MNs, but not for high proliferative cells like muscle cells.

Although gene therapy seems to be the most promising, results are in line with the oligonucleotide therapy, confirming that the therapeutic window is very narrow and that it is very important the timely intervention for best therapeutic improvement.

3.5.3 MUSCLE TARGETING APPROACHES

As previously describe, SMA is characterized by the loss of MNs, leading to the loss of muscle strength. Another group of therapies has been developed to ameliorate and improve neuromuscular functions, muscular weakness and fatigue.

3.5.3.1 CK2127107

CK2127107 (also called Reldesemtiv or CK107) is a troponin complex activator developed by Cytoskeleton Inc. in collaboration with Astellas Pharma (Stevens et al., 2008). This compound is able to slow down the release of calcium from fast skeletal muscle troponin to sensitize the sarcomere to calcium, resulting in an increased force output at submaximal frequencies of MN nerve stimulation [100]. Briefly, this treatment allowed the increase of the capability of skeletal muscle to contract, although the nerve signalling is reduced. In May 2015, FDA accorded orphan drug designation for the potential treatment of SMA patients.

3.5.3.2 SRK-015

This compound has been developed by a biotech company, Scholar Rock, and it is a local and selective inhibitor of the activation latent myostatin. Myostatin is a protein highly express in the skeletal muscle, whose role is to inhibit myogenesis. In particular, SP-015

binds the latent myostatin and halts protease cleavage, resulting in the inactivation of latent myostatin and consequent increasing of the muscle cell growth (especially of the fast-twitch muscle fibers) and differentiation [101]. The efficiency of neuroprotective and muscular enhancing of this compound has not to be determined yet and because of the dysregulation in the myostatin pathway, its therapeutic effects could be limited.
In March 2018, FDA accorded orphan drug designation for the potential treatment of SMA patients.

3.6 Preclinical Models for SMA

Besides human, only chimpanzees possessed SMN gene duplication, although only Homo sapiens carries the modification of SMN2 [102].

In all the species used to model SMA, complete loss of SMN causes lethality due to the absence of SMN2, which produces at least a small amount of functional SMN. Nevertheless, thanks to engineering progresses, nowadays there are a lot of different models to mimic SMA, both *in vivo* and *in vitro*.

Concerning *in vivo*, different types of animals have been used: Drosophila [103,104], Caenorhabditis elegans [105], zebrafish [106], pigs [99] and murine models.

So far, the best model to study SMA is the mouse. Indeed, *SMN* gene in mice shares 83% amino acid homology with human *SMN* [61].

It has been showed that the knockout of *SMN* gene in mice led to an early embryonic death, meanwhile the heterozygous animals did not present SMA phenotype [61].

As mentioned above, only humans carry *SMN2* gene, thus SMA mice ($SMN1^{-/-}$; $SMN2^{Tg/Tg}$) were created using an insertion of one or two copies of a full-length human *SMN2* transgene on a background of homozygous SMN1 deletion [107]. These mice survival is around 4-6 days and after 48 hours they present decreased movement, laboured breathing and tremor of the limbs [107]. Interesting, mice with higher copies (more than eight) of SMN2 transgene were phenotypically normal, likewise in humans. Indeed, these mice did not present any decrease movement and they presented no MNs death or a smaller number of Gems.

A variety of mice models have been developed to study SMA (list in table 3), but the two most used are Taiwanese and the SMNΔ7 mouse (which mimics the acute phase of severe SMA) [108].

Genotype	Survival	Phenotype	Reference
Smn $^{-/-}$	Embryonic lethal	/	Schrank et al., 1997
Smn $^{-/-}$; SMN2 $^{+/+}$	5 Days	Very severe SMA phenotype	Monani et al., 2000
Smn $^{-/-}$; SMN2 high copies (8 copies)	Normal	Normal, with short and thick tail	Monani et al., 2000
Smn $^{-/-}$; SMN2	Severe: 10 days Intermediate: 2-4 weeks Mild: Normal	Depending on SMN2 copies number it could be Severe, intermediate or mild	Hsieh-Li et al., 2000
Smn $^{-/-}$; SMN2 $^{+/+}$; SMNΔ7	13.3 Days	Severe SMA phenotype	Le et al., 2005
Smn $^{-/-}$; SMN2 $^{+/+}$; SMNA2G	Normal	Mild SMA phenotype	Monani et al., 2003
Smn $^{-/-}$; SMN2 $^{+/+}$; SMNA111G	Normal	Normal	Workman et al., 2009

Table 3. List of murine models to study SMA.

List of mice model used for study SMA.

In addition to in vivo models, in vitro models represent the other powerful tool to study SMA. In particular a great improvement was produced with the generation of the induce pluripotent stem cells (iPSCs).

iPSCs were first described by Takahashi and Yamanaka in 2006; these cells were obtained from human tissues (especially from fibroblast or blood cells) by administration of four reprogramming factors (also called Yamanaka's factors): Oct4, Sox2, Klf4 and c-Myc [109]. Many are the advantages resulting from the use of iPSCs. First of all, iPSCs are easily to obtain, indeed they can be derived from fibroblast or blood cells (Lynphocytes), and also easily to grow and maintain in culture; in addition, iPSCs could be differentiated into all three different germ layers (mesoderm, ectoderm and endoderm) (Fig. 8). For this reason, they can be used for a variety of purposes, such as drug screening and disease modelling [110]. Another great advantage is that they can be generated directly from affected subjects, leading to an individualize and patient-specific stem cell specific treatment replacing embryonic stem cell (hES), without both ethical issue and immunological rejection.

Moreover, iPSCs could be also used to study disease modifiers, indeed they could be obtained from subjects belonging to the same family, with the same genotype, but different phenotype [108,111] .

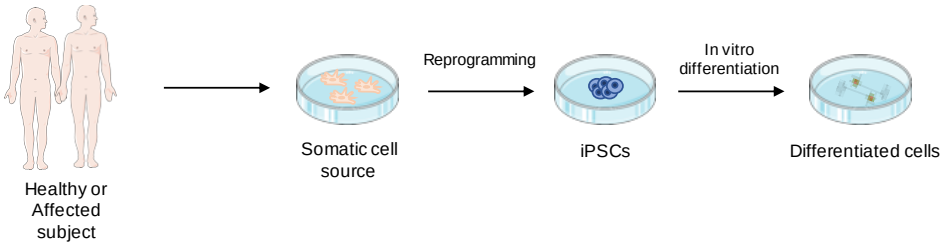

Fig. 8. Schematic representation of the generation of differentiated cells.

Somatic cells from human healthy or affected subjects are cultured and subsequently reprogrammed into iPSCs. Next iPSCs can be differentiated into different types of cells.

IPSCs for study SMA were first described by Ebert and collaborators in 2009. They generated iPSCs from 3 years old SMA I patient and as a healthy control they used the mother. They first analysed SMN mRNA expression level in both fibroblasts and iPSCs. Results showed a normal level of SMN in the control cells and a lower level in the SMA affected cells. Since SMA is an MND, the authors differentiated iPSCs into MNs, using a protocol based on the addition of retinoic acid and sonic hedgehog to the media. iPSCs-derived MNs were positive to the classical neuronal markers, such as Islet I, HB9, SMI 32 and ChAT. Interestingly, at early stages of the differentiation there were no differences between SMA and control iPSCs-derived MNs, but a few weeks later, SMA-iPSCs derived MNs showed differences in numbers and morphology compared to the control ones. This could be due to the fact that the absence of SMN1 gene did not impair the development of SMA MNs, but it caused a

post-developmental selective neurodegeneration of α-MNs. Furthermore, in the same study, two different compound, valproate and tobramycin, were administered, which are known to increase the SMN level, thus these cells could be used for drug screening. Results showed a significant increase of Gems [112].

In order to better understand the post-developmental mechanism underlying this pathology another group, Sareen and Svendsen's group, performed more experiment on iPSC-derived MNs. They obtain the same results as the previous work, indeed, there were no signs of degeneration in the early stages of the differentiation, but after 4 weeks, SMA iPSCs-derived MNs underwent to a reduction both in numbers and in size compared to the control. The possible explanation provided was the activation of the apoptotic pathway around 7-10 weeks of differentiation, because of the high level of caspase-3 and caspase-8, which are the triggers of the apoptotic cascade [113].

Another great contribute was given by Corti's laboratory, which was able to reprogram fibroblast using non-viral/transgenec method by nucleofection of plasmids encoding pluripotency factors (OCT4, SOX2, NANOG, LIN28, c-Myc, and KLF4). Moreover, a small portion of obtained SMA iPSCs were genetically corrected with SMN2 sequence-specific oligonucleotides. In line with previous studies, iPSCs-derived SMA MNs after 8 weeks of differentiation presented signs of degeneration, with the decrease in size of the soma and reduction of the axonal elongation. On the other hand, treated SMA iPSCs-derived MNs presented a rescue of the cellular damage and

significantly increase in gems numbers [114]. Nowadays a lot of studies have been published regarding the mechanism of MNs degeneration derived from SMA iPSCs [110].

Undoubtedly, study of SMA in animal models give a more complete view of the disease. Unfortunately, results obtained from animal model have to be validated in human cellular model, due to the natural lack of the homologous gene SMN2, which plays a crucial role in establishing the clinical phenotype. The generation of iPSCs gave rise to a new technology able to provide an unlimited amount of human pluripotent stem cells to study the pathology mechanisms in vitro and bypass the ethical issues. In conclusion, the development and optimization of iPSCs has permitted to elucidate disease-specific mechanisms and also to open new path to fully understand the key pathogenic events, resulting in a development of efficient treatments.

3.7 3D Culture

Our knowledge regarding neurogenesis, neural process and neurological disorders is limited due to an insufficient availability of human brain tissue. Indeed, the only way to study the CNS is through post-mortem human tissue or the use of animal models; the last one, gave a great contribute to study CNS, but is not sufficient because of cross-species differences, such as species-specific functions. A great revolution started with the ability to reprogram human somatic cells into iPSCs and then guide them over a specific cell fate, in fact, as mentioned in the previous paragraph, these cells are able to mimic

some cell-to-cell interactions and single populations. Although these 2D cultures represent a helpful tool to study cell biology, they do not provide a full understand of the whole organ, which is composed by different type of cells well organized. This is also a problem for the translation of many drugs from preclinical *in vitro* models into clinical setting. Another obstacle is the level of maturity that the cells can reach, indeed, for instance iPSCs-derive neurons are not as mature as adult human neurons.

In 1975, Green and collaborators were the first to perform a transplant in a burn patient with cultured autologous keratinocytes sheets. Indeed, they discovered the ability to keratinocytes to self-organized in sheets; on the bottom layer of the culture dish was presented the basal layer of the growing clones, meanwhile in the superficial layer were presented fully differentiated keratinocytes [115]. Few years later, in the same laboratory, they also developed a new method to culture the cornea [116], which was also successfully transplanted. These two were the first pioneers' studies on organoids.

Nowadays, the term organoid refers to stem cell–derived three-dimensional cultures which contain more than one cell type organized resembling the mimic organ and present some specific function of the organ [117].

Many are the advantages derived from this new technique. Mentioning few of them, they can be grown from human stem cell and from patient-derived iPSCs, thus they can be used both to model human development and disease. Moreover, interactions between

cell-cell and cell-extracellular matrix, which influence important cellular behaviour, are more complex and depicted in organoids. Most important features are that they present a spatial organization and a higher level of complexity compare to 2D culture; however, the 3D spatial organization is not completely the same as *in vivo* in human, for instance in the case of the brain, due to the lack of anterior-posterior and dorsal-ventral axes.

Organoids could be generated both from mouse and human pluripotent stem cells. To date different types of organoids from human pluripotent stem cells have been generated, such as intestinal, kidney, brain, retinal organoids, and liver buds (liver organoid-like) (Fig. 9).

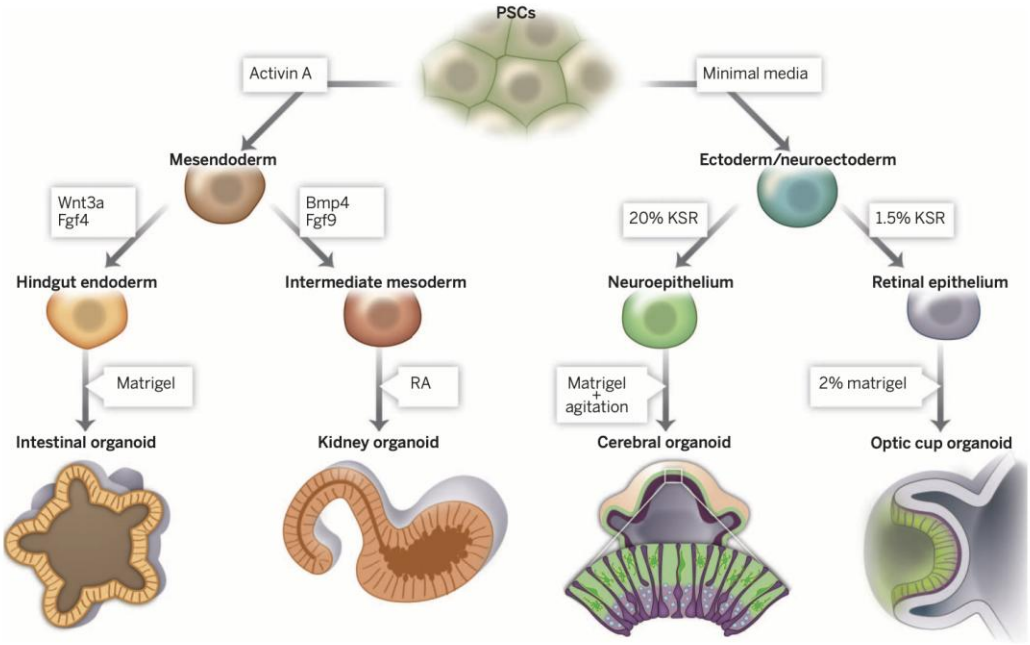

Fig. 9. Overview of organoid methodologies.

Using several factors, it is possible to induce different pathway of differentiation. [117].

Concerning the CNS, different types of 3D culture can be used: brain organotypic slices, neurospheroids and organoids.

3.7.1 Brain Organotypic Slices

Brain organotypic slides are referred to sliced brain usually obtained from young animals (around P3 and P10) and rarely from adult tissue. The age of the donor is really important, because this technique is well established for tissue from embryos, besides they survive better and increase the size [118]. Slides can be obtained from

any parts of the brain, but the more studied regions are subgranular zone of the hippocampus (SGZ) in the dentate gyrus and the subventricular zone (SVZ) of the lateral ventricle in the olfactory bulb, because it is where the adult neurogenesis takes place. Moreover, in order to promote the neurogenesis, slides are kept on a semiporous membrane in the air-liquid interface [119]. Furthermore, it has been reported that the brain slides in the presence of brain capillary were able to release important molecules for brain survival and development in absence of an active circulation [120].

Although some papers have been published on adult organotypic mice brain and some promising results have been achieved, these studies were performed for a very short-living period, thus neurodegenerative disease with an adult onset are difficult to study with this method. Moreover, but there are several obstacles that need to be overcome, such as for example the long-term culture of adult brain slides, the improvement of the method to obtain adult brain slides and the reconstruction of vascular system with the BBB.

3.7.2 Neurospheroids

Neurospheroids are an *in vitro* system composed by free-floating cluster of embryonic or adult neural stem cells maintained in a neuronal media, containing either N2 and/or B27 with growing factors, such as basic fibroblast growing factor (bFGF) and epiderma growth factor (EGF). Neurospheroids can be fate-induced by modulating specific pathways and they could contain different type of

neuronal cells, such as neurons, astrocytes and oligodendrocytes [121]. This type of technology is commonly used to drug screening and disease modelling. Nowadays, neurospheroids are obtained through the isolation of primary rat or mice cortex and maintained in culture for several weeks. After the dissociation, they are able to aggregate and self-organized [122]. In literature are present different protocols to obtain this type of culture, the more recent is called SFEBq (serum-free culture of embryoid body-like aggregates) and it was published from Eiraku and collaborators [123]. In this study, authors modified the SFEBq technique by adding Matrigel (aliminin-rich extracellular matrix) demonstrating the capability of neurosphere (derived from mice or humans embryonic stem cells) to form neural rosette and differentiate into cortical progenitors with functional projections, presenting also an apico-basal polarization and developing cortical tissue with four different zones (ventricular, early and late cortical plate, and an outer zone containing Cajal–Retzius cells) and, if no inhibitors of neural differentiation are added to the media, acquiring rostral hypothalamic-like fate. Furthermore, neurospheroids presented spontaneous electrical activity and are able to make synaptogenesis [124].

Moreover, Eiraku and colleagues affirmed that, using SFEBq method, were able to mimic the early corticogenesis *in vitro* [123]. Another study confirms the fact that neurospheroids behaved in the same way of the tissue from where they derived [125]. It seems that not only the developmental age influences the proliferation ability of the cells, but also the region of origin could partially impact on their differentiation capacity [126,127].

As all technologies, also neurospheroids have pros and cons. This method is a great tool to study neural stem cell biology, such as the ability to self-renewal and proliferation. They could be used to study neurogenesis, neurodevelopment and neurodegenerative disease, thanks to their ability to recapitulate the disease phenotype. Neurospheroids have been used for different purposes, such as study the origin and the role of tumour stem cells [128] and investigate neurodegenerative diseases, such as Parkinson's disease (PD) and Alzheimer's disease (AD). Last year, Chen and colleagues, have improved an already existing protocol to generate neurosphere for AD in order to analyse proteomic expression between neurospheroids with different derivation and phenotype. Results showed a dysfunction in metabolism of different proteins, some of them involved in axon transport [129]. In the same year, also Jorfi's group generated neurospheroids for modelling AD modifying the already existing protocol in order to obtain homogenous cultures (same size, cell density, rate of differentiation and cell composition) [122]. This model was also used to study peripheral nerve regeneration, because of the better neurite outgrowth in 3D culture compared to 2D [130].

Concerning the cons, although efforts made to avoid this issue, these type of culture are heterogenous, not only in size, but also in the stage of differentiation and in cell composition. Indeed, they are sensitive to even small variation, such as for instance the cell density, the passage or the medium composition. As a matter of fact, Gabay and colleagues demonstrated that the addition of bFGF in the media was able to induce the differentiation of the cells into neurons,

oligodendrocytes or astrocytes, whereas *in vivo* bFGF induces the differentiation only in the last two type of cells [131] (Gabay et al., 2003).

Thus, it is really challenging to reproduce and consolidate the data obtained not only between different studies, but even between different batches [132].

3.7.3 Organoids

The need to create a more effective and tissue-like *in vitro* model for neuroscience application and for the study of human brain complexity leads to the development in 2013 of the first model of cerebral organoid that was established to study microcephaly [133].

The huge difference between organoids and neurospheroids is that the first model can recapitulate different brain regions and the neural progenitor can differentiate into complete mature neuronal cells giving new insights into brain development both in physiological and pathological conditions.

Other aspects that distinguish organoids from neurospheroids are self-organization and self-assembly without the use of any exogenous factor.

Nowadays, organoids are used not only to study organogenesis, but also for drug screening. For instance, Watanabe and collaborators, studied organoids in order to develop an effective treatment for Zika

virus infection. Results showed that the majority of genes activated after infection have a role in antiviral or anti-inflammatory pathway [134]. Another group, Takasato and colleagues, tested the toxicity of cisplatin in kidney organoids. This type of organoids contained all the major features of a kidney, such as nephrons and ducts with interstitium and endothelial cells [135].

Despite all advantages that this method provided, a quite fundamental limitation has to be overpass, which is the lack of vascularization. Indeed, the absence of blood vessel prevents the delivery of small molecules and oxygen deep in the organoids, more often resulting in necrosis in the centre of the organoids [136].

At the present days, different types of healthy organoids have been generated, such as lung, gastric, intestinal, liver, pancreas, kidney, prostate, retina and brain.

3.7.3.1 THE NEOCORTEX

In nature the most fascinating biological process is neurodevelopment, due to the fact that the nervous system is a really complex system and it is at the base of survival.

Neurodevelopment could be divided into two processes: on one side neurogenesis, which consists in the migration and differentiation of neuronal cells, dendrite and axons formation, neuronal network formation and synaptogenesis; on the other side non-neuronal

processes, which involved myelinization, angiogenesis and generation of the BBB.

In the brain, the neocortex has the most important role. It is made from six layers of cells and it is in charge of different and complex functions such as generation of motor control, sensory and spatial perception, cognition and language. Human neocortex is highly specialized and evolved through the millennia; for this reason, the animal model, although really useful in other cases, cannot provide a valuable model to study human neurogenesis. Neocortex is composed by a variety of types of cells and can be classified horizontally into six different areas, also called layers, where the first is the outermost and the sixth is the innermost and each of them have specific function, from the processing of different stimuli, to the cytoarchitecture; it can also be divided according the function in a vertical way called columns [137] (Fig. 10).

Cortical neurogenesis occurs in a specific temporal sequence between the 5th gestational week and ends around the 20th [138]. As mentioned above, the pattern followed by migrating cells is the inside-out, where the deep layer is generated first (VI layer) followed by those of the upper layer (V, IV, III, II and I layer) [139,140].

Concerning the subtypes of neurons presented in the cerebral cortex, they are extremely heterogeneous and not all of them are classified yet or known. Generally, we can classify them into two groups: excitatory pyramidal (or projection) neurons (PNs) and inhibitory local cortical interneurons (INs) in accordance to their neurite target. PNs represent about 80% of cortical neurons and they are able to project

their neurite to distant cortical, subcortical and subcerebral cells. On the other side, cortical interneurons represent the last 20% of neurons and their role is to make local connection within the cortex.

When neurogenesis starts, neuroepithelial (NE) cells become neuronal progenitors and give rise to radial glia cells (RGCs), which further expands in the ventricle in the ventricular zone (VZ). This type of cells can generate three different types of cells, such as intermediate progenitors (IPs), outer RGs and PNs. Among the aforementioned progenitors (NE, RGCs and IPCs) in the cortex is present another one, which is called subapical progenitors (SAPs) and it is located in the VZ [139,141].

Opposite to PNs development, cortical INs are generated outside the cortex, within the medial and caudal ganglionic eminence (MGE and CGE) and the preoptic area (POA) by ventrally located progenitors [142–144]. From this area, they tangentially migrate through the subventricular zone (SVZ) and marginal zone (MZ) to rich the cortical plate.

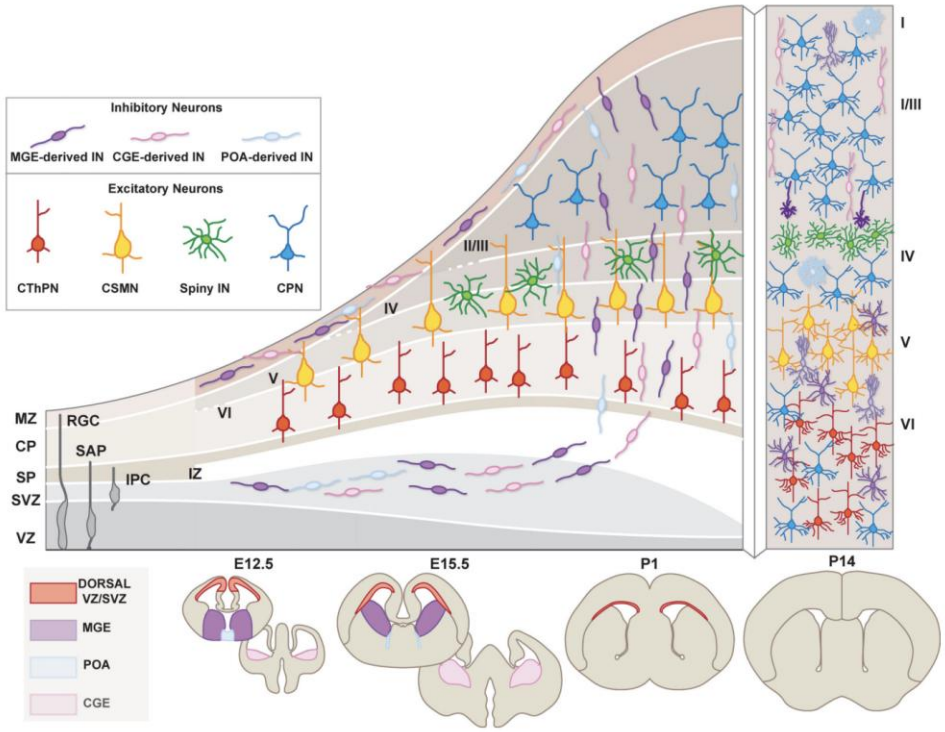

Fig. 10. Schematic representation of cortical layers and cell types.

During the embryogenesis, neurons are self-organized in specific layers. In each layer is present a specific cell type population. [145]

3.7.3.2 CEREBRAL ORGANOIDS

For centuries, neurobiologists, and in particular developmental ones, have tried to study the human brain formation and complexity through different approaches. Lately, the development of new 3D *in vitro* models has extremely helped neuroscientist and provided a great benefit to the field of neurodevelopment studies.

Brain organoids formation is a relatively new technique, but the protocol has rapidly evolved since the 2013. Indeed, after the generation in 2008 of neurospheres, in 2013 Lancaster and Knoblich discovered that embryoid bodies (EBs) left in Matrigel without any kind of factor to promote regional identity, displayed larger neuroepithelial buds that spontaneously generated multiple brain regions [133]. This research led to an increasing study of cerebral organoids as a neurodevelopment model.

Cerebral organoids (also called “mini-brains”) can grow up to 4 mm in diameter within 60 days, thus, besides the use of Matrigel (used as a scaffold), they need continuous and sufficient oxygenation; for this reason, Lancaster and collaborators placed cerebral organoids in spinning reactor. In this way, they showed more extended surrounding neuroepithelium. After ten days neural progenitors started to form inside the cerebral organoids, and after one-month, specific brain regions, such as cerebral cortex, plexi, meninges and retina appeared.

Although the use of the spinning flask, when the aggregates reach conspicuous size, due to the lack of a circulatory system, they started

to show necrosis within the centre. Moreover, the absence of circulation could interfere with some pathways necessary for cerebral organoids to develop and progenitor differentiation. Indeed, *in vivo* in the latest stages of development niches of neural progenitors are placed in proximity to vessels.

It has been suggested that the combination between microfluidic technology and organoid culture, may overcome this issue. For instance, endothelial cells could be cultured inside the microfluidic channels, thus modelling angiogenesis inside the brain organoids [146,147]. Another strategy was the embedding of iPSC-derived endothelial cells into the Matrigel droplets containing organoids [148]. Results showed a robust vascularization of the organoids within 5 weeks.

Mansour and collaborators engrafted cerebral organoids inside adult mice brain to promote the vascularization. Data showed an improvement in the viability and synaptic connectivity, and the formation of a microvascular network in the grafted organoids [149].

Although the problem of vascularization, cerebral organoids, are able over time to acquire a complete mature identity. Indeed, RT-PCR analyses confirmed the downregulation of pluripotency markers and the upregulation of region-specific markers, such as *BF1* and *Six3* for the forebrain and *Krox20* and *Isl1* for hindbrain [133]. These data were confirmed also through immunohistochemical analysis. Cerebral organoids showed also a sub-regional organization, with the presence of interneurons. The most interesting part, was the spatial separation displayed by organoids, in fact it was possible to identify a

lower ($Ctip2^+$) and upper ($Satb2^+$) layer, although they did not show any stereotypical II-VI layers organization, maybe due to the lack of later spatial organization into the cortical plate.

In 2017, Renner and collaborators, performed several experiments to better characterize cerebral organoids [150]. Results showed that “mini-brains” displayed the spatial and temporal pathway events that govern also human brain development *in vivo*.

Lancaster and collaborators tested also the electrical activity of brain organoids through the use of Calcium dye live imaging. Results showed a spontaneous calcium basal activity, which was promoted using exogenous glutamate and inhibit by the administration of tetrodotoxin administration [133].

Many are the studies have been performed to ameliorate the brain organoids protocol. For instance, Qian et al., identified a new method using specific pattering-factors in order to produce large numbers of organoids with the minimum variability among them [151]. Lee and collaborators developed brain organoids able to recapitulate all the stages of cortical development [152]. In this study, they generated neocortical organoids through the administration of SMAD and FGF inhibiting factors and the harvesting of single rosette-like structure. At late stages, organoids displayed typical neocortical feature.

Although it is known that cerebral organoids are able to self-organized and differentiate into different brain area, there is still a gap in the fully understanding of cellular composition of them and of their potential to create a functional neural network. For this reason,

Quadrato et al., studied the composition through droplet-based single-cell mRNA sequencing (Drop-seq) [153]. They analysed 31 organoids cultured in different bioreactors for over 9 months, modifying the already existing protocol in order to obtain the minimum level of hypoxia and cell death. Single-cell analysis was performed on organoids at different time points, one, three and six months. On the first months they displayed the formation of different brain regions, such as forebrain, midbrain, hindbrain and retina. At six months of age, seven clusters of cells were identified. Only one of them belonged to the mesodermal lineage and the rest had neuroectodermal origin. The six clusters were composed by cluster c2 which contained cells expressing astrocytes markers (Aquaporin 4 (AQP4) and GFAP), cluster c3 was composed by dopaminergic neurons (expressing tyrosine hydrolase (TH) and Early B-cell factor 1 (EBF1)), cluster c4 with neurons and precursor of cerebral cortex (in particular, PNs corticofugal and callosal, radial glial and interneurons), cluster c5 with retinal neurons, cluster c9 with oligodendrocyte precursor-like identity and cluster c10 with highly proliferative progenitors. The majority of these clusters were present in all organoids, indicating that there is a sort of reproducibility among them, although they were grown in different bioreactors. Regarding the three months old organoids analyses, data showed some cluster in common with older ones, but they did not present more mature cell types, such as callosal neurons, which are typical of late corticogenesis. Moreover, in six months organoids they could find dendrites and spines able to connect to one another. Electrophysiological analysis revealed spontaneous neuronal activity,

and light test, performed to verify whereas the organoids could be stimulated by light, showed that a small but specific subset of neurons was responsive by diminishing their firing rate [154].

All these studies demonstrated that 3D brain organoids have not only the capability to self-organize in some specific regions of the brain, but also to model high-order functions of human brain, such as neural circuit and cellular interaction.

Other interesting studies have been performed by Pasca laboratory [155,156]. They first generated from human pluripotent stem cell both dorsal (palladium) and ventral (subpalladium) forebrain spheroids, which contained cortical glutamatergic and GABAergic neurons respectively, and subsequently they placed them together in order to mimic the saltatory migration of interneurons. Results showed that interneurons not only were able to migrate toward the cerebral cortex, but they could also form a micro-physiological system integrating with glutamatergic neurons.

Many were the regional identities that many groups have engineered, such as dorsal cortex [157], ventral forebrain [158,159], midbrain and hindbrain [151,160,161], choroid plexus [162], hypothalamus and hippocampus [151,162].

3.7.3.2.1 Cerebral Organoids to Model Diseases

For all the characteristic reported in the previous paragraph, brain organoids could be used to study both the neurodevelopmental disorder, which it has been difficult to do in animal model, and to model neurodegenerative diseases.

Brain organoids have been already used to model disorders such as microcephaly, autism, schizophrenia and adult onset disorders like Alzheimer's disease (AD), frontotemporal dementia (FTD) and Parkinson's disease (PD).

Microcephaly is an autosomal recessive disorder characterized by reduced brain size. Many genes are involved in this disorder, and the majority of them have a role in mitotic division. Lancaster et al., 2013 used organoids to mimic this disease [133]. They used cells deriving from patients with CDK5 Regulatory Subunit Associated Protein 2 (CDK5RAP2) mutation. Results showed not only a reduced size of affected organoids, but also a decrease in neuroepithelium formation and a reduced number of regions containing neural progenitors compared to the control. They also demonstrated that they could rescue the phenotype through the electroporation of CDK5RAP2. Indeed, electroporated cerebral organoids presented a larger neuroepithelium and a normal organization of radial glia.

Microcephaly could be also caused by the infection of Zika virus of pregnant women. For this reason, some studies were published using infected organoids with Zika virus [163,164]. In accordance with Lancaster study, Zika infected organoids presented not only a reduce

size but also a premature death of neural progenitors, a decrease of $Tbr1^+$ and $CTIP2^+$ cells, indicating a reduced presence of cortical cells and a lower mitotic activity.

Autism is a spectrum disorder, which means that the symptoms could present in a wide variety of combination. It is a developmental disorder that impairs communication and behaviour of the affected subject. The cause is still unknown due to the lack of a proper model to study this disorder, the only information that we have derived from post-mortem and magnetic resonance imaging (MRI). The advent of organoids changed this field. For the first time organoids to study autism were generated from Mariani and collaborators. These organoids did not present genomic mutations, but an upregulation of genes involved in cell-cycle, differentiation and synaptogenesis. In particular results showed an overproduction of GABAergic neurons also confirmed by electrophysiological analysis [165]. This data is in line with the findings in post-mortem tissue, indicating that nowadays, cerebral organoids represent the best option to study autism.

Regarding disorder with an adult onset, AD is a chronic neurodegenerative disease. One of the groups that tested 3D culture as model is the one of Raja and colleagues. In this study, they developed patient-derived cerebral organoids with early familial onset of AD. Organoids were able to recapitulate the disease phenotype; indeed, results showed the presence of β-amyloid aggregation, hyperphosphorylated tau proteins and abnormalities in endosomes similar to those in the mouse model [166]. Moreover, they demonstrated that the treatment with β-secretase and γ-secretase

inhibitor could reverse the phenotype. Same results were obtained in other studies [167,168].

PD is another long-term neurodegenerative disease, whose exact cause is still unknown. However, based on neuropathological findings, it seems to be caused by toxic aggregation of α-synuclein, which is able to propagate through the brainstem. Among the genetic mutation that can cause PD, the most common genetic variant is LRRK2 (variant G2019S, N551K, N2081D). Studies performed on PD midbrain organoids showed α-synuclein aggregation and mislocalization, besides the fact the presence of dopaminergic neurons was 3-fold less compare with the controls [169,170]. Midbrain organoids also showed the typical neuropathological hallmarks of PD thus they can be used as a tool to study the pathway involved in the pathogenesis.

In conclusion, several types of organoids using different protocol have been generated to induce the formation of region-specific organoids. Brain organoids can be used not only to study the neurodevelopment in physiological conditions, but also to study neurodegenerative disease.

In the following table is schematizing the specific brain organoids to study *in vitro* neurobiology and disease modelling. Understanding the development and dysfunction of the human brain is a major goal of neurobiology. Recent advances in stem cell technologies that enable the generation of human brain organoids from pluripotent stem cell will likely profoundly change our understanding of the development of

the human brain and enable a detailed study of the pathogenesis of inherited and acquired brain diseases.

Type of organoid	Aspect of neurobiology studied	Disease modeled/potential application	Mechanisms revealed	References
Cerebral/early brain organoids	-Neural progenitor maintenance	-Genetically caused microcephaly	-Premature differentiation of neural progenitors	[4–6,51]
	-Corticogenesis	-Zika virus mediated microcephaly	-Neural progenitor depletion and cell death	
	-Neural migration	-Miller–Dieker syndrome	-Disrupted microtubule network	
Midbrain organoids	-Differentiation of dopaminergic neurons and neuromelanin-containing neurons	-Potential to model Parkinson's disease	-Not yet used for disease modeling	[52,53]
Hypothalamus organoids	-Differentiation of hypothalamic neurons and POMC-positive peptidergic neurons	-Potential to model hormonal and metabolic disorders including Prader–Willi syndrome	-Not yet used for disease modeling	[38]
Adenohypophysis organoids	-Generation of Lim3-positive pituitary progenitors	-Potential to model pituitary dysfunction	-Not yet used for disease modeling	[54]
Hippocampus organoids	-Dorsomedial telencephalon development	-Potential to model cognitive dysfunctions due to Alzheimer's disease	-Not yet used for disease modeling	[55]
	-Choroid plexus development			
Cerebellum organoids	-Cerebellum development	-Potential to model SCA and Dandy–Walker syndrome	-Purkinje neurons are vulnerable to triiodothyronine depletion	[56,57]
	-Differentiation of Purkinje neurons			
Dorsaltelencephalon organoids	-FOXG1-positive forebrain development	-ASD	- Imbalance between GABAergic and glutamatergic neuronal fates	[14]
Forebrain assembloids	-Interneuron migration and circuit formation	-Timothy syndrome	-Abnormal saltatory migration	[3]
Photosensitive organoids	-Vast diversity of cells and network activities of neurons	-Potential to model disorders of mature brain	-Dendritic spines and spontaneously active neuronal networks	[11]
Retinal organoids	-Retinal pigment epithelia development	-Neuroretinal disorders and retinal dystrophy due to ciliary defects	-Impaired ciliogenesis	[58]
	-Rod and cone cell development	-Potential to model wide range of neural retina disorders and retinitis pigmentosa		

Table 4. Summary of region-specific brain organoids that could be generated using different signalling molecules. [171]**.**

3.7.3.3 Spinal Organoids

Unfortunately, there are limited studies to date that uses spinal organoids to model MNDs, indeed in literature there are only two studies.

Kawada and collaborators [172] took advantage from microfluidic technology to generate axon fascicles from neural spheres. Their protocol was based on the differentiation of iPSCs into MNs prior to neural sphere formation, using retinoic acid, Smoothened and FGFR antagonist. Results showed around 60% of cells positive to classical MNs markers (such as HB9), a small fraction of cells expressed astrocytes marker (GFAP) and no expression of oligodendrocytes or neuronal stem cell marker. Subsequently, neurospheres were placed in the recipient chamber and axons started to grow spontaneously in the microchannels; by 20 days, a single straight and unidirectional axons were generated. Fascicles were positive both for axonal marker, such as Tau1 and presynaptic marker, such as synapsin1. Moreover, electrophysiological activity was recorded.

Another group generated ventral spinal cord organoids to study spinal muscular atrophy [173]. In this study, they used a different protocol, generating organoids form both control and SMA Type I and II patients by adding small molecules, growing factors, Retinoic Acid and Sonic Hedgehog and Matrigel as scaffold. Although, they showed interesting results, such as the capability of these organoids to develop neural rosette and synapsis, there are still a lot of gap to fill in. For instance, they cultured organoids for a short period (35 days). Moreover, they obtain only the ventral part of the spinal cord, leading to a problem with the definition of organoids, because their model did not represent the all spinal cord.

For these reasons, it is still necessary to study and generate a better 3D model for spinal cord. the biggest issue is represented by the lack

of an establish gradient of caudal and ventral differentiation factors for the generation of a faithful model, although the structure of the spinal cord is relatively easy compared to the brain.

4. MATERIAL AND METHOD

4.1 Generation and Characterization of Induce Pluripotent Stem Cells (iPSCs)

A total of 3 controls and 3 SMA type 1 human pluripotent stem cell lines were used. 1 control (C1) and 1 SMA type 1 (S3) were provided by Cesar Sinai Biobank. Meanwhile, the other 2 controls (C2 and C3) and 2 SMA type 1 (S1 and S2) were reprogrammed from human skin biopsy fibroblasts using CytoTune-iPS Sendai 2.0 Reprogramming kit (Thermo Fisher) (See Table 5).

This kit uses modified, non-integrating Sendai viruses which carry the four Yamanaka factors, Oct3/4, Sox2, Klf4, and L-Myc. Human Fibroblasts were plated on a 6-well plate (Sarsted) using fibroblasts media (DMEM with 15% of fetal bovine serum (FBS, Euroclone). Reached 80% confluency, cells were transduced using the CytoTune™ 2.0 Sendai Reprogramming vectors and 24 hours later, media was replaced. Culture media was changed every other day. On day 5, trypsin (Thermo Fisher Scientific) was used to harvest transduced fibroblasts and plated on a 6-well plated, previously coated with human embryonic feeder (ATCC® SCRC-1041™, HFF-1). At day 8, fibroblast media was replaced by iPSCs specific medium, Essential 8 (E8, Life Technologies). When iPSC colonies began to appear, they were manually picked and transferred into 6-well plate covered with Cultrex® Stem Cell Qualified Reduced Growth Factor Basement Membrane Extract PathClear® (Cultrex BME, Tema Ricerca).

All iPSCs were cultured in feeder-free conditions on Cultrex-coated 6-well plate costars, using E8 medium at 37°C in 5% CO_2. This study was conducted in compliance with the Code of Ethics of the World Medical Association (Declaration of Helsinki) and with national legislation and institutional guidelines. Ethical committee approved the use of these samples at the IRCCS Foundation Ca' Granda Ospedale Maggiore Policlinico.

iPSCs line	Diagnosis	Sex	Age	Reprogramming strategy
Ctrl1	Healthy donor	Male	Newborn	Episomial 6factors:OSKM+LN
Ctrl2	Healthy donor	Male	34 years old	CytoTune-iPS Sendai
Ctrl3	Healthy donor	Male	67 years old	CytoTune-iPS Sendai
S1	SMA type 1	Male	Newborn	CytoTune-iPS Sendai
S2	SMA type 1	Male	3 years old	Episiomal 6factors:OSKM+LN
S3	SMA type 1	Male	7 months	Episomial 6factors:OSKM+LN

Table 5. List of cell lines used for the study.

Ctrl: control, SMA: Spinal Muscular atrophy.

4.2 Generation of Organoids

To generate brain organoids and spinal cord like-spheroids, we used and readapted an already published protocol. For brain organoids we followed Lancaster protocol [133], meanwhile for the generation of spinal cord like spheroids we developed a new protocol. Indeed, at the time of institution of this study, no protocols for the generation of spinal cord like spheroids were published yet.

At the beginning, the medium to generate organoids is similar to brain organoids and spinal cord like spheroids, only from differentiation day 6, in the spinal cord like spheroids, we started to add specific molecules to induce the activation of dorsal-ventralization pathway.

In particular, on day 0, human iPSCs (80-90% confluency) were dissociated using first EDTA (Life Technologies) for 4 minutes at 37°C and afterward Accutase (GIBCO) for an additional 4 minutes at 37°C. In order to inactivate the Accutase a double volume of E8 media containing Rock inhibitor (Y-27632, Millipore) was added. Subsequently cells were centrifuged at 270g for 5 minutes.

Cells were counted using Trypan Blu and Bürker chamber. The following formula was applied:

$$\frac{Total\ number\ of\ counted\ cells}{Number\ of\ counted\ squares} * Volume\ of\ resuspension\ (ml) * Dilution\ factor * 10^4$$

Obtained the number of the total cells, we used the following formula:

$$\left[\frac{Total\ number\ of\ cells}{Volume\ of\ resuspension\ (ml)}\right] * Vi = \left[\frac{9000\ cells}{150\ \mu l}\right] * 15\ ml$$

9,000 cells per well were seeded in ultra-low-attachment 96-well plates with U-bottomed wells (Corning) in HES media with 4ng/ml bFGF (Sigma-Aldrich), 50uM Rock Inhibitor.

- **Media Composition:**

HES media composition: 80% Dulbecco's modified Eagle's medium (DMEM)/F-12 (Life Technologies), 20% Knockout Serum Replacement (KOSR) (Gibco), 3% Fetal Bovine Serum (FBS, Euroclone), 1% GlutaMax supplement (100X Life Technologies), 1% Minimum Essential Medium non-essential amino acids (MEM-NEAA) (Gibco), 0.3% 2-Mercaptoethanol (BME, 50mM, Life Technologies) and 1% penicillin-streptomycin (LONZA).

Neural Induction media (NIM): DMEM-F12; 1% N2 supplement (Life Technologies); 1% Glutamax supplement (100X life Technologies); 1% MEM-NEAA (Gibco) and Heparin (final Concentration 1µg/ml).

CNS organoid differentiation media 1: 50% DMEM-F12, 50% Neurobasal (Life Technologies), 0.5% N2 supplement (Life Technologies), 0.025% Insulin (SIGMA), 1% Glutamax supplement, 0.5% MEM-NEAA, 1% penicillin-streptomycin, 0.3% BME, 1% B27 supplement without vitamin A (Life Technologies).

CNS organoid differentiation media 2: 50% DMEM-F12, 50% Neurobasal (Life Technologies), 0.5% N2 supplement (Life

Technologies), 0.025% Insulin (SIGMA), 1% Glutamax supplement, 0.5% MEM-NEAA, 1% penicillin-streptomycin, 0.3% BME, 1% B27 supplement with vitamin A (Life Technologies).

4.2.1 Brain Organoids Generation

The specific protocol used to develop brain organoids is set out below:

- **Day 2:** Half of media were removed and double volume of fresh media plus 4 ng/ml Basic fibroblast growth factor (bFGF, Sigma-Aldrich) and 50 μM Rock Inhibitor was added.
- **Day 4:** Half of the media was changed and double volume of fresh media were added. At this time bFGF and Rock Inhibitor were no longer added to the media.
- **Day 6:** Embryoid bodies (Ebs) were transferred into ultra-low attachment 24-well plates (Corning) using a 200 µl pipette with cut tip. At this stage we used as media NIM.
- **Day 8:** 1:1 Volume of fresh NIM media was added.
- **Day 10:** 90% of the media was changed and replaced with fresh media.
- **Day 12:** Media was changed as previously described.

- **Day 13/14:** Ebs were embedded in Cultrex® Basement Membrane Matrix, Type 2 (BME type 2, Tema Ricerca) droplets and placed at 37°C for 20 minutes. Once solidified, 7 ml of CNS organoid differentiation media 1 were added. 16 organoids were placed per each 60cm dish.

- **Day 16:** All the culture media was changed.

- **Day 18:** Organoids were transferred into spinning bioreactors (Corning). The number of organoids placed in each bioreactor changed based on their volume. In 125 ml bioreactors around 32 organoids could be added, meanwhile the 250 ml could contain around 60 organoids. The media used was CNS organoid differentiation media 2.

After one week the media was change. After the first change, media was replaced every 10 days. The speed of the spinning bioreactors was 45 r.p.m. Organoids were collected for analysis at day 25, 50 and 90.

4.2.2 Spinal Cord-Like Spheroids Generation

The specific protocol that was used to develop spinal cord like-spheroids is set out below:

- **Day 2:** Half of media were removed and double of fresh media containing 4 ng/ml bFGF, 50 μM Rock Inhibitor and cytokines, such as 3μM CHIR 99021 (GSK3 inhibitor, Sigma-Adrich), 2 μM SB 431542 (Activin/BMP/TGF-β pathway inhibitor, Sigma-Aldrich) and 0.2 μM LDN 193189 (inhibitor of the bone morphogenetic (BMP) pathway, Stemgent).

- **Day 4:** Half of the media was changed and fresh media was added. Cytokines were added in the media, without bFGF and Rock Inhibitor.

- **Day 6:** Ebs were transferred into ultra-low attachment 24-well plates (Corning) using a 200 μl pipette with cut tip. At this stage we used NIM plus cytokines. In order to induce dorsal-ventral pattern, 100 nM of Retinoic Acid (RA, Sigma-Aldrich) was also added in the media.

- **Day 8:** 1:1 Volume of fresh NIM media was added. RA was kept in the media, but Cytokines were no longer added.

- **Day 10:** 90% of the media was changed and replaced with fresh media. RA was added.

- **Day 12:** Media was changed as previously described. At this time in order to induce the ventralization of the spheroids, 1 μM Smoothened Agonist (SAG, Calbiochem) was added in the media. Since now, RA and SAG were always added in the media at the previous mentioned concentration.

- **Day 13/14:** Ebs were embedded in Cultrex® Basement Membrane Matrix, Type 2 (BME type 2, Tema Ricerca) droplets and placed at 37°C for 20 minutes. Once solidified 7 ml of CNS organoid differentiation media 1 were added. 16 organoids were placed per each 60 cm dish. RA and SAG were added.

- **Day 16:** All the culture media was changed. RA and SAG were added.

- **Day 18:** Spheroids were transferred into spinning bioreactors (CORNING). The number of organoids placed in each bioreactor changed based on their volume. In 125 ml bioreactors around 32 organoids could be added, meanwhile the 250 ml could contain around 60 organoids. The media used was CNS organoid differentiation media 2. RA and SAG were added

After one week the media was change. After the first change, media was replaced every 10 days.

- **From Day 28 on:** CNS organoid media 2 was used, concentrations of RA and SAG were halved and 10 ng/ml of growth factors such as brain-derived neurotrophic factor

(BDNF, Peprotech), insulin-like growth factor 2 (IGF2, Sigma-Adrich) and glial cell-derived neurotrophic factor (GDNF, Peprotech) were added.

The speed of the spinning bioreactors was 45 r.p.m. Spinal cord-like spheroids were collected for analysis at day 25, 50 and 90.

4.3 Characterization Of Brain Organoids And Spinal Cord-Like Spheroids

4.3.1 Immunohistochemistry For 3D Culture

Selected organoids or spheroids were washed with PBS 1X and fixed with 4% paraformaldehyde for 15 minutes at 4C, followed by washing in PBS 1X three times for 5min each. Tissues were placed in eppendorf tube with 30% sucrose overnight at 4°C. The next day, organoids or spheroids were embedded in 10%-7.5% gelatin/sucrose as following: a thin layer of gelatin was placed in the mold in order to cover the bottom and let them solidify at 4°C. Subsequently organoids or spheroids were placed at the center of the mold and covered with a thick layer of gelatin. Thereafter gelatin bulk was cut with a scalpel to obtain a pointy shape (the point indicates where the organoid or spheroid is placed) and then they were immersed in cold isopropanol (between -20°C and -30°C) for 45 seconds. Organoids or spheroids were then placed at -80°C overnight and cryosectioning at 10 µm. Slides were kept at -20°C freezer before being stained.

Sections were permeabilized for 1 hour in PBS 1X with 0.3% Tryton-X (Sigma) and 10% donkey serum (Jackson Innunoresearch) at room temperature. Subsequently, primary antibody was diluted in fresh permeabilized solution (for the dilution see the table of the antibodies) and placed on top of slides in order to cover all sections. These were kept overnight at 4°C. The following day, slides were washed with PBS 1x 3 times for 5 minutes each. Secondary antibodies were added with DAPI (1:500, Sigma-Aldrich) in PBS 1X for 90 minutes at room temperature. Secondary antibodies used were donkey AlexaFluor 488, 594 and 647 conjugates (1:1000, Invitrogen). Slides were washed in PBS 1X 3 times for 5 minutes each. DAKO mounting media (DAKO) was used to mount coverglasses and slides were preserved at -20°C.

4.3.2 Immunohistochemistry For 2D Culture

For immunostaining analysis of 2D culture, cells on coverslips were washed carefully once with PBS 1X and fixed using 4% paraformaldehyde 6 minutes at room temperature, followed by three washes with PBS 1X. In order to permeabilized the cells, PBS 1X with 0.2% Tryton-X (Sigma) and 10% donkey serum (Jackson Immunoresearch) was used and added on the coverslip for 1h at room temperature.

Thereafter, primary antibody was diluted in fresh permeabilized solution (for the dilution see the table of the antibodies, table 4), and

added on the coverslips, which was placed at 4°C overnight. The following day coverslips were washed three times with PBS 1X. Subsequently cells on the coverslips were covered with the secondary antibody (Alexa Fluor®, Thermo Fisher Scientific, 1:1000) and DAPI (1:500), previously diluted in PBS 1X with 0.1% Tryton-X and 5% donkey serum. This solution was left for 90 minutes at room temperature.

Afterwards, coverslips were washed three times in PBS 1X and mounted on slides using DAKO mounting media (DAKO) and preserved at -20°C.

4.3.3 Whole Mount Staining For 3D Culture

Selected organoids or spheroids were taken from the flask with a cut tip, subsequently washed in PBS 1X and then placed in Eppendorf tubes containing 4% paraformaldehyde on a spinning wheel at 4°C overnight. The day after, in order to remove the excess of paraformaldehyde, 5 times washes (10 minutes each) in PBS 1X were performed on the spinning wheel at room temperature.

Organoids or spheroids were permeabilized with 0.25% Tryton in PBS 1X for 15 minutes on the spinning wheel at room temperature. In order to prevent non-specific bindings of the antibodies organoids or spheroids were placed on the spinning wheel for 3 hours at room temperature in PBS 1X with 10% FBS and 0.5% serum of the same species as primary antibodies.

Primary antibodies were changed three times. The first time, they were diluted in PBS 1X with 5% FBS, 0.5% serum of the same species as primary antibodies and 0.1% Tryton, subsequently added to the Eppendorf containing the organoid or spheroid at room temperature on the spinning wheel. After 2 hours, primary antibodies were added for a second time. They were diluted in PBS 1X with 5% FBS and 0.5% of serum of the same species as primary antibodies and incubated at room temperature overnight on the spinning wheel. The third time, primary antibodies were diluted in PBS 1X with 5% FBS and 0,5% of serum of the same species as primary antibodies for 5 hours on the spinning wheel at room temperature. Afterward, organoids or spheroids were washed 6 times 5 minutes each in PBS 1X on the spinning wheel at room temperature. Secondary antibodies were diluted in the previous described solution for primary antibodies (PBS 1X with 5% FBS and 0,5% of serum) and incubated at room temperature overnight on the spinning wheel in the dark. The next day, organoids or spheroids were washed with PBS 1X 6 times, 15 minutes each on the spinning wheel at room temperature.

Meanwhile organoids or spheroids were washing, a small chamber with staples was made on the slide. Organoids or spheroids were placed in the middle of the chamber with PBS 1X. Afterward, PBS 1X was completely removed and mounting media was added avoiding bobbles. A square coverslip was added on top to seal the chamber.

Images were acquired with Nikon's A1 R MP+ multiphoton microscope by Alembic Facility (IRCCS Ospedale San Raffaele).

ANTIBODY	DILUTION
Sex-determining region Y-box 2 (SOX2), abcam, ab97959	1:100
BIII tubulin (Tuj1) Biolegend 801201	1:1000
Microtubule associated protein 2 (MAP2), Sigma Aldrich, M9942	1:100
Doublecortin (DCX), Abcam, ab18723	1:100
Forkhead box protein G1 (FOXG1), abcam, ab 18259	1:100
Special AT-rich sequence-binding protein 2 (SATB2), abcam ab 51502	1:100
Glial fibrillary acidic protein (GFAP), Sigma, G3893	1:100
Neurofilament H/SMI32, Abcam, ab8185	1:100
OLIG2, Sigma-Aldrich, SAB1404798	1:100
PAX6, Invitrogen, 42660	1:100
OCT-4, Thermofisher, 701756	1:100
S100 calcium-binding protein B (S100B), abcam, ab52642	1:100
HB9, DSHB, 81.5C10-s	1:50
NESTIN, abcam, ab27952	1:100
ChAT, Millipore, AB144P	1:250
CTIP2, abcam, ab18465	1:100

Table 4. List of antibodies used for Immunostaining and whole mount.

4.4 Dissociation

Brain organoids and spinal cord like spheroids were centrifuged at 300g for 5 minutes in a 15ml falcon tube to remove all the media. The supernatant was discarded, PBS 1X was added and they were centrifuged again with the same parameters. Supernatant was discarded and a solution of PBS 1X containing 1% of trypsin was added. The falcon tube was placed in the water bath at 37°C for 5 minutes. A double volume of Horse Serum (Euroclone) was used to inactivate the trypsin and the samples were centrifuged 300g for 3 minutes at room temperature. Cerebral organoid differentiation media 2 was added to the tube and the pellet was dissociated by pipetting vigorously up and down with a p1000 pipette.

Two days before dissociation 24-wells plates with coverslips were coated with poly-L-ornithine and laminin. 50 µg/ml poly-L-ornithine (Sigma-Aldrich) were resuspended in sterile water and incubated overnight at 37°C. The following day, poly-L-ornithine was removed and 20µg/ml natural mouse laminin (Sigma-Aldrich) were resuspended in DMEM/F12 (Thermo Fisher) and incubated for 4h at 37°C. Laminin was discarded and plates were washed twice with DMEM/F12.

After dissociation, 50.000 cells were seeded in each well using CNS organoid differentiation media 2 (in the case of spinal cord like spheroids were added also RA, SAG and growth factors at the same concentration of differentiation day 28). The media was changed every other day.

Immunostaining analysis were performed as describe in paragraph 4.3.2.

4.5 GENE EXPRESSION ANALYSIS

4.5.1 Matrigel Depolymerization

In order to study biochemical processes, it is necessary to separate organoids from their scaffold. For this purpose, we used Trevigen's Cultrex® Organoid Harvesting Solution (OHS, Tema Ricerca), a non-enzymatic method for the depolymerization of extracellular matrix proteins, as followed.

Organoids or spheroids were harvested and placed into 24-well plates on ice. Wells were washed 1 time with cold PBS 1X and next OHS was added. Costars were placed at 4°C on a shaker with moderate speed for at least 3 hours. When Cultrex scaffold was completely dissolved, organoids were collected separately in an Eppendorf tube and centrifuged at 500g for 5 minutes at 4°C. The supernatant was removed, the pellet was washed with cold PBS 1X and then centrifuged again with the same parameters. Once removed the supernatant, pellets could be used directly for RNA extraction or stored at - 80°C.

4.5.2 Real-Time PCR

Total RNAs was extracted from brain organoids and spinal cord-like spheroids pellets (previously stored at -80°C) using ReliaPrep™ RNA Cell Miniprep System (Promega). Total RNAs was eluted in 15 µL of nuclease-free water and we evaluate the concentration of RNAs using Nanodrop (Thermo Fisher Scientific). The reverse transcription was performed using SuperScript IV VILO Master Mix (Thermo Fisher Scientific). 150ng of template total RNA were retrotranscripted and blank RT was used as control reaction.

Different probes were used for brain organoids and spinal cord-like spheroids (for the specific probes see the table 5). For the assay, 96 well-plates (7500 Real Time PCR System, Applied Biosystem) and 384 well-plates (7900HT Fast Real-Time PCR System, Applied Biosystem) were used. 20 µl of total reaction volume were used for the 96 wells-plates and 10 µl were used for the 384 wells-plates. We used 5ng of cDNA and we run the experiment in triplicates. As blank we used blank RT as well as blank qPCR. GAPDH was considered as reference gene.

To analyze the data ΔΔCT method was used to calculate relative changes in gene expression. The thermal cycling condition was as followed:

Parameter	UNG incubation†	Polymerase activation‡	PCR (40 cycles)	
	Hold	Hold	Denature	Anneal/extend
Temperature	50°C	95°C	95°C	60°C
Time (mm:ss)	02:00	10:00	00:15	01:00

Statistical analyses were performed using *t*-test.

TYPE OF SAMPLE	GENE	COMPLETE NAME	PROBE
BRAIN	POU5F1 (OCT4)	Trascription factor with POU domain	Hs00742896_s1
BRAIN	TBR1	T-box, brain 1	Hs00232429_m1
BRAIN	BCL11B (CTIP2)	B-cell CLL/lymphoma 11B	Hs01102259_m1
BRAIN	FOXG1	forkhead box G1	Hs01850784_s1
BRAIN	PAX6	paired box 6	Hs00240871_m1
SPINAL	MAP2	microtubule-associated protein tau	Hs00258900_m1
SPINAL	CHAT	Choline O-Acetyltransferasi	Hs00252848_m1
SPINAL	MNX1 (HB9)	Motor neuron and pancreas homeobox type 1	Hs_00232128_m1
SPINAL	ISL1	Islet 1	Hs00158126_m1
SPINAL	OLIG2	oligodendrocyte transcription factor 2	Hs00300164_s1
BRAIN/SPINAL	TUJ1	Class 3 member of Beta-Tubulin family	Hs00801390_s1
BRAIN/SPINAL	SOX2	SRY (sex determining region Y)-box 2	Hs01053049_s1
BRAIN/SPINAL	GAPDH	glyceraldehyde-3-phosphate dehydrogenase	Hs99999905_m1

Table 5. List of qPCR probes.
List of the probes used for brain organoids and spinal cord like-spheroids q-PCR.

4.6 Calcium Imaging

Fluo-4 AM (Thermo fisher), a cell permeant assay, was used to image the spatial dynamics of Ca^{2+} signaling, in both brain organoids and spinal cord-like spheroids.

As a first step, DMSO was used to resuspend Fluo-4 powder to obtain a final concentration of 10mM. Selected organoids or spheroids were placed in 8 wells chamber (Sarsted), one in each well, and washed with PBS 1X without Ca^{2+} and Mg (Euroclone). A final concentration of 100 µM of Fluo-4 was diluted in opti-MEM (Thermo fisher) and added to the wells. Organoids or spheroids were placed at 37°C and incubated for 1 hour. Afterward, wells were washed 3 times with PBS 1X without Ca^{2+} and Mg. Organoids were incubated with pure opti-MEM for 30 minutes at 37°C. Calcium fluxes were visualized and acquired though a LED-illuminated automated widefield time-lapse microscope (Ti; Nikon), using both 4x and 20x dry objectives.

After 10 minutes evaluation, a Glutamate solution (100 µM in opti-MEM, Sigma-Aldrich) was added in order to stimulate organoids and spheroids and the subsequently changes were recorded for an additional 10 minutes. Imaging time-laps was acquired every 5 seconds for a total of 20 minutes recording.

Statistic was conducted using non-parametric Kruskal Wallis tests with an n=5 per each type.

4.7 Electrophysiology

High-density multielectrode array (HD-MEA) was used to record extracellular spontaneous activity of both brain organoids and spinal cord-like spheroids. This device consists of 4096 planar electrodes measuring 21µm x 21µm and placed in a 2,67mm x 2,67mm chip (Biocam X, 3Brain AG, Swiss).

Organoids and spheroids were situated on chip and a platinum anchor (with the same size of the chip) with nylon strings was used to keep them on place. Before and during recordings, organoids or spheroids were submerged in a fluid mimicking neuronal extracellular liquid (Kreb's solution), which was composed by: 120mM NaCl, 2mM KCl, 1.19mM MgSO4, 26mM NaHCO3, 1.18mM KH2PO4, 11mM glucose, 2mM CaCl2, oxygenized with a blend composed of 95% O2 - 5% CO2 to obtain a 7,4 pH (buffer CO2 /NaCHO3 which stabilizes pH). Organoids or spheroids were recorded at baseline for 15 minutes and afterward induction of stimuli with 100 µM of Glutamate (L-glutamic acid, Sigma-Aldrich) for an additional 15 minutes.

Some organoids were also tested using a mix of 10 µM gabazine and 1 µM strychnine (ABCAM), in order to block GABA-a and glycine receptors and evaluate the electrophysiological response. The effects were recorder for 15 minutes during the exposure.

Brainwave X (3Brain AG) software was used to register all signals coming from the chip at a sampling frequency of 17kHz. Spontaneous activity (registered as action potential) of single organoid or spheroid was recorded off-line. Brainwave 4 software

was used to both manually select channels which action potentials were clearly visible and identify action potential. The precise time spike detection (PTSD) algorithm was used to detect the spikes (the parameters used were: positive and negative peak, peak duration less than 1 ms, refractory period of at least 1ms and detection threshold set for signals at least 7 times higher than standard deviation of signal recorded without neural activity). In order to recognize artefact spikes sorting was used. To cluster the spikes K-means analysis (silhouette method) was used using the following parameters: maximum 3 cluster per electrode and 3 spikes per cluster.

Further and refine validation was performed by the researcher, indeed, all these signals were analyzed one by one, removing confounding signal. For the analysis were taken in consideration only electrodes presenting stable activity during the control period, which means for example without any fluctuations superior to 20% in spike frequency.

Statistical significance was assessed using paired or unpaired Student's t test. Data are reported as mean ± SEM (standard error of the mean).

4.8 RNA-seq

RNA-seq analyses were performed as service at Humanitas Hospital NGS facility.

Single cells from 2 affected SMA spinal cord-like spheroids were analyzed using the 10X Chromium system (10X Genomics). The cells were divided into Gel Beads-In-Emulsions and prepared using the single-cell 3′ mRNA kit (V3; 10X Genomics). Bioninformatics was performed at Humanitas hospital in Milan.

4.9 Statistical analyses

Continuous variables have been analysed through descriptive statistics and reported as mean±SD or median [IQR], as appropriate. Normality of distributions was visually inspected with box-plot representation and formally tested with the D'Agostino-Pearson and Shapiro-Wilk tests. Changes with respect to baseline have been analysed with paired t-test or Wilcoxon matched pairs signed rank test, as appropriate. Differences between groups have been analyzed with unpaired t-test or Mann-Whitney U-test (two groups), as appropriate. ANOVA or Kruskal-Wallis test were used for comparisons of more than two groups; appropriate follow-up tests for multiple comparisons (Tukey HSD) were used in case of significant differences. All p-values were two sided and statistical significance was assumed at the 5% level of probability. GraphPad Prism v.8 was used for all analyses.

5. RESULTS

5.1 Generation And Characterization Of Induce Pluripotent Stem Cells (iPSCs)

We generated and fully characterized iPSCs lines from both control and SMA affected subjects. Fibroblasts were obtained from skin biopsy and they have been reprogrammed to iPSCs using a viral non-integrating approach, as described in Materials and Methods. The colonies were first grown on feeder and subsequently isolated and placed on Matrigel coated 6-wells plates. All cell lines were assessed for karyotype (G-banded karyotype test, performed by Genetica medica Policlinico di Milano) and mycoplasma (assayed with the MycoAlert Mycoplasma Detection Kit). We successfully generated iPSCs, as demonstrated by the proper morphology and the positivity for pluripotency markers, such as OCT4, TRA1-60 and SSEA4. (Fig.11)

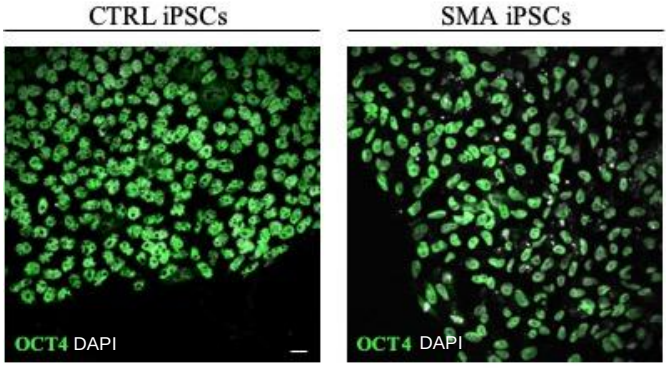

Fig. 11. Representative images of pluripotency markers.

iPSCs were stained for pluripotency markers, here is reported representative images of pluripotency marker OCT4 (green) in CTRL and SMA affected iPSCs. Nuclei were stained with DAPI (grey). Scale bar 20 μm.

5.2 BRAIN ORGANOIDS GENERATION

Through the use of a readapted version of Lancaster's protocol [117], we successfully obtained 3 different controls and 3 different SMA brain organoids. This method is based on *in vitro* development of neural differentiation through embryoid bodies to obtain mature and differentiated cortical neurons. Mature neurons are able to form functional connections and self-organized in circuit similar to those of a human brain.

Briefly, iPSCs were seeded in 6-well plates and kept in Essential 8 media until they reached 70% confluency, when they were detached and placed in ultra-low attachment 96-well plates to form Embryoid Bodies (EBs) using HES media. After six days, EBs were gently transferred into ultra-low attachment 24-well plates and grew in Neural Induction Media (NIM) in order to induce their differentiation and organization into cortical structure. Over time, organoids need a scaffold in order to grow and project axons outside the body, thus we used as a substrate Cultrex® Basement Membrane Matrix, Type 2 (BME type 2), a hydrogel extracellular matrix. Organoids have been embedded into Cultrex droplets. Ultimately, they were moved into the spinning flask to provide sufficient oxygenation throughout the whole organoid especially to the center (Fig. 12A).

At the beginning of the differentiation, control EBs showed well defined border compared to the SMA ones. Moreover, during the differentiation protocol, EBs form both control and SMA showed a

bright border, which represents the double layer of the neuroepithelium (Fig. 12B red arrows). Interestingly, we observed that affected EBs developed later the double layer compared to the control, and their form was more irregular and they are less. This was probably due to a difficult progression in differentiation of SMA organoids.

Cerebral organoids were maintained in culture for 90 days. At different time points (day 25, day 50 and day 90), they were harvested (n=3/group) in order to perform gene expression and functional analyses.

Fig. 12. Brain organoids generation from iPSCs colonies timeline.

iPSCs: Induced pluripotent stem cells; EBs: embryoid bodies; CTRL: Control

A. Schematic representation of human brain organoids generation. After iPSCs reached the proper confluency, they were seeded into 96-well plates with HES media. As EBs started to growth, they were placed in 24-well plates using NIM media. Around a week later, EBs were included in Cultrex droplets. After a few days, organoids were moved into the spinning flask.

B. Representation of brightfield images of differentiation pathway progression. The first two right images represent the iPSCs colonies of control and SMA, meanwhile the other 3 images represent EBs and brain organoids. (Scale bar 100 μm).

5.2.1 Brain Organoids Express Typical Neuronal Marker and Show A Preliminary Formation of The Cortex Layers

Several analyses were performed at different developmental phases on obtained brain organoids. Stages were divided as follow: early stage from day 15 to day 35, intermediate stage between day 60 and 70 and late stage organoids later than days. Analyses of gene expression were first performed with immunohistochemical staining in order to investigate whether, at different time points, it is possible to visualize an increase of the level of specific protein of neuron maturation. Subsequently some of these markers were investigate using RT-qPCR method in order to have more accurate information on gene expression profile.

5.2.2 Immunohistochemestry

At first, we performed immunohistochemistry for sex determining region Y-box 2 (SOX2), to follow the development of the brain organoids. SOX2 is a neural precursor marker, thus its expression supposed to decrease during the development. In combination we used Neuron-specific Class III b-tubulin (TUJ1), which is a post-mitotic pan-neuronal marker [174,175].

Regarding SOX2, its expression was present, in small portion until late developmental stages in controls. In both control and SMA organoids it was localized in niche (neural rosette), indicating that

with the progression of the differentiation, some cells lost their stem phenotype to acquire a more committed one. Notably, in SMA compared to the control in the course of the time, the expression of SOX2 did not decrease, suggesting a possible delay in the development in affected compared to healthy organoids (Fig. 13).

Concerning TUJ1, it resulted already expressed in both control and SMA at the early stages (Fig. 13). While in the control organoids TUJ1 appeared filamentous, in SMA organoids, it appeared organized in agglomerates, probably indicating a dysfunction in the neuronal outgrowth.

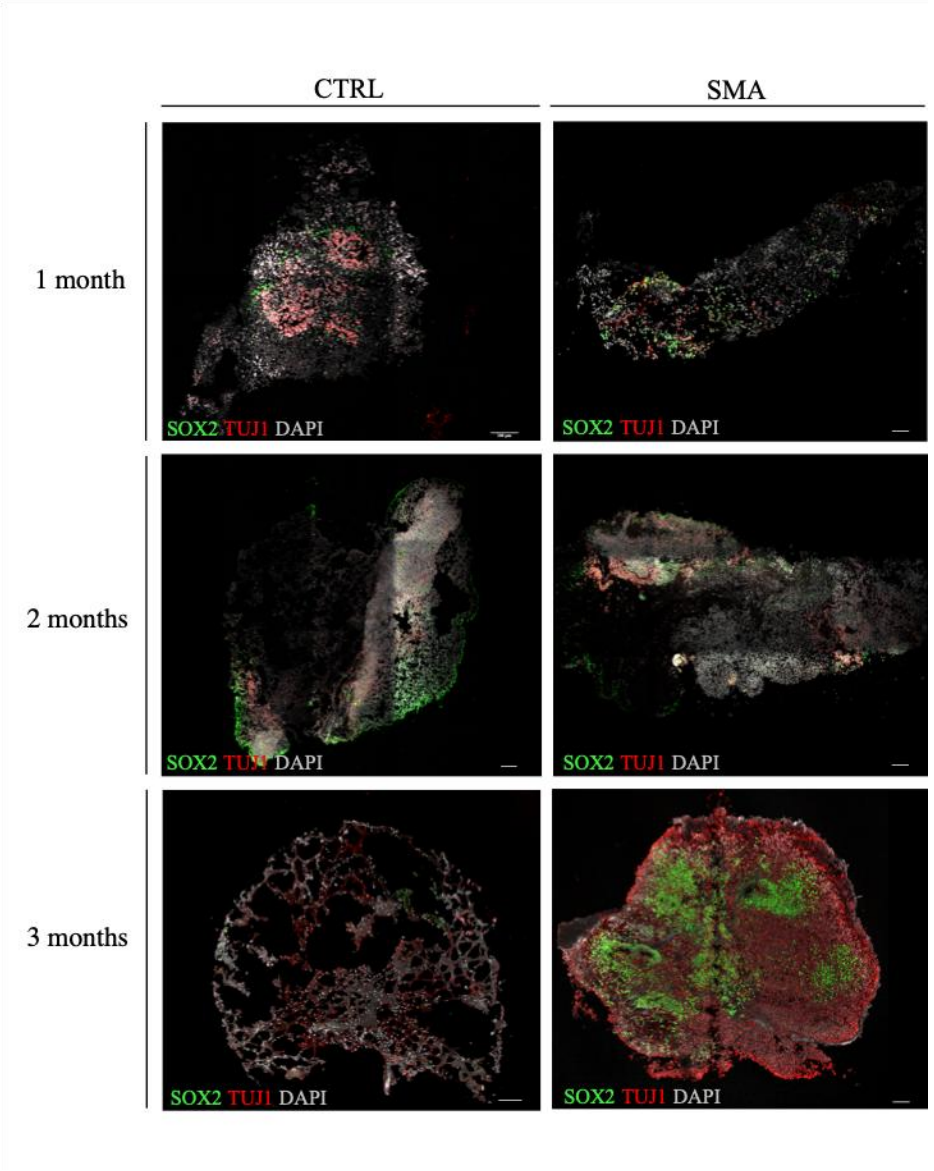

Fig. 13. Immunohistochemistry for SOX2 and TUJ1.

Immunohistochemistry of SOX2 (nuclear, green) and TUJ1 (cytoplasmatic, red) at different stages of the development of CTRL and SMA brain organoids:1 month, 2 months and 3 months. Nuclei were stained with DAPI (grey). Scale bar 100 μm.

Aiming to test the grade of the maturation of both control and SMA brain organoids, we performed immunohistochemistry with several differentiation markers (Fig. 14).

Doublecortin, or DCX, is a protein associate with the neurogenesis. It is expressed by neural precursor and immature neurons, which are actively dividing during neuronal migration. During the development its expression could be found only in small regions and it has been showed that a low level of this marker is expressed in adult brain, where NSCs are localized [176]. Besides DCX, we detected also the expression of Microtubule-associated protein 2 (MAP2), which is another protein involved in neurogenesis and whose function is associated with microtubules assembly and dendrites stabilization [177]. Its localization is both in the soma and dendrites of the neurons. Both markers were expressed and co-localized in our organoids, both in the control and in SMA, indicating a progression of the neurogenesis (Fig. 14A).

Immunohistochemestry showed also a partial differentiation in telencephalon, indeed, control and SMA organoids were positive for FOXG1, which is a common marker expressed during the neurogenesis and in particular in the development of the telencephalon (Fig. 14B).

Moreover, our interest was addressed to the capability of our organoids to self-organize and express typical markers of upper and lower layers of the cortex. For this reason, we tested the expression of cortical layer markers, Special AT-rich sequence-binding protein 2 (Satb2) and COUP-TF-interacting protein 2 (Ctip2) for the lower and upper cortical layer respectively (Fig. 14C,D). Results showed an

expression of these markers in both control and SMA cerebral organoids, starting from intermediate time point, indicating a preliminary formation of the double cortex layer.

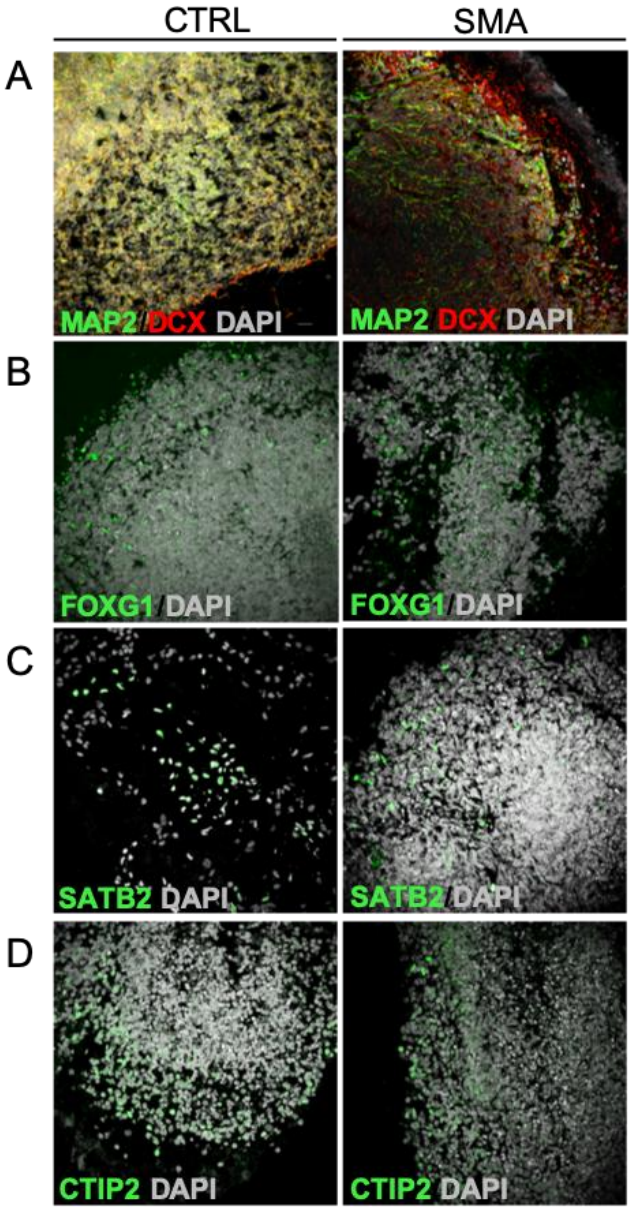

Fig. 14. Immunohistochemistry for developmental markers.

The first two images (A) of the panel represented MAP2 (green) and DCX (red) in CTRL and SMA brain organoids. The other images showed staining for FOXG1 (B, green), CTIP2 (C, green) and SATB2 (D, green). All organoids were at their intermediate (2 months) and late stage (3 months) of the development. Nuclei were stained with DAPI (grey). Scale bar 20μm.

5.2.3 Whole Mount Staining

Immunohistochemistry does not give insight about the population of the cells in the whole tissue. For this reason, we decided to perform the whole mount staining, which is used to stain small tissues without sectioning. We modified the standard staining protocol to obtain a higher penetration of the antibody inside organoids.

Control brain organoids were stained for TUJ1, and GFAP to analyse the presence of radial glia. Results confirmed data obtained from 2D-confocal imaging. TUJ1 was express in all organoid, and it was organized in clusters delimiting areas that could resemble brain *sulci* (Fig. 15A). Moreover, we demonstrated the presence of radial glia, indeed images showed clear filaments positive for GFAP. In particular, in control sample, we were able to follow a single cell express GFAP with its filaments spreading among other cells (Fig. 5A). A co-staining of TUJ1 and GFAP was also performed. Images showed a defined organization of radial glia and other neuronal cells (Fig. 15B).

All these data suggest the capability of brain organoids to self-differentiate into several subtypes of neurons and to self-organize.

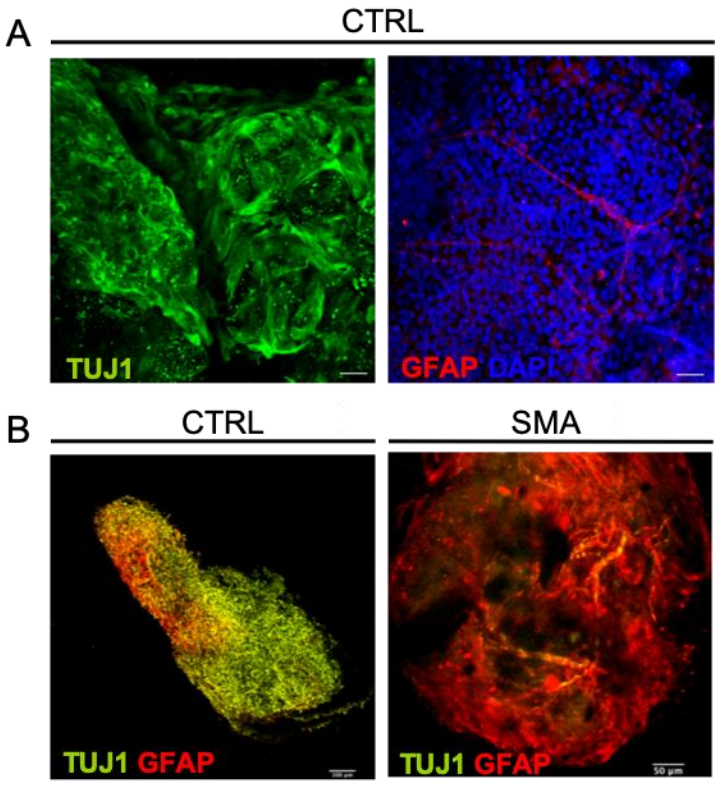

Fig. 15. Whole mount staining.

Whole mount staining was performed on organoids control and SMA.

A. Control brain organoids were stained with TUJ1 (green) and GFAP (red). Nuclei were stained in DAPI (blue). Scale bar 50 μm.

B. Both control and SMA organoids were stained with TUJ1 and GFAP. Scale bar 100 μm in the right image and 50 μm in the left image.

5.2.4 Real-Time PCR

Real-Time PCR technique was used to characterize brain organoids. This method allowed to perform a relative quantification of gene expression. Cerebral organoids were harvested at late stage of the development. mRNA was extracted from cryopreserved organoids' pellets and retrotranscripted into cDNA. Several genes were evaluated in order to assess the maturation stage of both control and SMA organoids. All mature markers were compared to starting iPSCs.

Results showed a reduction of the expression of stem cell genes OCT4 as well as SOX2 in cerebral organoids compare with the starting iPSCs. Moreover, SMA organoids showed a trend towards increase of PAX6 expression, which is a neuronal precursor marker, while both control and SMA brain organoids expressed mature neurons markers, such as MAP2 and TUJ1.

To evaluate the self-organization ability of cerebral organoids, we assessed the expression of lower cortical layer markers, such as CTIP2 and TBR1. Data revealed that both cerebral organoids groups expressed the lower cortical layer markers. Ultimately, we tested the expression of FOXG1, which resulted overexpressed in healthy and SMA affected organoids.

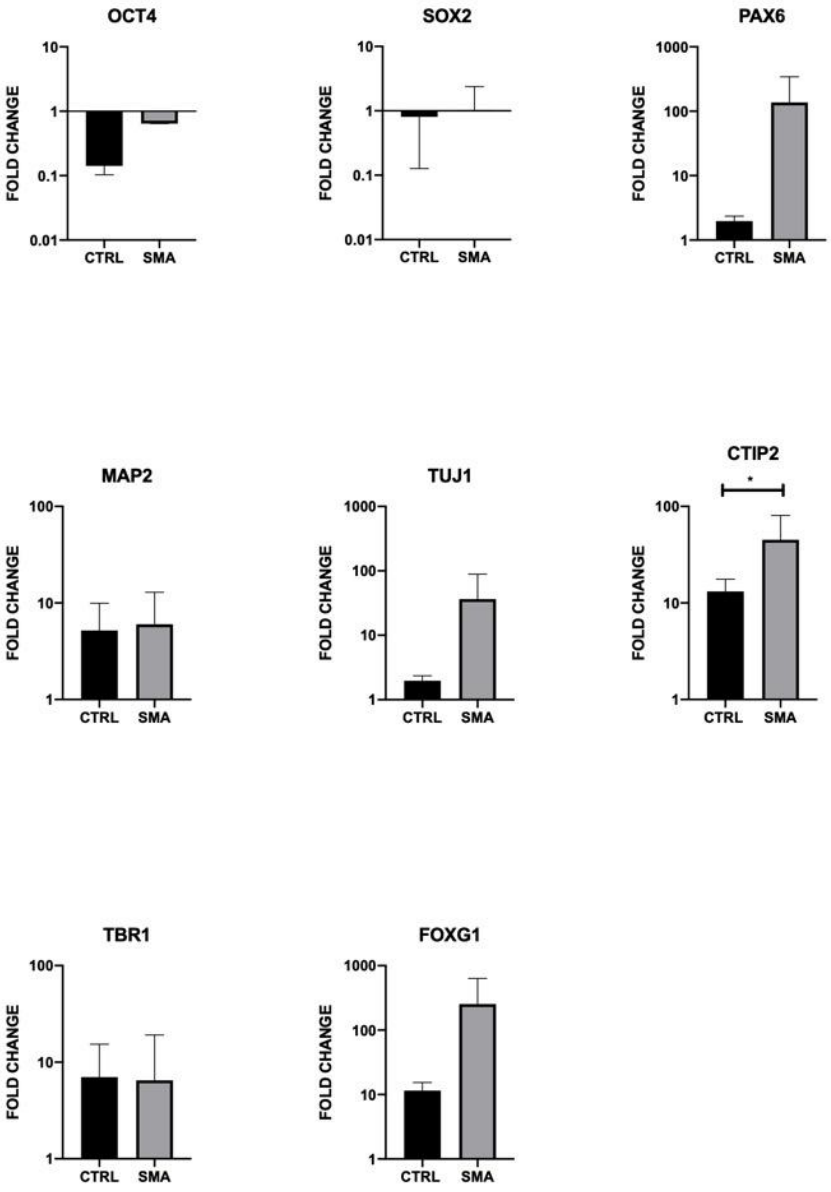

Fig. 16. Real Time PCR analysis.

Gene expression was analysed with Real Time-PCR on brain organoids harvested at late developmental stages. Analysed genes were SOX2 and OCT4 (stem gene markers), PAX6 (neural precursors marker) TUJ1 (pan-neural marker), CTIP2 and TBR1 (cortical mature neurons marker) and FOXG1 (telencephalon neurons marker).

5.3 Calcium Imaging Analyses Reveal the Basal Activity of The Cerebral Organoids And The Ability To Respond To Stimuli

We investigated the basal activity of cerebral organoids and whether they were able to react to stimuli performing FLUO-4 calcium analyses using with Nikon Time-Lapse.

In particular, the intra-cellular calcium in cerebral organoids was visualized using Fluo-4 calcium loading dye for over 20 minutes in both control and SMA organoids at day 80. After the first 10 minutes of basal activity recording, we added an excitatory neurotransmitter, glutamate. The subsequent fluctuations were recorded for an additional 10 minutes.

We evaluated the differences data distribution in control and affected organoids of calcium maximum variation amplitude (Fig. 7B-C) in basal versus glutamate stimulated conditions. The maximum calcium variation amlitude for each analysed brain organoid was reported as a dot-plot chart (Fig.7D-E). Data showed the presence of a basal activity in and its increase after glutamate treatment in both control and SMA cerebral organoids. Results showed the presence of spontaneous calcium activity, which increased in frequency after the application of an exogenous glutamatergic stimulus. Interestingly, SMA brain organoids presented a trend towards lower basal calcium amplitude oscillations and significantly higher response to the glutamatergic stimulus in comparison with controls (Figure 7 A-E).

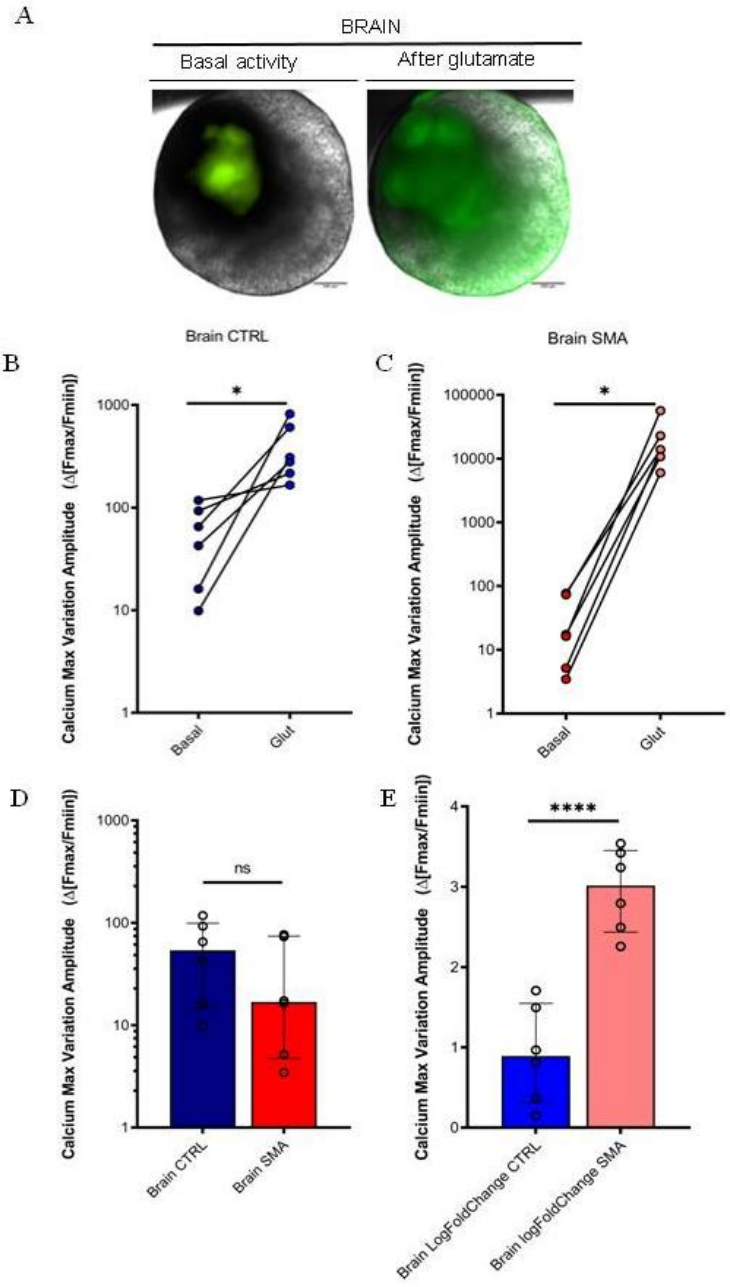
A
BRAIN
Basal activity
After glutamate
B
Brain CTRL
Calcium Max Variation Amplitude (Δ[Fmax/Fmiin])
1000
100
10
1
*
Basal
Glut
C
Brain SMA
Calcium Max Variation Amplitude (Δ[Fmax/Fmiin])
100000
10000
1000
100
10
1
*
Basal
Glut
D
Calcium Max Variation Amplitude (Δ[Fmax/Fmiin])
1000
100
10
1
ns
Brain CTRL
Brain SMA
E
Calcium Max Variation Amplitude (Δ[Fmax/Fmiin])
4
3
2
1
0
****
Brain LogFoldChange CTRL
Brain logFoldChange SMA

Fig. 17. Calcium fluctuation in brain organoids.

Organoids were assayed for a calcium response to glutamate (100 µM) stimulation using the Fluo-4 direct assay in different areas at the edge of the organoids. Measurements are given in relative fluorescent units as the maximum response minus the minimum response divided by the minimum response.

A. Representative image of brain organoids Fluo-4 calcium loading dye before and after glutamate administration. Scale bar 500 µm.

B-C. Calcium maximum variation amplitude in control and SMA organoids in basal condition versus glutamate stimulated condition.

D-E Log Fold Change of maximum variation amplitude in basal vs stimulated condition in CTRL vs SMA organoids.

5.4 Brain Organoids Showed A Basal Electrophysiological Activity and Are Able to Response to Stimuli

Exploratory data from calcium analysis revealed a basal activity of cerebral organoids, and also the ability to response to stimuli.

For a better and deeper analyses, we used Multielectrode array (MEA) technique for both type of organoids, at the late stages of their development ($n \geq 7$). We tested electrophysiological activity and the response to exogenous stimuli, through the glutamate administration.

Basal recording of both control and SMA organoids showed that they were functional and active with a spontaneous inner frequency. This result suggested that they were alive and able to self-organize to form synaptic circuits. In particular, we observed that spikes in control samples occurred at higher frequency compared to SMA

organoids spikes. Indeed, there is a statistically significant difference between the two types of organoids (Fig. 18A).

After the basal activity recording, 100µM glutamate was gently added in the Kreb's solution in order to verify the responsiveness to exogenous stimuli. Relevant was the fact that the firing frequency of SMA brain organoids increased more than 100%, which was more than the increase of control organoids (Fig. 18B). This data suggested a greater and earlier response of SMA compared to the control organoids, suggesting that they were more susceptible to excitatory stimuli.

No differences in spikes amplitude was detected in controls vs SMA, or before and after glutamate administration.

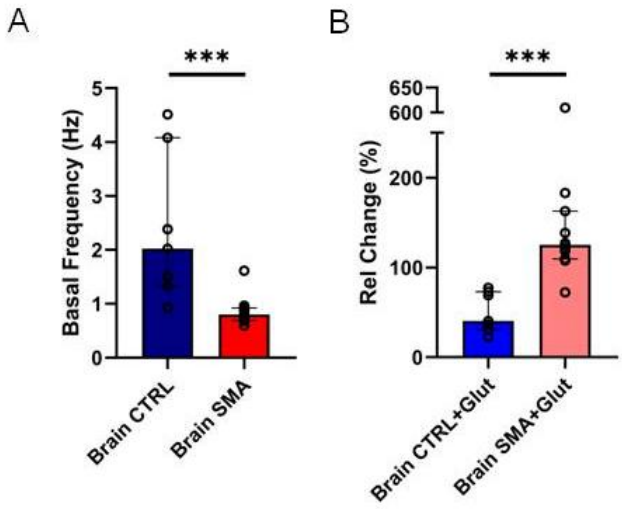

Fig. 18. Electrophysiology of control and SMA cerebral organoids.

- **A.** Basal activity of control and SMA brain organoids. They both showed the spontaneous action potential.
- **B.** Comparison between the control and SMA brain organoids electrophysiological activity after the glutamate administration.

5.5 Spinal Cord-Like Spheroids Generation

As mentioned before, SMA is a neuromuscular disease that mainly affects the second MN in the spinal cord. For this reason, we decided to develop a new 3D *in vitro* model: spinal cord like-spheroids.

Since no protocol has been published in literature at the time this project began, we generated a new one, by combining Lancaster's protocol to generate organoids, and Amoroso's protocol to induce the ventralization and caudalization of MNs in 2D [178] (Fig. 19A).

The generation of ventral spinal cord-like spheroids protocol started as the one brain organoids, but at different time points specific factors, such as cytokines and growing factors, were added to induce the motor neuronal development and the ventral-caudal pattern. At the beginning SB-431542, LDN-193189 and CHIR-99021cytokines were added, whereas Retinoic Acid (RA) and Smoothened Agonist (SAG) were administrated form day 6 till the end of the protocol. After one week in the spinning flask (around day 28) growing factors, such as BDNF, GDNF and IGF were added to the media.

According to the brightfield images (Fig. 19B) and to the immunohistochemistry, we can affirm that we successfully obtained of the ventral spinal cord-like spheroids, indicating that the protocol established was able to produce spheroids and induce the ventral-caudal pattern.

The workflow was the same as the one to generate brain organoids (Fig. 9A). At the early stages of the differentiation, EBs engaged in

ventral differentiation fate showed filaments outgrowth from the bodies, which were very evident during the latest stages of the differentiation (Fig. 9B, green arrow). Moreover, EBs showed a brighter layer of neuroepithelium (Fig. 9B red arrow).

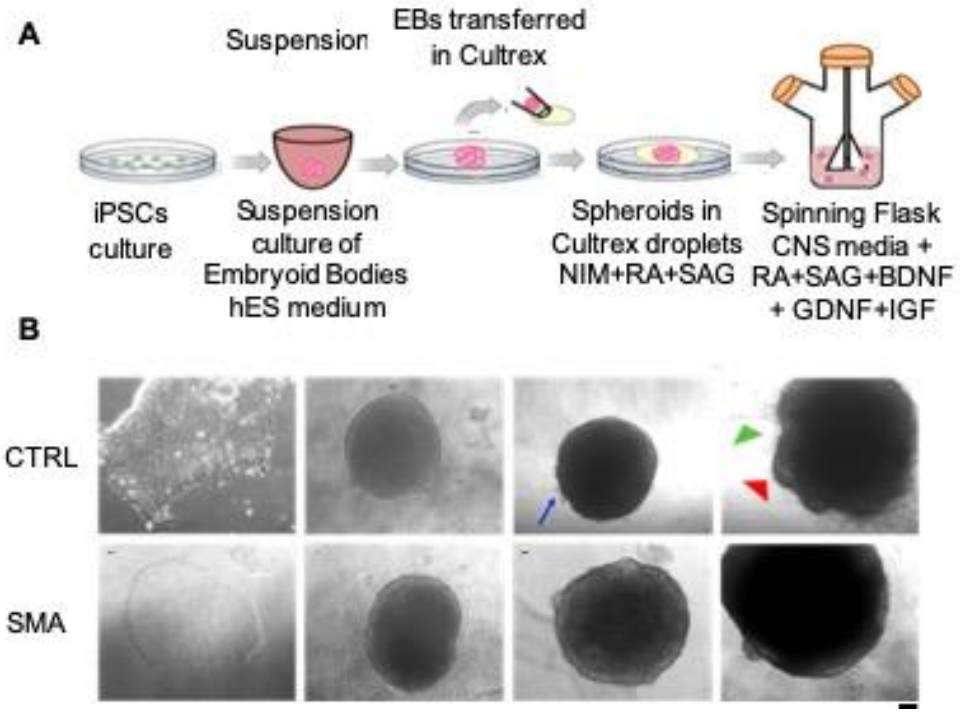

Fig. 19. Ventral Spinal Cord-like spheroids generation from iPSCs colonies timeline.

iPSCs: Induced pluripotent stem cells; EBs: embryoid bodies; CTRL: Control

A. Schematic representation of human spinal cord-like spheroids generation. After iPSCs reached the proper confluency, they were seeded into 96-well plates with HES media and cytokines, such as LDN, CHIR and SB. As EBs started to growth, they were placed in 24-well plates using NIM media with RA. Around a week later, EBs were included in Cultrex droplets and SAG was added in the media. After a few days, spheroids were moved into the spinning flask with CNS media and the trophic factors, such as BDNF, GDNF and IGF.

B. Representation of brightfield images of the differentiation pathway progression. The first two right images represented the iPSCs colonies, meanwhile the other 3 represented brain EBs and spheroids. Moreover, spinal spheroids showed the generation of radial outgrowing filaments (blue arrow) that kept growing as the spheroid developed (green arrowhead). Moreover, spheroids showed sign of neuroepithelium (red arrow) (Scale bar 100 μm).

As mentioned in the previous paragraph, to generate this protocol we used a combination of two different methods: one for the generation of organoids and one for the differentiation into 2D-MNs through EBs. In order to verify that our protocol induces the generation of ventral-spinal cord structure and does not produce only MNs, we stained EBs for 2D-MNs differentiation and spheroids with SMI32, which is the most common marker of MN filaments (Fig.20). The EBs stained imaged showed a ubiquitously expression of SMI32, with no differences in the expression and no regionalization, while the spheroids presented SMI32 expression in specific regions. On the other hand, ventral spinal cord-like spheroids showed regionalized expression of SMI32 and the presence of neural rosette, indicating

the capability of self-inner functional circuit and morphological organization.

These are the essential differences from the already known model of EBs to generate only MNs in 2D culture and our 3D spinal cord-like spheroids.

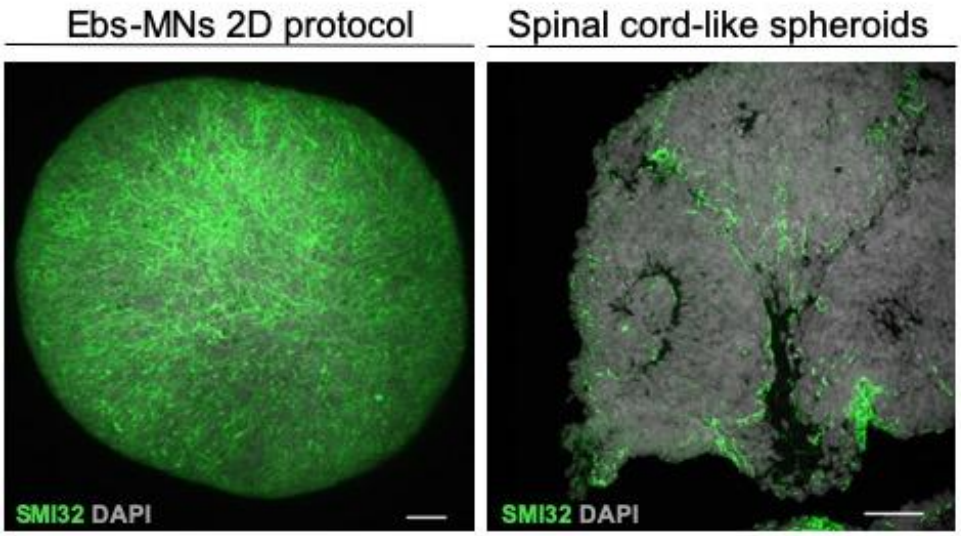

Fig. 20. Comparison between Ebs for 2D-MNs differentiation and spinal cord-like spheroids.

EBs cultured to generate 2D-MNs were stained with SMI32 (green) and no regionalization of its expression could be observed. On the other side, 3D spinal cord like-spheroids stained for SMI32 (green) showed regional differences and a pattern of expression. Nuclei were stained in grey. Scale bar 100 μm.

5.5.1 Control and SMA Ventral Spinal Cord-Like Spheroids Express Proper Differentiation Markers

The next step was to understand whether our protocol was able to give rise to different types of cells present in the spinal cord. Thus, we tested spheroids for different neuronal markers. We performed several types of analysis, such as immunohistochemistry, Real time PCR and whole mount staining.

5.5.2 Immunohistochemestry

We tested the expression of SOX2 and TUJ1. As assessed for brain organoids, we evaluated the time course of the expression rate of these two markers (Fig. 21). At the beginning of the differentiation, control as well as SMA spheroids showed the formation of neural rosette (Fig. 21, yellow arrows), indicating the progression of cells maturation. In the same way as brain organoids, the expression of SOX2 seemed to decrease during the differentiation. In parallel, TUJ1 seemed to be expressed from the second month of the differentiation protocol.

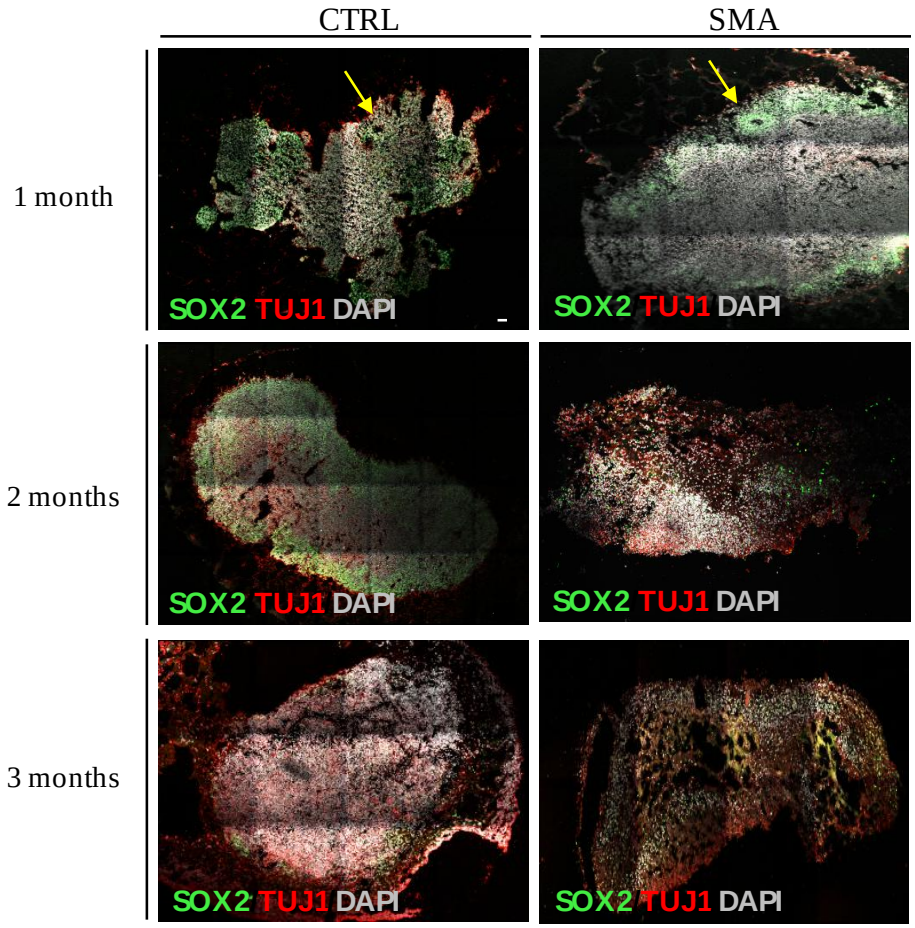

Fig. 21. Immunohistochemistry for SOX2 and TUJ1.

Immunohistochemistry of SOX2 (nuclear, green) and TUJ1 (cytoplasmatic, red) at different stages of the development of CTRL and SMA spinal cord-like spheroids:1 month, 2 months and 3 months. At the beginning of the development control as well as SMA spheroids formed neural rosette (yellow arrow). Nuclei were stained with DAPI (grey). Scale bar 100 μm.

Immunohistochemestry of early differentiated ventral spinal cord-like spheroids showed (in both control and affected) the expression of neural precursor markers, such as NESTIN and PAX6, which are neuroectodermal stem cell markers (Fig. 22A,C). NESTIN is a

member of intermediate filaments proteins family and is involved in axonal outgrowth. It is usually express in the early embryonic development and subsequently replaced by more specific filament proteins such as neurofilament heavy (NF-H) in MNs and GFAP in astrocytes [179]. Images of both control and SMA spheroids at early stages showed a high expression of this marker, suggesting the neural differentiation of spheroids. Since the early stages of the development spheroids presented the formation of the neural rosette (yellow arrow). Regarding PAX6, it is a transcription factor, which is expressed by neural precursor and it plays a key role in the neural tissue development. Sections stained with this antibody showed a positivity for this marker in both control and SMA spheroids.

To verify the presence of different cell population, we stained our spheroids for oligodendrocytes markers, Oligodendrocyte Transcription Factor 2 (OLIG2) (Fig.12B). OLIG2 is a protein mainly express in the nervous system, and its role is different depending on the developmental stage. Indeed, at the beginning of the development it supports the mitotic renewable pool of progenitors, in early stages it promotes the ventralization of the tissue, inducing the differentiation into MNs, meanwhile in late stages it induces cell differentiation into oligodendrocytes. In our model, OLIG2 was expressed in both control and SMA, supporting the ventralization of our spheroids.

All together, these data sustained the fact that the spinal cord-like spheroids at early stages started to express neural stem cell marker and presented typical structure for the development of CNS.

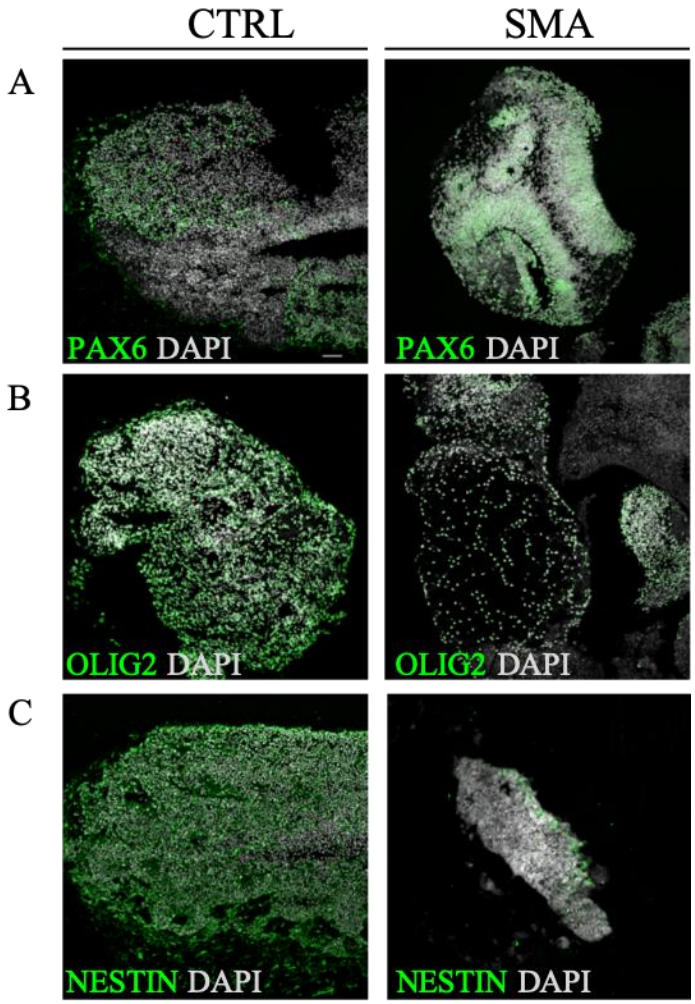

Fig. 22. Immunohistochemistry for precursor neuronal markers.

Immunohistochemistry for PAX6 (A, green), OLIG2 (B, green) and NESTIN (C, green) during 2 months of development in both control and SMA spheroids. Nuclei were stained in DAPI (grey). Scale bar 50 μm.

For the purpose to verify the ability of newly generated spinal cord-like spheroids to maturate and differentiate into spinal cord-like structure and the ability to generate different types of cells, we

stained sections with different markers, such as s100b, TUJ1, HB9 and SMI32 (Fig.23).

S100b is a marker for astrocytes. In the images it is possible to appreciate a clear signal of this marker, even if SMA spheroids did not showed the same signal of the control.

Ventral spinal cord-like spheroids showed positivity for MNs markers in both control and SMA. Indeed, they expressed HB9, which is the most common used marker for MNs, and it has a fundamental role in determining and consolidating motoneuronal identity [178,180]. Furthermore, both samples resulted positive for SMI32, which is a marker for the Neurofilament Heavy non phosphorylated (part of the cytoskeletal intermediate filaments). During the development its expression is low, and increases in post-mitotic myelinated neurons, which presented thicker axons [181,182].

In conclusion, we can affirm that both control and spinal cord-like spheroids presented different types of cells (astrocytes, oligodendrocytes and MNs).

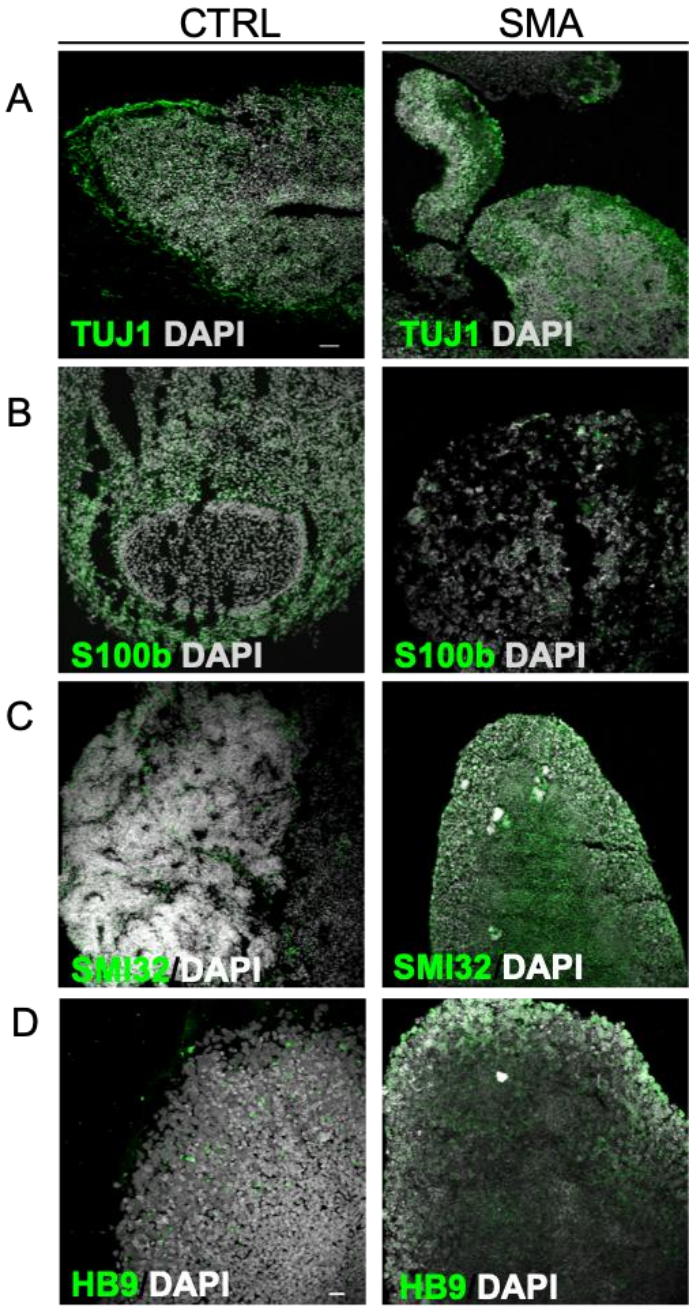

Fig. 23. Immunohistochemistry for TUJ1, GFAP and HB9/SMI32.

In the late stages of the developments, spheroids were stained for neuronal marker, TUJ1 (A, green), for astrocyte markers, s100b (B, green) and for MNs markers such as SMI32 (C, green) and HB9 (D, green). Nuclei were stained with DAPI (grey). Scale bar 50 μm.

5.5.3 Whole Mount Staining

In order to verify the structure of our spinal cord-like spheroids, we performed the whole mount staining in the same way of cerebral organoids. For spheroids we used SMI32 antibody to see the MNs axonal outgrowth (Fig. 24).

Results showed a signal distributed in the whole spheroids in the control and a more localized one in the SMA sample.

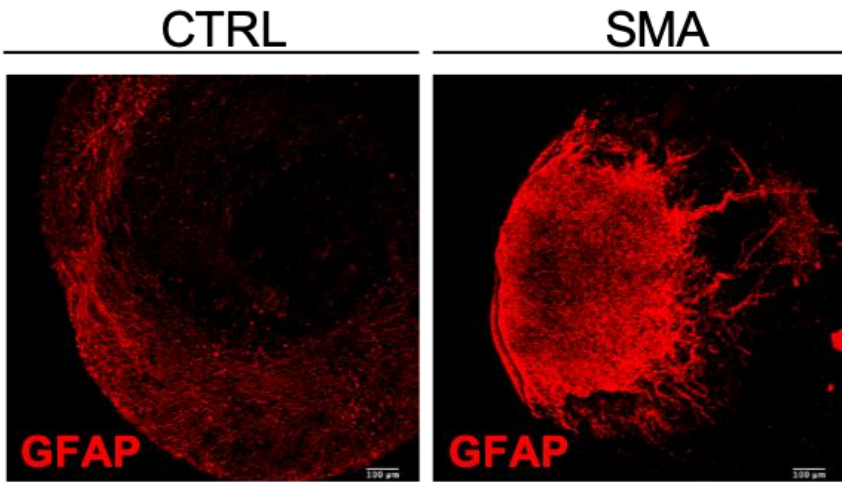

Fig. 14. Whole mount staining.

Whole mount was performed on control and SMA spheroids. Both spheroids were stained for SMI32 (red). Scale bar 100 μm.

5.5.4 Real-Time PCR

Real-Time PCR technique was used to characterize gene expression of ventral spinal cord-like spheroids at the late stage of the differentiation (Fig. 25). All markers were compared to starting iPSCs.

Results showed a significant increase of SOX2 gene expression in the SMA compared to the control spheroids, suggesting a possible delay in the maturation of the affected in respect with the control. Indeed, also OLIG2 marker showed a trend towards increase in SMA organoids compared to the control.

Concerning neuronal markers, we evaluated the expression of MAP2 and TUJ1.

Ultimately, we assessed the presence of MN gene expression using Insulin gene enhancer protein (ISL1), Homeobox HB9 (HB9) and Anti-Choline Acetyltransferase ChAT. ISL1 and HB9 are early MN markers, while ChAT is a late MN marker.

To conclude, we can affirm that we successfully differentiated both control and SMA into spinal cord-like spheroids and they were able to recapitulate the neural development of the spinal cord *in vivo*.

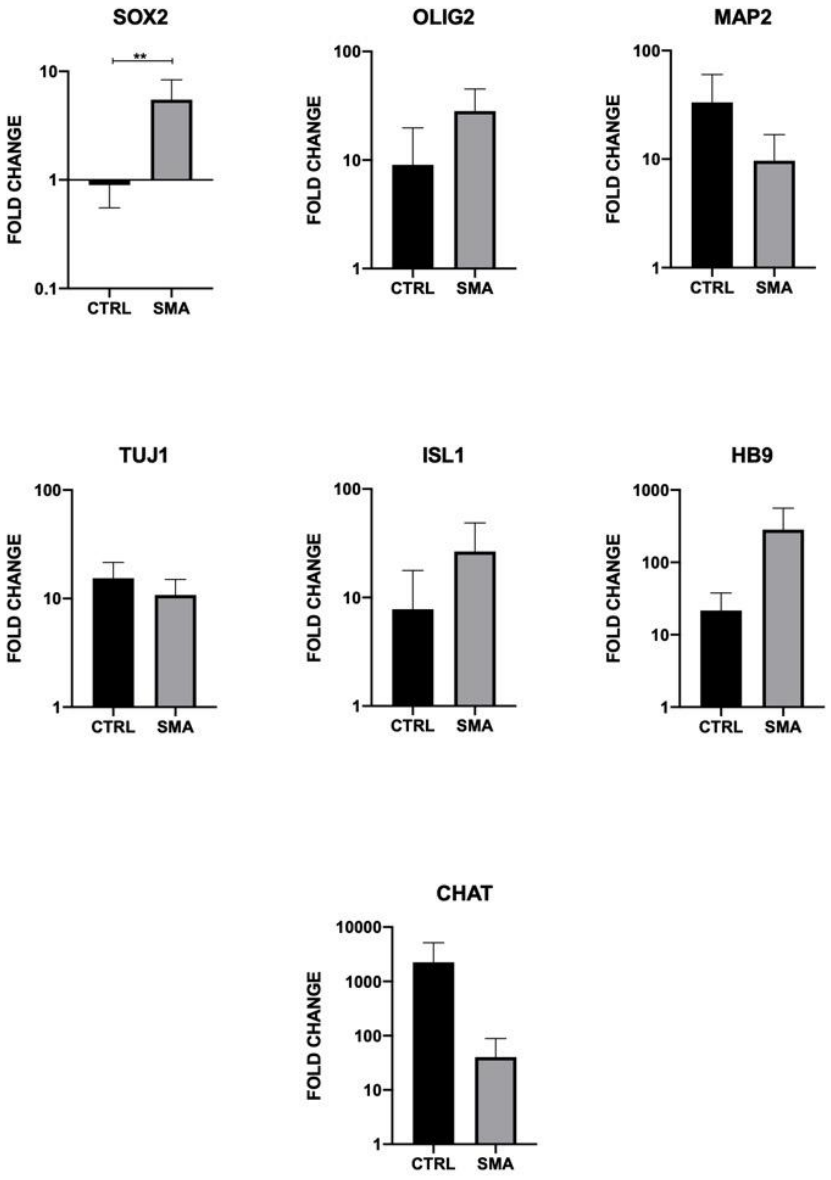

Fig. 25. Real Time PCR analysis.

Gene expression was analysed with Real Time-PCR on spinal cord-like spheroids harvested at late developmental stages. Analysed genes were SOX2 (stem gene marker), OLIG2 (neural precursors marker), MAP2 and TUJ1 (pan-neural markers), ISL1 and HB9 (early MN markers) and ChAT (mature MN marker).

5.6 Calcium Imaging Analyses Reveal the Basal Activity of The Ventral Spinal Cord-Like Spheroids and The Ability To Respond To Stimuli

As already done for brain organoids, we performed the Fluo-4 calcium loading dye experiment on both healthy and affected ventral spinal cord-like spheroids.
In particular, the intra-cellular calcium was visualized using Fluo-4 calcium loading dye for over 20 minutes in both control and SMA spheroids. After the first 10 minutes of basal activity recording, we added an excitatory neurotransmitter, glutamate. The subsequent fluctuations were recorded for an additional 10 minutes.

Maximum calcium oscillation for each analysed spinal spheroids are also reported as a dot-plot to better evaluate differences data distribution in HD and SMA organoids of calcium maximum oscillations (Fig. 26A) and calcium maximum variation amplitude (Fig. 26B) in basal conditions versus Glutamate- stimulated conditions (Fig.26). Exploratory data obtained with the calcium imaging revealed a basal activity of spheroids and also their ability to response to stimuli.

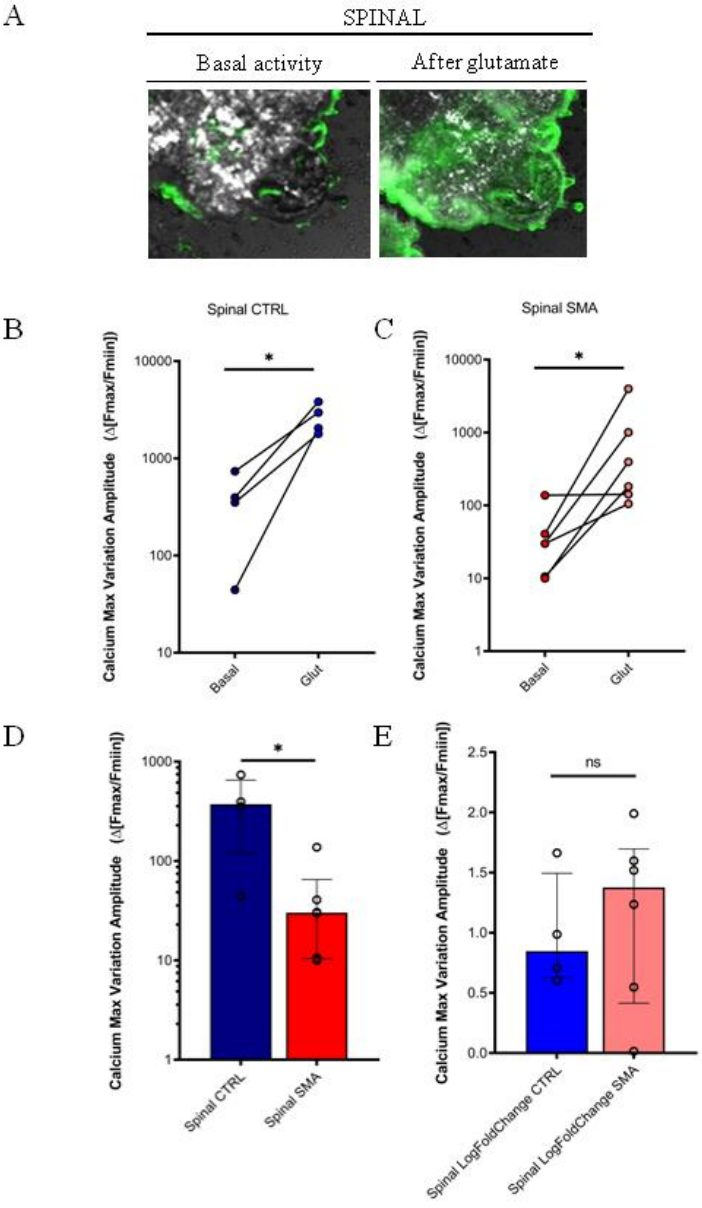
A
SPINAL
Basal activity
After glutamate
B
Spinal CTRL
Calcium Max Variation Amplitude (Δ[Fmax/Fmiin])
10000
1000
100
10
*
Basal
Glut
C
Spinal SMA
Calcium Max Variation Amplitude (Δ[Fmax/Fmiin])
10000
1000
100
10
1
*
Basal
Glut
D
Calcium Max Variation Amplitude (Δ[Fmax/Fmiin])
1000
100
10
1
*
Spinal CTRL
Spinal SMA
E
Calcium Max Variation Amplitude (Δ[Fmax/Fmiin])
2.5
2.0
1.5
1.0
0.5
0.0
ns
Spinal LogFoldChange CTRL
Spinal LogFoldChange SMA

Fig.26. Calcium fluctuation in ventral spinal cord-like spheroids.

Spheroids were assayed for a calcium response to glutamate (100 µM) stimulation using the Fluo-4 direct assay in different areas at the edge of the spheroids. Measurements are given in relative fluorescent units as the maximum response minus the minimum response divided by the minimum response.

A. Representative image of brain organoids Fluo-4 calcium loading dye before and after glutamate administration. Scale bar 500 µm.

B-C. Calcium maximum variation amplitude in control and SMA organoids in basal condition versus glutamate stimulated condition.

D-E Log Fold Change of maximum variation amplitude in basal vs stimulated condition in CTRL vs SMA organoids.

5.7 Ventral Spinal Cord-Like Spheroids Show A Basal Electrophysiological Activity And Are Able to Response To Stimuli

In the same way we tested brain organoids, ventral spinal cord-like spheroids have been tested for vitality and the capability to respond to stimuli to deepen calcium data.

We used Multielectrode array (MEA) technique for both type of spheroids, at the late stages of their development. We tested them for electrophysiological activity and the response to exogenous stimuli with glutamate administration.

Both control and SMA spheroids resulted functional and active with a spontaneous inner frequency. This result suggested that they were alive and able to self-organized in order to form synaptic circuits. In particular, we observed that control spikes occurred at higher

frequency compared to SMA organoids spikes. Indeed, there is a statistically significant difference between the two types of organoids, control fired 1,71±0,66Hz and SMA organoids fired 1,38±0,69Hz (Fig. 27A); this data showed that the control fired almost the double of the SMA, indicating a possible pathological activity of the SMA.

After the addition of glutamate, statistical increase of both control and SMA spheroids' spiking frequency was observed (Fig. 27B). Relevant was the fact that the firing frequency of SMA spinal cord-like spheroids, increased more (91±29%) than the increase of controls (55±22,37%). This data suggests a greater and earlier response of SMA compared to the control organoids, confirming data obtained in brain organoids.

No differences in spikes amplitude was detected in controls compared to SMA, before and after glutamate administration.

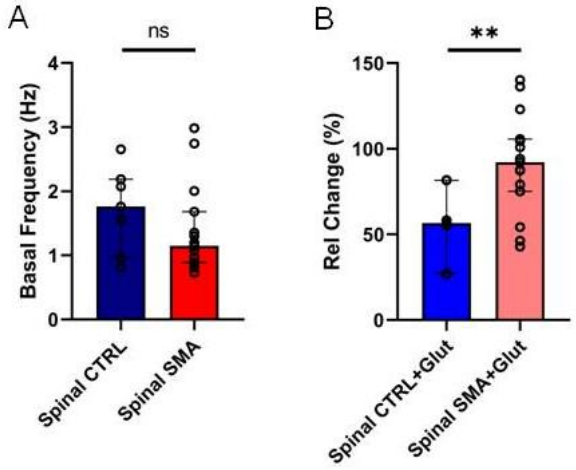

Fig. 27. Electrophysiology of control and SMA ventral spinal cord-like spheroids.

- **A.** Representation of the basal activity of control and SMA ventral spinal cord-like spheroids. They both showed spontaneous action potential.
- **B.** Comparison between the control and SMA ventral spinal cord-like organoids electrophysiological activity after the glutamate administration.

6. SMA Motor Neurons Derived From Organoids Display Reduced Axon Lenght

We dissociated ventral spinal cord-like spheroids to better verify the presence of MNs, and whether SMA spheroids showed same phenotypical hallmarks of 2D SMA MNs.

Three months old spheroids were dissociated and placed onto coverslips already coated with poly-Ornithine and Laminin. Subsequently, we evaluate the presence of the MNs through immunohistochemical analysis, using SMI32 antibody. Results showed a positivity for both markers in the control as well in the SMA, although it seems to be present a different outgrowth and axon length in SMA MNs compared to the controls (Fig. 28).

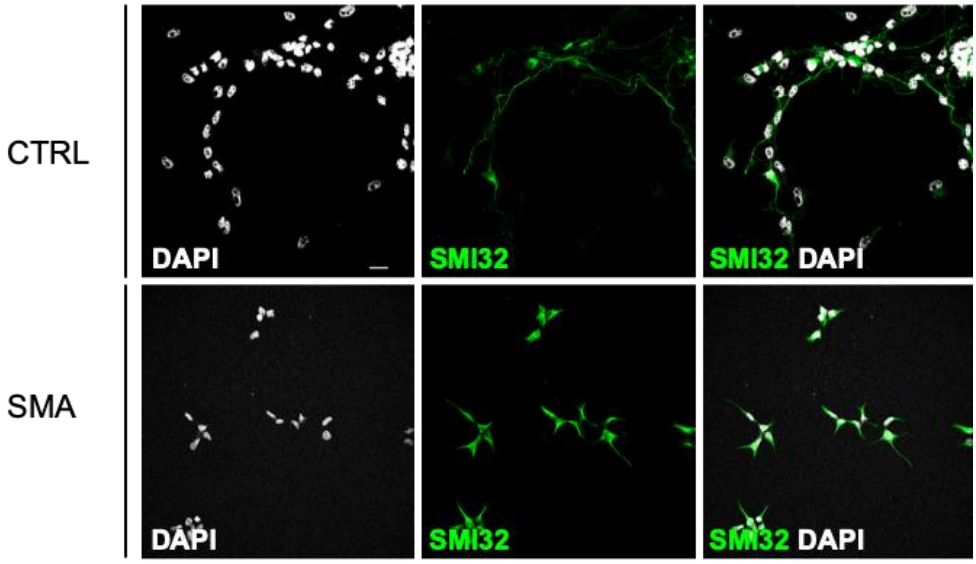

Fig. 28. Immunohistochemistry for SMI32 of dissociated ventral spinal cord-like spheroids.
Representative images of dissociated spheroids at the third month of their development. Fixed cells were stained with SMI32 (green). Nuclei were stained with DAPI (grey). Scale bar 20μm

7. Single Cell RNA-Seq

In order to have more detailed information about the different type of cells composing spinal cord-like spheroids, we performed single cells RNA sequencing (scRNA-seq).

For preliminary analyses were used two SMA spinal cord-like spheroids (Fig. 29). Results showed the presence of six different cluster of cells. Interesting is the fact that these cluster are similar between the two different organoids, indicating a possible reproducibility in spinal cord-like spheroids. More analyses are needed. The sc-RNA-seq for control spinal cord-like spheroids are still ongoing.

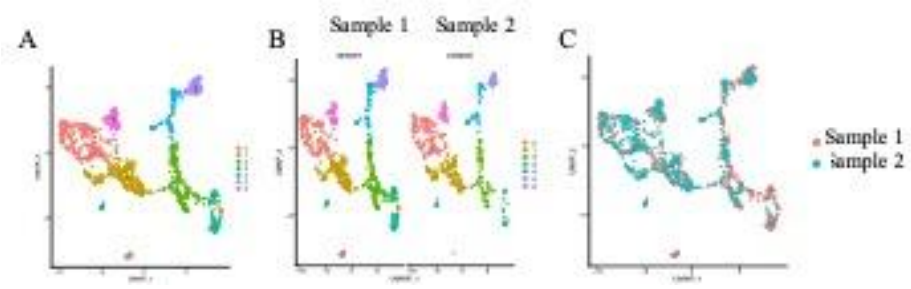

Fig. 29. Vulcano plot of scRNA-seq analyses.

These graphs represent the cluster of the different cells in SMA organoids. In the first graph (A) is represented the Vulcano plot of one sample of SMA spheroid; (B) Vulcano plot of both the SMA samples analysed; (C) Merged Vulcano plot of the two samples analysed.

8. Discussion

Spinal Muscular Atrophy (SMA) is one of the most common inherited form of motor neuron disorder and a leading cause of early childhood mortality. It is caused by mutations in *Survival Motor Neurons 1* gene (*SMN1*), leading to the reduction of SMN protein, which causes the selectively degeneration of lower MNs in the spinal cord. The degeneration of the MNs causes a progressive weakness and atrophy of the limb and the trunk muscle, eventually leading to respiratory failure. SMA has been classified in four different forms based on the gravity of the symptoms (from I, the most severe to IV, the less severe). The human genome contains a *SMN1* paralogous, called *SMN2*, whose genomic sequence differs from *SMN1* by a single important nucleotide from C to T. This change results in an alternative spliced transcript missing exon 7 and to the production of a truncated and non-functional SMN protein in the majority of the cases. Interesting is the fact that the SMA phenotype is related to the number of *SMN2* copies that each patient retains, with a proven inverse relationship between *SMN2* copies and disease severity [44] Therefore, acting on SMN2 has been one of the most common therapeutic approach. As a matter of fact, nowadays two treatments are approved from FDA and administrated to patients: Antisense Oligonucleotide (ASO) therapy and gene therapy.

ASO therapy (Nusinersen) is based on the modulation of *SMN2* splicing, increasing the level of the full-length SMN, meanwhile gene therapy uses the vector self-complementary AAV9 (scAAV9) to deliver wild-type human *SMN1* gene.

Although first results with both therapies seem to be promising and the SMA phenotype seems to improve, there are still some concerns. For instance, not all type of patients has a good response to ASO therapy or can be recruited for gene therapy (because of for instance the presence of antibodies against the virus). Moreover, the way of administration of ASO is invasive and the injection is difficult to be performed in patient with scoliosis, which is often present. Furthermore, a possible toxic accumulation in patients' liver treated with scAAV9 has been shown.

For all this reason it is necessary to continue investigating the pathogenetic mechanisms and likely new combined therapies for SMA.

As a matter of fact, a new way to model organs *in vitro* has been developed, called 3D *in vitro* cultures. Some of the advantages of these cultures on the traditional 2D are for instance the increasing of differentiation activity, more realistic gene expression levels, better cell-cell interaction and, most importantly, the capability to self-assembly and self-organized. These 3D *in vitro* cultures are called organoids. In this study, we generated cerebral organoids and we developed a new protocol for the generation of ventral spinal cord-like spheroids.

We generated cerebral organoids readapting the already published protocol from Lancaster [133]. Our control cerebral organoids, at the beginning of differentiation, presented the same morphology of brain organoids generated in other laboratories, with defined and regular borders and the formation of neuroepithelium (bright double layer).

Although later in the development, also SMA cerebral organoids presented the formation of the neuroepithelium layer. This backwardness in formation of the neuroepithelium could already indicate a delay in the development of the SMA organoids compared to the control. As expected, control brain organoids changed their precursor protein markers expression into a more mature ones with the progression of the differentiation. We tested SOX2 presence, a transcription factor expressed during neurogenesis by ectodermal cells committed to the neural fate, which marks the developing nervous system from its earliest developmental stages [183]. Organoids expressed high level of SOX2 in the first month of the differentiation, which decreased at the third month. This data was also confirmed through qPCR; indeed, the expression of SOX2 in organoids at late stage was decreased compared to starting iPSCs. The same result was obtained for OCT4, which is involved in the embryonic development [184]. On the other hand, SMA organoids seemed to express the same level of SOX2 during the whole differentiation time course. Moreover, by qPCR we observed the same level of SOX2 as in iPSCs at later time points, suggesting a possible delay in the differentiation rate compared to the control. Concerning OCT4, which is a stem cell marker, it was not expressed in SMA late stage organoids, implying that they were able to differentiate in more committed tissue.

In order to verify the ability of cerebral organoids to self-organize, thus assessing the presence of different types of mature neurons, we used markers such as MAP2 and Doublecortin (proteins associated with the microtubule-assembly during neurodevelopment) [185–187];

SATB2 and CTIP2 markers were tested in order to verify the formation of the upper and lower cortex layer, and FOXG1 to validate the presence of cells forming the telencephalon [133].

As also demonstrated by other groups [133,188] our cerebral organoids, both control and SMA, expressed both markers of upper and lower cortical layers at three months. On the contrary, we did not identify a stratification of cortical layers, but only the single expression of CTIP2 and SATB2. However, our organoids displayed the presence of mature neurons, as demonstrated by the expression of MAP2 and DCX.

Furthermore, whole mount staining revealed the presence in our control cerebral organoids of radial glia (GFAP positive cells). Radial glia cells are an embryonic transient population, which, during the CNS development, extends fibres from the soma to the ventricular zone (VZ) [189]. Its role in the development of the CNS consists in forming a scaffold to guide neuroblasts during their migration in the VZ [190]. Radial glia cells have a distinctive morphology and they can be clearly distinguished from other neurons by the expression of glial marker such as GFAP [191,192]. The presence of this type of cells in cerebral organoids is another evidence of their ability to recapitulate part of the embryonal neurogenesis process. Besides, in the control organoids, there was a spatial organization between radial glia and other types of neurons (TUJ1 positive cells) which was not present in the affected ones.

We demonstrated also that our cerebral organoids were electrophysiologically active. At the beginning, as preliminary

experiment, we assessed FLUO-4 calcium activity. Results showed that both control and SMA organoids have a basal activity as already reported in literature by Lancaster group [133]. Moreover, organoids were able to respond to stimuli. Indeed, when a solution containing glutamate (excitatory neurotransmitter) was added, an increase of the activity was detected. Interestingly, SMA organoids showed a higher increase of the activity after glutamate induction.

To verify these data, we performed multielectrode array (MEA) analysis. Results confirmed what previously reported with the FLUO-4 calcium assay. Control organoids had higher basal activity compared to the affected ones, but SMA were more responsive to stimuli.

At the present time, there is only one reported study on the electrophysiology of the brain in SMA patients [193]. In this study possible alteration of somatosensory thalamocortical evoke potential in a group of type I and type II patients compared to the control was investigated. Results showed not only an alteration of the response by somatosensory thalamocortical pathway, but also a delay in the central conduction time, likely associated with the brain atrophy. This study is perfectly in line with our model of cerebral SMA organoids, which showed a low basal activity compared to the control. Moreover, we also reported the possible hyperexcitability of SMA organoids compared to the control, which was never investigate *in vivo* or *in vitro* before.

SMA is a neurodegenerative disorder which mainly affect MNs in the spinal cord. For this reason, we generated for the first-time spinal

cord-like spheroids, indeed, when we started this project, no protocols were available in literature for developing such model.

We established a protocol based on MNs embryonic development stages. We combined the protocol already described for the generation of cerebral organoids adding at different times point cytokines and growth factors to induce the formation of the ventral part of the spinal cord taking into account the protocol used for the generation of 2D-MNs [178]. To induce the neural differentiation, we used cytokines such as SB, CHIR and LDN, while we used RA and SAG to induce the formation of caudal and ventral part, respectively. The crucial 2D-MN differentiation protocol step is the formation of the EBs, at the end completely composed by MNs; besides, 3D spheroids should be able to self-organize and generate different types of cells besides MNs. A first comparison between EBs and spheroids showed a different organization; spheroids showed the formation of neural rosette and an organized expression of SMI32, the most common MN axons marker. EBs from 2D-MNs protocol instead presented a generalized expression of this marker and no organization. This result suggested the potential efficacy of our protocol in modelling ventral spinal cord.

Concerning the morphology of spheroids at early differentiation state, both control and SMA had round shape and clear edges. During the time, and after the supplied scaffold, from the body of spheroids was visible the axonal outgrowth, which was more evident in the control compared to the affected ones. This delay in the outgrowth of SMA axons could be due to a possible impairment of the axons' elongation

or to the delay in the development of the SMA compared to control organoids.

Immunohistochemical analyses revealed the expression of neural precursor markers such as SOX2. Interestingly, in the control organoids SOX2 expression decreased at the third month compared to the first month of differentiation, which is in line with the only recently published study in which authors generated spinal organoids [173]. SMA organoids instead, expressed high level of SOX2 also at the third month of differentiation. This data was confirmed by qPCR, indeed SOX2 expression was significantly higher in SMA spheroids compared to the controls. Nevertheless, more experiments, as the counting of SOX2 positive cells, have to be done.

Another important phenotypic aspect is the formation of neural rosettes. The neural rosettes formation is a critical morphogenic process during *in vivo* neural development, indeed, during the neural tube development, neural stem cells (NSCs) placed inside the tube organize in round shape niches to proliferate and differentiate into neurons, oligodendrocytes or astrocytes [194]. With the progress of differentiation, data showed the formation of neuroectodermal tissue and the differentiation of several types of cells populations. At one month, spheroids expressed neural precursor markers, such as NESTIN, PAX6 and OLIG2; at the third month of differentiation, spinal cord like spheroids expressed more mature neural markers, such as HB9, SMI32, s100b and TUJ1.

We performed a 3D reconstruction of control as well as SMA spheroids using the whole mount staining. Data showed an

organization of MN axons in control spheroids, which was not visible in the SMA ones.

Interesting was the data of the qPCR, that showed a trend towards increase in the expression of OLIG2 in the SMA spheroids compared to the control ones, but on the contrary the markers of more mature markers MAP2 and TUJ1 were more expressed in the control compared to the affected ones.

Moreover, SMA spheroids showed also a trend towards the increase in the expression of HB9 and ISL1, but less expression of ChAT compared to the controls. The possible explanation of these results could be the fact that HB9 and ISL1 are markers of MNs, but they are expressed at the beginning of their formation, meanwhile ChAT is expressed by mature MNs; thus, SMA MNs might be more immature compared to the control MNs. We did not investigate markers of cervical, thoracic or lumbar spinal cord parts in our ventral spinal cord-like spheroids, as Hor in his study did, but we decided to perform FLUO-4 calcium assay in order to have preliminary results on the basal activity and on the response to stimuli. Control spheroids presented a higher basal activity compare to SMA ones; moreover, after stimulation through glutamate, the activity of control and SMA increased. These data confirmed data obtained with the same assay in brain organoids.

In literature are reported different studies on the spinal cord electrophysiology of SMA mice model. It has been demonstrated that MNs in the ventral spinal cord derived from SMA mice model at postnatal day 5 and 6 (P5-P6) are no longer active and those that

remain are less active compared to control [195]. Our study confirmed the same results, indeed, control spheroids were significantly more active compared to the SMA. In the same study mentioned above, it has been reported that MNs from SMA mice are less able to respond to stimuli. Our results are in contrast with that study, indeed the increase of the activity in SMA spheroids is significantly higher compare to the control, although both activity increase after glutamate induction. The discordance can be correlated to the different time point of analysis and to the different used models. However, our results are in line with the study performed in SMAΔ7 mice in 2013 [196]. Indeed, Mentis and collaborators performed electrophysiological analyses on post-natal mice (P0-P4), when the MNs number is not reduced as at P5-P6. Results showed an impairment between the excitatory and inhibitory inputs leading to a decrease in MN activity and a MN hyperexcitability in order to compensate the reduction of presynaptic activity. We suppose that our spinal cold-like spheroids display the same behaviour, since the MNs loss was not evident, but the MNs circuit could be already damaged.

9. CONCLUSIONS

Organoids are a useful tool for the study of neurodevelopment and the interaction of different types of neurons. Nevertheless, there are some issues, such as for example the high level of cell-packing that limits the possibility of quantification and cell analysis. To overcome this problem, it can be useful to perform clarity technique, which provides accessibility to the whole organ, or to dissociate the organoids. In our study, to better asses the MN phenotype of our control and SMA spinal cord-like spheroids, we dissociated them. Immunohistochemistry analyses suggested a reduction in the SMA axon length compared to the control, although the quantification of the axon length has to be performed.

All these results are really promising, but further analyses have to be done in order to better characterize SMA cerebral organoids and both control and SMA spinal cord-like spheroids. For this reason, RNA-seq (bulk and single-cell) analyses are ongoing. Preliminary data of RNA singe cell analysis on SMA spinal cord-like spheroids were promising, because the two different spheroids analyzed expressed the same set of cells and we could observed the presence of different cell population. The identification of which type of cell belongs to the each cluster is ongoing.

Another issue regards the formation of spinal cord-like spheroids. With our protocol we could generate only the ventral part of the spinal cord. The use of proper scaffold with specific gradient is likely needed in order to obtain the whole organ. Indeed, during

embryogenesis, several proteins involved in the generation of the spinal cord have different gradient. Bone morphogen protein (BMP) is expressed in high concentration in the dorsal part of the neural tube and decreases along the ventral part, meanwhile Sonic hedgehog (Shh) is not expressed in the dorsal part but is concentrated in the ventral part. Retinoic Acid (RA) expression level increases in the ventral part and decreases in the dorsal one [110].

It should be taken into account the heterogeneity among the organoids and spheroids and the absence of the vascularization. Velasco group optimized a new protocol for the generation of the cerebral organoids, and they declared that their organoids have a 95% similarity among them [188]. The lack of the vascular system prevents the delivery of small molecules and oxygen deep in the organoids or spheroids, leading to the formation of necrosis. As mentioned in the introduction, different groups exploited the possibility to generate blood vessel-like structure in 3D-cultures [146–149]. Although results are promising, further experiments need to be done.

Despite these issues, cerebral organoids and spinal cord-like spheroids represent revolutionary tools to study the pathogenic mechanisms of different types of disorders. As a matter of fact, nowadays different type of disease has been modelled through brain organoids, such as microcephaly, autism, schizophrenia and adult onset disorders like Alzheimer's disease (AD), frontotemporal dementia (FTD) and Parkinson's disease (PD). Moreover, spinal cord-like spheroids have been generated to study SMA.

This model could be also used to test new drugs to find new therapy for SMA. Indeed, it would be interesting to test the increase of SMN through the use of ASO or gene therapy. In our lab, we started to test the ASO therapy in SMA type I spinal cord-like spheroids. Preliminary results suggested an increase of SMN in treated spheroids compared to non-treated ones.

Nowadays, modern medicine is able to replace damage and non-functional tissue with healthy tissue by allogenic transplantation, even if the healthy donor tissue is limited and side effects, such as rejection, could occur. For this reason, additional tissue sources are needed. Organoids technology could represent a new possibility for the transplant use, because they are obtained from isogenic tissue derived from a non-invasive biopsy. In literature, several studies reported functional engraftment of orthotopically transplanted organoids in the colon, pancreas and liver as a therapy for repair diseased or damaged tissue [197–200] For instance, Fordham et al., transplanted intestinal organoids into damage colon in mice for tissue repair [200]. Dekkers et al., demonstrated the ability of intestinal generated organoids to repopulate diseased tissue after transplantation [197].

Overall, organoids represent an innovative and a promising tool for the study of pathological mechanisms underlying diseases, drug screening and a possible treatment for injuries.

11. BIBLIOGRAPHY

1. Verhaart, I. E. C. *et al.* Prevalence, incidence and carrier frequency of 5q-linked spinal muscular atrophy - A literature review. *Orphanet Journal of Rare Diseases* (2017). doi:10.1186/s13023-017-0671-8

2. Prior, T. W. Spinal muscular atrophy: newborn and carrier screening. *Obstet. Gynecol. Clin. North Am.* **37**, 23–36, Table of Contents (2010).

3. Sugarman, E. A. *et al.* Pan-ethnic carrier screening and prenatal diagnosis for spinal muscular atrophy: clinical laboratory analysis of >72 400 specimens. *Eur. J. Hum. Genet.* **20**, 27–32 (2012).

4. Hendrickson, B. C. *et al.* Differences in SMN1 allele frequencies among ethnic groups within North America. *J. Med. Genet.* (2009). doi:10.1136/jmg.2009.066969

5. Beevor, C. E. A case of congenital spinal muscular atrophy (family type), and a case of hæmorrhage into the spinal cord at birth, giving similar symptoms. *Brain* **25**, 85–108 (1902).

6. Werdnig, G. Zwei frühinfantile hereditäre Fälle von progressiver Muskelatrophie unter dem Bilde der Dystrophie, aber anf neurotischer Grundlage. *Arch. Psychiatr. Nervenkr.* **22**, 437–480 (1891).

7. Lefebvre, S. *et al.* Identification and characterization of a spinal muscular atrophy-determining gene. *Cell* **80**, 155–65 (1995).

8. Rudnik-Schöneborn, S. *et al.* Congenital heart disease is a feature of severe infantile spinal muscular atrophy. *J. Med. Genet.* **45**, 635–638 (2008).

9. Govoni, A., Gagliardi, D., Comi, G. P. & Corti, S. Time Is Motor Neuron: Therapeutic Window and Its Correlation with Pathogenetic Mechanisms in Spinal Muscular Atrophy. *Molecular Neurobiology* **55**, 6307–6318 (2018).

10. Kolb, S. J. & Kissel, J. T. Spinal Muscular Atrophy: A Timely

Review. *Arch Neurol* **68**, (2011).

11. Liu, Q., Fischer, U., Wang, F. & Dreyfuss, G. The spinal muscular atrophy disease gene product, SMN, and its associated protein SIP1 are in a complex with spliceosomal snRNP proteins. *Cell* **90**, 1013–1021 (1997).

12. Sun, Y. *et al.* Molecular and functional analysis of intragenic SMN1 mutations in patients with spinal muscular atrophy. *Hum. Mutat.* **25**, 64–71 (2005).

13. Coovert, D. D. *et al.* The survival motor neuron protein in spinal muscular atrophy. *Hum. Mol. Genet.* **6**, 1205–1214 (1997).

14. Singh, N. N., Howell, M. D., Androphy, E. J. & Singh, R. N. How the discovery of ISS-N1 led to the first medical therapy for spinal muscular atrophy. *Gene Therapy* **24**, 520–526 (2017).

15. Young, P. J., Jensen, K. T., Burger, L. R., Pintel, D. J. & Lorson, C. L. Minute virus of mice NS1 interacts with the SMN protein, and they colocalize in novel nuclear bodies induced by parvovirus infection. *J. Virol.* **76**, 3892–904 (2002).

16. Lorson, C. L., Hahnen, E., Androphy, E. J. & Wirth, B. A single nucleotide in the SMN gene regulates splicing and is responsible for spinal muscular atrophy. *Proc. Natl. Acad. Sci.* (1999). doi:10.1073/pnas.96.11.6307

17. Bertrandy, S. *et al.* The RNA-binding properties of SMN: Deletion analysis of the zebrafish orthologue defines domains conserved in evolution. *Hum. Mol. Genet.* **8**, 775–782 (1999).

18. Selenko, P. *et al.* SMN tudor domain structure and its interaction with the Sm proteins. *Nat. Struct. Biol.* **8**, 27–31 (2001).

19. Bühler, D., Raker, V., Lührmann, R. & Fischer, U. Essential role for the tudor domain of SMN in spliceosomal U snRNP assembly: Implications for spinal muscular atrophy. *Hum. Mol. Genet.* **8**, 2351–2357 (1999).

20. Cuscó, I., Barceló, M. J., Del Río, E., Baiget, M. & Tizzano, E. F. Detection of novel mutations in the SMN Tudor domain in

type I SMA patients. *Neurology* **63**, 146–149 (2004).

21. Sanchez, G. *et al.* A novel function for the survival motoneuron protein as a translational regulator. *Hum. Mol. Genet.* **22**, 668–684 (2013).

22. Carlsson, L., Nyström, L. E., Sundkvist, I., Markey, F. & Lindberg, U. Actin polymerizability is influenced by profilin, a low molecular weight protein in non-muscle cells. *J. Mol. Biol.* **115**, 465–483 (1977).

23. Talbot, K., Rodrigues, N. R., Ignatius, J., Muntoni, F. & Davies, K. E. Gene conversion at the SMN locus in autosomal recessive spinal muscular atrophy does not predict a mild phenotype. *Neuromuscul. Disord.* **7**, 198–201 (1997).

24. Carissimi, C. *et al.* Unrip is a component of SMN complexes active in snRNP assembly. *FEBS Lett.* **579**, 2348–2354 (2005).

25. Carissimi, C. *et al.* Gemin8 is a novel component of the survival motor neuron complex and functions in small nuclear ribonucleoprotein assembly. *J. Biol. Chem.* **281**, 8126–34 (2006).

26. Charroux, B. *et al.* Gemin4. A novel component of the SMN complex that is found in both gems and nucleoli. *J. Cell Biol.* **148**, 1177–86 (2000).

27. Charroux, B. *et al.* Gemin3: A novel DEAD box protein that interacts with SMN, the spinal muscular atrophy gene product, and is a component of gems. *J. Cell Biol.* **147**, 1181–1193 (1999).

28. Gubitz, A. K. *et al.* Gemin5, a novel WD repeat protein component of the SMN complex that binds Sm proteins. *J. Biol. Chem.* **277**, 5631–5636 (2002).

29. Gubitz, A. K., Feng, W. & Dreyfuss, G. The SMN complex. (2004). doi:10.1016/j.yexcr.2004.03.022

30. Otter, S. *et al.* A comprehensive interaction map of the human survival of motor neuron (SMN) complex. *J. Biol. Chem.* **282**, 5825–33 (2007).

31. Singh, R. N., Howell, M. D., Ottesen, E. W. & Singh, N. N. Diverse role of survival motor neuron protein. *Biochimica et Biophysica Acta - Gene Regulatory Mechanisms* **1860**, 299–315 (2017).

32. Battle, D. J. *et al.* The SMN complex: An assembly machine for RNPs. in *Cold Spring Harbor Symposia on Quantitative Biology* (2006). doi:10.1101/sqb.2006.71.001

33. Meister, G. & Fischer, U. Assisted RNP assembly: SMN and PRMT5 complexes cooperate in the formation of spliceosomal UsnRNPs. *EMBO J.* **21**, 5853–5863 (2002).

34. Pellizzoni, L., Kataoka, N., Charroux, B. & Dreyfuss, G. A novel function for SMN, the spinal muscular atrophy disease gene product, in pre-mRNA splicing. *Cell* **95**, 615–24 (1998).

35. Lanfranco, M., Vassallo, N. & Cauchi, R. J. Spinal Muscular Atrophy: From Defective Chaperoning of snRNP Assembly to Neuromuscular Dysfunction. *Front. Mol. Biosci.* **4**, 41 (2017).

36. Chaytow, H., Huang, Y. T., Gillingwater, T. H. & Faller, K. M. E. The role of survival motor neuron protein (SMN) in protein homeostasis. *Cellular and Molecular Life Sciences* **75**, 3877–3894 (2018).

37. Rossoll, W. *et al.* Smn, the spinal muscular atrophy-determining gene product, modulates axon growth and localization of β-actin mRNA in growth cones of motoneurons. *J. Cell Biol.* **163**, 801–812 (2003).

38. Sharma, A. *et al.* A role for complexes of survival of motor neurons (SMN) protein with gemins and profilin in neurite-like cytoplasmic extensions of cultured nerve cells. *Exp. Cell Res.* **309**, 185–197 (2005).

39. Akten, B. *et al.* Interaction of survival of motor neuron (SMN) and HuD proteins with mRNA cpg15 rescues motor neuron axonal deficits. *Proc. Natl. Acad. Sci. U. S. A.* **108**, 10337–42 (2011).

40. Rage, F. *et al.* Genome-wide identification of mRNAs associated with the protein SMN whose depletion decreases

their axonal localization. *RNA* **19**, 1755–1766 (2013).

41. Fallini, C. *et al.* The Survival of Motor Neuron (SMN) protein interacts with the mRNA-binding protein HuD and regulates localization of poly(A) mRNA in primary motor neuron axons. *J. Neurosci.* **31**, 3914–3925 (2011).

42. Sumner, C. J. Molecular Mechanisms of Spinal Muscular Atrophy. *J. Child Neurol.* **22**, 979–989 (2007).

43. Biros, I. & Forrest, S. Spinal muscular atrophy: Untangling the knot? *Journal of Medical Genetics* (1999).

44. Mailman, M. D. *et al.* Molecular analysis of spinal muscular atrophy and modification of the phenotype by SMN2. *Genet. Med.* (2002). doi:10.1097/00125817-200201000-00004

45. Burnett, B. G. *et al.* Regulation of SMN Protein Stability. *Mol. Cell. Biol.* (2009). doi:10.1128/mcb.01262-08

46. Dimitriadi, M. *et al.* Conserved genes act as modifiers of invertebrate SMN loss of function defects. *PLoS Genet.* **6**, e1001172 (2010).

47. Wishart, T. M. *et al.* Dysregulation of ubiquitin homeostasis and β-catenin signaling promote spinal muscular atrophy. *J. Clin. Invest.* **124**, 1821–1834 (2014).

48. Little, D. *et al.* PTEN depletion decreases disease severity and modestly prolongs survival in a mouse model of spinal muscular atrophy. *Mol. Ther.* **23**, 270–7 (2015).

49. Wirth, B. An update of the mutation spectrum of the survival motor neuron gene (SMN1) in autosomal recessive spinal muscular atrophy (SMA). *Human Mutation* **15**, 228–237 (2000).

50. Velasco, E., Valero, C., Valero, A., Moreno, F. & Hernández-Chico, C. Molecular analysis of the SMN and NAIP genes in Spanish spinal muscular atrophy (SMA) families and correlation between number of copies of cBCD541 and SMA phenotype. *Hum. Mol. Genet.* **5**, 257–263 (1996).

51. Amara, A. *et al.* Correlation of SMN2, NAIP, p44, H4F5 and

Occludin genes copy number with spinal muscular atrophy phenotype in Tunisian patients. *Eur. J. Paediatr. Neurol.* **16**, 167–74 (2012).

52. Derakhshandeh-Peykar, P. *et al.* Molecular analysis of the SMN1 and NAIP genes in Iranian patients with spinal muscular atrophy. *Ann. Acad. Med. Singapore* **36**, 937–41 (2007).

53. Hosseinibarkooie, S. *et al.* The Power of Human Protective Modifiers: PLS3 and CORO1C Unravel Impaired Endocytosis in Spinal Muscular Atrophy and Rescue SMA Phenotype. *Am. J. Hum. Genet.* (2016). doi:10.1016/j.ajhg.2016.07.014

54. Oprea, G. E. *et al.* Plastin 3 is a protective modifier of autosomal recessive spinal muscular atrophy. *Science (80-.).* (2008). doi:10.1126/science.1155085

55. Ackermann, B. *et al.* Plastin 3 ameliorates spinal muscular atrophy via delayed axon pruning and improves neuromuscular junction functionality. *Hum. Mol. Genet.* (2013). doi:10.1093/hmg/dds540

56. Helmken, C. *et al.* Evidence for a modifying pathway in SMA discordant families: Reduced SMN level decreases the amount of its interacting partners and Htra2-beta1. *Hum. Genet.* (2003). doi:10.1007/s00439-003-1025-2

57. Gangwani, L., Mikrut, M., Theroux, S., Sharma, M. & Davis, R. J. Spinal muscular atrophy disrupts the interaction of ZPR1 with the SMN protein. *Nat. Cell Biol.* (2001). doi:10.1038/35070059

58. Ahmad, S., Wang, Y., Shaik, G. M., Burghes, A. H. & Gangwani, L. The zinc finger protein ZPR1 is a potential modifier of spinal muscular atrophy. *Hum. Mol. Genet.* (2012). doi:10.1093/hmg/dds102

59. L.-K., T. *et al.* Systemic administration of a recombinant AAV1 vector encoding IGF-1 improves disease manifestations in SMA mice. *Mol. Ther.* (2014).

60. Riessland, M. *et al.* Neurocalcin Delta Suppression Protects against Spinal Muscular Atrophy in Humans and across

Species by Restoring Impaired Endocytosis. *Am. J. Hum. Genet.* (2017). doi:10.1016/j.ajhg.2017.01.005

61. Schrank, B. *et al.* Inactivation of the survival motor neuron gene, a candidate gene for human spinal muscular atrophy, leads to massive cell death in early mouse embryos. *Proc. Natl. Acad. Sci. U. S. A.* (1997). doi:10.1073/pnas.94.18.9920

62. Ruggiu, M. *et al.* A Role for SMN Exon 7 Splicing in the Selective Vulnerability of Motor Neurons in Spinal Muscular Atrophy Downloaded from. (2011). doi:10.1128/MCB.06077-11

63. Soler-Botija, C. *et al.* Implication of fetal SMN2 expression in type I SMA pathogenesis: Protection or pathological gain of function? *J. Neuropathol. Exp. Neurol.* **64**, 215–223 (2005).

64. Burlet, P. *et al.* The distribution of SMN protein complex in human fetal tissues and its alteration in spinal muscular atrophy. *Hum. Mol. Genet.* (1998). doi:10.1093/hmg/7.12.1927

65. Simic, G. *et al.* Ultrastructural analysis and TUNEL demonstrate motor neuron apoptosis in Werdnig-Hoffmann disease. *J. Neuropathol. Exp. Neurol.* (2000). doi:10.1093/jnen/59.5.398

66. Soler-Botija, C. Neuronal death is enhanced and begins during foetal development in type I spinal muscular atrophy spinal cord. *Brain* (2002). doi:10.1093/brain/awf155

67. Soler-Botija, C., Ferrer, I., Alvarez, J. L., Baiget, M. & Tizzano, E. F. Downregulation of Bcl-2 proteins in type I spinal muscular atrophy motor neurons during fetal development. *J. Neuropathol. Exp. Neurol.* (2003). doi:10.1093/jnen/62.4.420

68. Ng, S. Y. *et al.* Genome-wide RNA-Seq of Human Motor Neurons Implicates Selective ER Stress Activation in Spinal Muscular Atrophy. *Cell Stem Cell* (2015). doi:10.1016/j.stem.2015.08.003

69. Kariya, S., Mauricio, R., Dai, Y. & Monani, U. R. The neuroprotective factor Wld(s) fails to mitigate distal axonal and neuromuscular junction (NMJ) defects in mouse models of spinal muscular atrophy. *Neurosci. Lett.* **449**, 246–51 (2009).

70. Kong, L. *et al.* Impaired synaptic vesicle release and immaturity of neuromuscular junctions in spinal muscular atrophy mice. *J. Neurosci.* **29**, 842–851 (2009).

71. Dachs, E. *et al.* Defective neuromuscular junction organization and postnatal myogenesis in mice with severe spinal muscular atrophy. *J. Neuropathol. Exp. Neurol.* **70**, 444–61 (2011).

72. Martínez-Hernández, R. *et al.* The developmental pattern of myotubes in spinal muscular atrophy indicates prenatal delay of muscle maturation. *J. Neuropathol. Exp. Neurol.* **68**, 474–81 (2009).

73. Ghatak, N. R. Spinal roots in Werdnig-Hoffmann disease. *Acta Neuropathol.* **41**, 1–7 (1978).

74. Chou, S. M. & Nonaka, I. Werdnig-Hoffmann disease: Proposal of a pathogenetic mechanism. *Acta Neuropathol.* **41**, 45–54 (1978).

75. Mcgovern, V. L., Gavrilina, T. O., Beattie, C. E. & Burghes, A. H. M. Embryonic motor axon development in the severe SMA mouse. *Hum. Mol. Genet.* **17**, 2900–2909 (2008).

76. Brock, T. O. & McLlwain, D. L. Astrocytic proteins in the dorsal and ventral roots in amyotrophic lateral sclerosis and werdnig-hoffmann disease. *J. Neuropathol. Exp. Neurol.* (1984). doi:10.1097/00005072-198411000-00005

77. Van Alstyne, M., Lotti, F., Dal Mas, A., Area-Gomez, E. & Pellizzoni, L. Stasimon/Tmem41b localizes to mitochondria-associated ER membranes and is essential for mouse embryonic development. *Biochem. Biophys. Res. Commun.* **506**, 463–470 (2018).

78. F., L. *et al.* SMN-dependent U12 splicing defects cause synaptic dysfunction in a drosophila model of spinal muscular atrophy. *Mol. Biol. Cell* (2010). doi:10.1091/mbc.E10-10-0839

79. See, K. *et al.* SMN deficiency alters Nrxn2 expression and splicing in zebrafish and mouse models of spinal muscular atrophy. *Hum. Mol. Genet.* (2014). doi:10.1093/hmg/ddt567

80. Rizzo, F. *et al.* Key role of SMN/SYNCRIP and RNA-Motif 7 in spinal muscular atrophy: RNA-Seq and motif analysis of human motor neurons. *Brain* **142**, 276–294 (2019).

81. Probst, A. & Ulrich, J. Sensory ganglioneuropathy in infantile spinal muscular atrophy. Light and electronmicroscopic findings in two cases. *Neuropediatrics* (1981).

82. Towfighi, J., Young, R. S. K. & Ward, R. M. Is Werdnig-Hoffmann disease a pure lower motor neuron disorder? *Acta Neuropathol.* (1985). doi:10.1007/BF00687008

83. Harding, B. N. *et al.* Spectrum of neuropathophysiology in spinal muscular atrophy type i. *J. Neuropathol. Exp. Neurol.* **74**, 15–24 (2015).

84. Hua, Y. *et al.* Motor neuron cell-nonautonomous rescue of spinal muscular atrophy phenotypes in mild and severe transgenic mouse models. *Genes Dev.* **29**, 288–297 (2015).

85. Calder, A. N., Androphy, E. J. & Hodgetts, K. J. Small Molecules in Development for the Treatment of Spinal Muscular Atrophy. *Journal of Medicinal Chemistry* (2016). doi:10.1021/acs.jmedchem.6b00670

86. Zanetta, C. *et al.* Molecular, genetic and stem cell-mediated therapeutic strategies for spinal muscular atrophy (SMA). *J. Cell. Mol. Med.* **18**, 187–196 (2014).

87. Gladman, J. T. & Chandler, D. S. Intron 7 conserved sequence elements regulate the splicing of the SMN genes. *Hum. Genet.* **126**, 833–41 (2009).

88. Singh, N. K., Singh, N. N., Androphy, E. J. & Singh, R. N. Splicing of a Critical Exon of Human Survival Motor Neuron Is Regulated by a Unique Silencer Element Located in the Last Intron. *Mol. Cell. Biol.* (2006). doi:10.1128/mcb.26.4.1333-1346.2006

89. Miller, C. M. & Harris, E. N. Antisense Oligonucleotides: Treatment Strategies and Cellular Internalization. *RNA Dis. (Houston, Tex.)* **3**, (2016).

90. Porensky, P. N. *et al.* A single administration of morpholino antisense oligomer rescues spinal muscular atrophy in mouse. *Hum. Mol. Genet.* **21**, 1625–1638 (2012).

91. Ramirez, A. *et al.* Investigation of New Morpholino Oligomers to Increase Survival Motor Neuron Protein Levels in Spinal Muscular Atrophy. doi:10.3390/ijms19010167

92. Arnold, W. D. *et al.* The neuromuscular impact of symptomatic SMN restoration in a mouse model of spinal muscular atrophy. *Neurobiol. Dis.* (2016). doi:10.1016/j.nbd.2015.12.014

93. Naryshkin, N. A. *et al.* SMN2 splicing modifiers improve motor function and longevity in mice with spinal muscular atrophy. *Science (80-.).* (2014). doi:10.1126/science.1250127

94. Bharucha-Goebel, D. & Kaufmann, P. Treatment Advances in Spinal Muscular Atrophy. *Current Neurology and Neuroscience Reports* (2017). doi:10.1007/s11910-017-0798-y

95. Duque, S. *et al.* Intravenous administration of self-complementary AAV9 enables transgene delivery to adult motor neurons. *Mol. Ther.* (2009). doi:10.1038/mt.2009.71

96. Foust, K. D. *et al.* Intravascular AAV9 preferentially targets neonatal neurons and adult astrocytes. *Nat. Biotechnol.* (2009). doi:10.1038/nbt.1515

97. Foust, K. D. *et al.* Rescue of the spinal muscular atrophy phenotype in a mouse model by early postnatal delivery of SMN. *Nat. Biotechnol.* (2010). doi:10.1038/nbt.1610

98. Bevan, A. K. *et al.* Systemic gene delivery in large species for targeting spinal cord, brain, and peripheral tissues for pediatric disorders. *Mol. Ther.* (2011). doi:10.1038/mt.2011.157

99. Duque, S. I. *et al.* A large animal model of spinal muscular atrophy and correction of phenotype. *Ann. Neurol.* (2015). doi:10.1002/ana.24332

100. Hwee, D. T. *et al.* The small-molecule fast skeletal troponin activator, CK-2127107, improves exercise tolerance in a rat model of heart failure. *J. Pharmacol. Exp. Ther.* **353**, 159–68

(2015).

101. Long, K. K. *et al.* Specific inhibition of myostatin activation is beneficial in mouse models of SMA therapy. *Hum. Mol. Genet.* (2019). doi:10.1093/hmg/ddy382

102. Rochette, C. F., Gilbert, N. & Simard, L. R. SMN gene duplication and the emergence of the SMN2 gene occurred in distinct hominids: SMN2 is unique to Homo sapiens. *Hum. Genet.* **108**, 255–66 (2001).

103. Aquilina, B. & Cauchi, R. J. Modelling motor neuron disease in fruit flies: Lessons from spinal muscular atrophy. *Journal of Neuroscience Methods* (2018). doi:10.1016/j.jneumeth.2018.04.003

104. Chan, Y. B. Neuromuscular defects in a Drosophila survival motor neuron gene mutant. *Hum. Mol. Genet.* (2003). doi:10.1093/hmg/ddg157

105. Burt, E. C., Towers, P. R. & Sattelle, D. B. Caenorhabditis elegans in the study of SMN-interacting proteins: A role for SMI-1, an orthologue of human Gemin2 and the identification of novel components of the SMN complex. *Invertebr. Neurosci.* (2006). doi:10.1007/s10158-006-0027-x

106. McWhorter, M. L., Monani, U. R., Burghes, A. H. M. & Beattie, C. E. Knockdown of the survival motor neuron (Smn) protein in zebrafish causes defects in motor axon outgrowth and pathfinding. *J. Cell Biol.* (2003). doi:10.1083/jcb.200303168

107. Monani, U. R. The human centromeric survival motor neuron gene (SMN2) rescues embryonic lethality in Smn-/- mice and results in a mouse with spinal muscular atrophy. *Hum. Mol. Genet.* (2000). doi:10.1093/hmg/9.3.333

108. Bowerman, M. *et al.* Therapeutic strategies for spinal muscular atrophy: SMN and beyond. *Dis. Model. Mech.* **10**, 943–954 (2017).

109. Maherali, N. & Hochedlinger, K. Guidelines and Techniques for the Generation of Induced Pluripotent Stem Cells. *Cell Stem Cell* (2008). doi:10.1016/j.stem.2008.11.008

110. Faravelli, I. *et al.* Motor neuron derivation from human embryonic and induced pluripotent stem cells: Experimental approaches and clinical perspectives. *Stem Cell Research and Therapy* **5**, (2014).

111. Boza-Morán, M. G. *et al.* Decay in survival motor neuron and plastin 3 levels during differentiation of iPSC-derived human motor neurons. *Sci. Rep.* (2015). doi:10.1038/srep11696

112. Ebert, A. D. *et al.* Induced pluripotent stem cells from a spinal muscular atrophy patient. *Nature* **457**, 277–280 (2009).

113. Sareen, D. *et al.* Inhibition of apoptosis blocks human motor neuron cell death in a stem cell model of spinal muscular atrophy. *PLoS One* (2012). doi:10.1371/journal.pone.0039113

114. Corti, S. *et al.* Genetic Correction of Human Induced Pluripotent Stem Cells from Patients with Spinal Muscular Atrophy. *Sci. Transl. Med.* **4**, 165ra162-165ra162 (2012).

115. Rheinwatd, J. G. & Green, H. Seria cultivation of strains of human epidemal keratinocytes: the formation keratinizin colonies from single cell is. *Cell* (1975). doi:10.1016/S0092-8674(75)80001-8

116. Lindberg, K., Brown, M. E., Chaves, H. V., Kenyon, K. R. & Rheinwald, J. G. In vitro propagation of human ocular surface epithelial cells for transplantation. *Investig. Ophthalmol. Vis. Sci.* (1993).

117. Lancaster, M. A. & Knoblich, J. A. Organogenesis in a dish: modeling development and disease using organoid technologies. *Science* **345**, 1247125 (2014).

118. Humpel, C. Organotypic brain slice cultures: A review. *Neuroscience* (2015). doi:10.1016/j.neuroscience.2015.07.086

119. Stoppini, L., Buchs, P. A. & Muller, D. A simple method for organotypic cultures of nervous tissue. *J. Neurosci. Methods* (1991). doi:10.1016/0165-0270(91)90128-M

120. Moser, K. V., Schmidt-Kastner, R., Hinterhuber, H. & Humpel, C. Brain capillaries and cholinergic neurons persist in

organotypic brain slices in the absence of blood flow. *Eur. J. Neurosci.* (2003). doi:10.1046/j.1460-9568.2003.02728.x

121. Gage, F. H. Neurogenesis in the Adult Brain. *J. Neurosci.* **22**, 612–613 (2002).

122. Jorfi, M., D'Avanzo, C., Tanzi, R. E., Kim, D. Y. & Irimia, D. Human Neurospheroid Arrays for In Vitro Studies of Alzheimer's Disease. *Sci. Rep.* (2018). doi:10.1038/s41598-018-20436-8

123. Eiraku, M. *et al.* Self-Organized Formation of Polarized Cortical Tissues from ESCs and Its Active Manipulation by Extrinsic Signals. *Cell Stem Cell* **3**, 519–532 (2008).

124. Pasca, A. M. *et al.* Functional cortical neurons and astrocytes from human pluripotent stem cells in 3D culture. *Nat. Methods* (2015). doi:10.1038/nmeth.3415

125. Ostenfeld, T. *et al.* Regional specification of rodent and human neurospheres. *Dev. Brain Res.* (2002). doi:10.1016/S0165-3806(01)00291-7

126. Santa-Olalla, J., Baizabal, J. M., Fregoso, M., Cárdenas, M. D. C. & Covarrubias, L. The in vivo positional identity gene expression code is not preserved in neural stem cells grown in culture. *Eur. J. Neurosci.* (2003). doi:10.1046/j.1460-9568.2003.02824.x

127. Klein, C., Butt, S. J. B., Machold, R. P., Johnson, J. E. & Fishell, G. Cerebellum- and forebrain-derived stem cells possess intrinsic regional character. *Development* (2005). doi:10.1242/dev.02037

128. Zaidi, H. A., Kosztowski, T., DiMeco, F. & Quiñones-Hinojosa, A. Origins and clinical implications of the brain tumor stem cell hypothesis. *Journal of Neuro-Oncology* (2009). doi:10.1007/s11060-009-9856-x

129. Chen, M. *et al.* Common proteomic profiles of induced pluripotent stem cell-derived three-dimensional neurons and brain tissue from Alzheimer patients. *J. Proteomics* (2018). doi:10.1016/j.jprot.2018.04.032

130. Kraus, D., Boyle, V., Leibig, N., Stark, G. B. & Penna, V. The Neuro-spheroid-A novel 3D in vitro model for peripheral nerve regeneration. *J. Neurosci. Methods* (2015). doi:10.1016/j.jneumeth.2015.03.004

131. Gabay, L., Lowell, S., Rubin, L. L. & Anderson, D. J. Deregulation of dorsoventral patterning by FGF confers trilineage differentiation capacity on CNS stem cells in vitro. *Neuron* (2003). doi:10.1016/S0896-6273(03)00637-8

132. Pastrana, E., Silva-Vargas, V. & Doetsch, F. Eyes wide open: A critical review of sphere-formation as an assay for stem cells. *Cell Stem Cell* (2011). doi:10.1016/j.stem.2011.04.007

133. Lancaster, M. A. *et al.* Cerebral organoids model human brain development and microcephaly. *Nature* **501**, 373–379 (2013).

134. Watanabe, M. *et al.* Self-Organized Cerebral Organoids with Human-Specific Features Predict Effective Drugs to Combat Zika Virus Infection. *Cell Rep.* (2017). doi:10.1016/j.celrep.2017.09.047

135. Takasato, M. *et al.* Directing human embryonic stem cell differentiation towards a renal lineage generates a self-organizing kidney. *Nat. Cell Biol.* (2014). doi:10.1038/ncb2894

136. Pacitti, D., Privolizzi, R. & Bax, B. E. Organs to cells and cells to organoids: The evolution of In vitro central nervous system modelling. *Frontiers in Cellular Neuroscience* (2019). doi:10.3389/fncel.2019.00129

137. MOUNTCASTLE, V. B. Modality and topographic properties of single neurons of cat's somatic sensory cortex. *J. Neurophysiol.* (1957).

138. Bystron, I., Blakemore, C. & Rakic, P. Development of the human cerebral cortex: Boulder Committee revisited. *Nature Reviews Neuroscience* (2008). doi:10.1038/nrn2252

139. Greig, L. C., Woodworth, M. B., Galazo, M. J., Padmanabhan, H. & Macklis, J. D. Molecular logic of neocortical projection neuron specification, development and diversity. *Nature Reviews Neuroscience* (2013). doi:10.1038/nrn3586

140. Kohwi, M. & Doe, C. Q. Temporal fate specification and neural progenitor competence during development. *Nature Reviews Neuroscience* (2013). doi:10.1038/nrn3618

141. Pilz, G. A. *et al.* Amplification of progenitors in the mammalian telencephalon includes a new radial glial cell type. *Nat. Commun.* (2013). doi:10.1038/ncomms3125

142. Gelman, D. M. *et al.* The embryonic preoptic area is a novel source of cortical GABAergic interneurons. *J. Neurosci.* (2009). doi:10.1523/JNEUROSCI.0604-09.2009

143. Anderson, S. A., Eisenstat, D. D., Shi, L. & Rubenstein, J. L. R. Interneuron migration from basal forebrain to neocortex: Dependence on Dlx genes. *Science (80-.).* (1997). doi:10.1126/science.278.5337.474

144. Tamamaki, N., Fujimori, K. E. & Takauji, R. Origin and route of tangentially migrating neurons in the developing neocortical intermediate zone. *J. Neurosci.* (1997).

145. Lodato, S. & Arlotta, P. Generating Neuronal Diversity in the Mammalian Cerebral Cortex. *Annu. Rev. Cell Dev. Biol.* **31**, 699–720 (2015).

146. Yin, X. *et al.* Engineering Stem Cell Organoids. *Cell Stem Cell* (2016). doi:10.1016/j.stem.2015.12.005

147. Auger, F. A., Gibot, L. & Lacroix, D. The Pivotal Role of Vascularization in Tissue Engineering. *Annu. Rev. Biomed. Eng.* (2013). doi:10.1146/annurev-bioeng-071812-152428

148. Pham, M. T. *et al.* Generation of human vascularized brain organoids. *Neuroreport* **29**, 588–593 (2018).

149. Mansour, A. A. *et al.* An in vivo model of functional and vascularized human brain organoids. *Nat. Biotechnol.* **36**, 432–441 (2018).

150. Renner, M. *et al.* Self-organized developmental patterning and differentiation in cerebral organoids. *EMBO J.* **36**, 1316–1329 (2017).

151. Qian, X. *et al.* Brain-Region-Specific Organoids Using Mini-bioreactors for Modeling ZIKV Exposure. *Cell* (2016). doi:10.1016/j.cell.2016.04.032

152. Lee, C. T. *et al.* CYP3A5 Mediates Effects of Cocaine on Human Neocorticogenesis: Studies using an in Vitro 3D Self-Organized hPSC Model with a Single Cortex-Like Unit. *Neuropsychopharmacology* (2017). doi:10.1038/npp.2016.156

153. Quadrato, G. & Arlotta, P. Present and future of modeling human brain development in 3D organoids. *Current Opinion in Cell Biology* (2017). doi:10.1016/j.ceb.2017.11.010

154. Quadrato, G. *et al.* Cell diversity and network dynamics in photosensitive human brain organoids. *Nature* **545**, 48–53 (2017).

155. Sloan, S. A., Andersen, J., Paşca, A. M., Birey, F. & Paşca, S. P. Generation and assembly of human brain region–specific three-dimensional cultures. *Nat. Protoc.* **13**, 2062–2085 (2018).

156. Birey, F. *et al.* Assembly of functionally integrated human forebrain spheroids. *Nature* **545**, 54–59 (2017).

157. Krefft, O., Jabali, A., Iefremova, V., Koch, P. & Ladewig, J. Generation of standardized and reproducible forebrain-type cerebral organoids from human induced pluripotent stem cells. *J. Vis. Exp.* (2018). doi:10.3791/56768

158. Xiang, Y. *et al.* Fusion of Regionally Specified hPSC-Derived Organoids Models Human Brain Development and Interneuron Migration. *Cell Stem Cell* (2017). doi:10.1016/j.stem.2017.07.007

159. Pas, S. P. The rise of three-dimensional human brain cultures. *Nature* (2018). doi:10.1038/nature25032

160. Jo, J. *et al.* Midbrain-like Organoids from Human Pluripotent Stem Cells Contain Functional Dopaminergic and Neuromelanin-Producing Neurons. *Cell Stem Cell* (2016). doi:10.1016/j.stem.2016.07.005

161. Monzel, A. S. *et al.* Derivation of Human Midbrain-Specific

Organoids from Neuroepithelial Stem Cells. *Stem Cell Reports* (2017). doi:10.1016/j.stemcr.2017.03.010

162. Sakaguchi, H. *et al.* Generation of functional hippocampal neurons from self-organizing human embryonic stem cell-derived dorsomedial telencephalic tissue. *Nat. Commun.* (2015). doi:10.1038/ncomms9896

163. Garcez, P. P. *et al.* Zika virus: Zika virus impairs growth in human neurospheres and brain organoids. *Science (80-.).* (2016). doi:10.1126/science.aaf6116

164. Cugola, F. R. *et al.* The Brazilian Zika virus strain causes birth defects in experimental models. *Nature* (2016). doi:10.1038/nature18296

165. Mariani, J. *et al.* FOXG1-Dependent Dysregulation of GABA/Glutamate Neuron Differentiation in Autism Spectrum Disorders. *Cell* **162**, 375–390 (2015).

166. Raja, W. K. *et al.* Self-organizing 3D human neural tissue derived from induced pluripotent stem cells recapitulate Alzheimer's disease phenotypes. *PLoS One* **11**, (2016).

167. Choi, S. H. *et al.* A three-dimensional human neural cell culture model of Alzheimer's disease. *Nature* (2014). doi:10.1038/nature13800

168. Lee, H. K. *et al.* Three dimensional human neuro-spheroid model of Alzheimer's disease based on differentiated induced pluripotent stem cells. *PLoS One* (2016). doi:10.1371/journal.pone.0163072

169. Smits, L. M. *et al.* Modeling Parkinson's disease in midbrain-like organoids. *npj Park. Dis.* (2019). doi:10.1038/s41531-019-0078-4

170. Kim, H. *et al.* Modeling G2019S-LRRK2 Sporadic Parkinson's Disease in 3D Midbrain Organoids. *Stem Cell Reports* (2019). doi:10.1016/j.stemcr.2019.01.020

171. Gopalakrishnan, J. The Emergence of Stem Cell-Based Brain Organoids: Trends and Challenges. *Bioessays* **41**, e1900011

(2019).

172. Kawada, J. *et al.* Generation of a Motor Nerve Organoid with Human Stem Cell-Derived Neurons. *Stem cell reports* **9**, 1441–1449 (2017).

173. Hor, J. H. *et al.* Cell cycle inhibitors protect motor neurons in an organoid model of Spinal Muscular Atrophy. *Cell Death Dis.* **9**, 1100 (2018).

174. Breuss, M. W., Leca, I., Gstrein, T., Hansen, A. H. & Keays, D. A. Tubulins and brain development – The origins of functional specification. *Molecular and Cellular Neuroscience* (2017). doi:10.1016/j.mcn.2017.03.002

175. Menezes, J. R. L. & Luskin, M. B. Expression of neuron-specific tubulin defines a novel population in the proliferative layers of the developing telencephalon. *J. Neurosci.* (1994).

176. Sossey-Alaoui, K. Human doublecortin (DCX) and the homologous gene in mouse encode a putative Ca2+-dependent signaling protein which is mutated in human X-linked neuronal migration defects. *Hum. Mol. Genet.* **7**, 1327–1332 (1998).

177. Izant, J. G. & McIntosh, J. R. Microtubule-associated proteins: a monoclonal antibody to MAP2 binds to differentiated neurons. *Proc. Natl. Acad. Sci. U. S. A.* **77**, 4741–5 (1980).

178. Amoroso, M. W. *et al.* Accelerated high-yield generation of limb-innervating motor neurons from human stem cells. *J. Neurosci.* **33**, 574–586 (2013).

179. Lendahl, U., Zimmerman, L. B. & McKay, R. D. G. CNS stem cells express a new class of intermediate filament protein. *Cell* (1990). doi:10.1016/0092-8674(90)90662-X

180. Arber, S. *et al.* Requirement for the homeobox gene Hb9 in the consolidation of motor neuron identity. *Neuron* **23**, 659–674 (1999).

181. M., N. *et al.* Human motor neuron generation from embryonic stem cells and induced pluripotent stem cells. *Cell. Mol. Life*

Sci. **67**, 3837–3847 (2010).

182. Qu, Q. *et al.* High-efficiency motor neuron differentiation from human pluripotent stem cells and the function of Islet-1. *Nat. Commun.* **5**, 3449 (2014).

183. Pevny, L. H., Sockanathan, S., Placzek, M. & Lovell-Badge, R. A role for SOX1 in neural determination. *Development* **125**, (1998).

184. Wu, G. & Schöler, H. R. Role of Oct4 in the early embryo development. *Cell Regen.* **3**, 3:7 (2014).

185. Francis, F. *et al.* Doublecortin is a developmentally regulated, microtubule-associated protein expressed in migrating and differentiating neurons. *Neuron* **23**, 247–56 (1999).

186. Couillard-Despres, S. *et al.* Doublecortin expression levels in adult brain reflect neurogenesis. *Eur. J. Neurosci.* **21**, 1–14 (2005).

187. Walker, T. L., Yasuda, T., Adams, D. J. & Bartlett, P. F. The doublecortin-expressing population in the developing and adult brain contains multipotential precursors in addition to neuronal-lineage cells. *J. Neurosci.* **27**, 3734–3742 (2007).

188. Velasco, S. *et al.* Individual brain organoids reproducibly form cell diversity of the human cerebral cortex. *Nature* **570**, 523–527 (2019).

189. Götz, M. & Bolz, J. Formation and preservation of cortical layers in slice cultures. *J. Neurobiol.* (1992). doi:10.1002/neu.480230702

190. Kawauchi, T. *et al.* Rab GTPases-dependent endocytic pathways regulate neuronal migration and maturation through N-cadherin trafficking. *Neuron* (2010). doi:10.1016/j.neuron.2010.07.007

191. Bignami, A., Eng, L. F., Dahl, D. & Uyeda, C. T. Localization of the glial fibrillary acidic protein in astrocytes by immunofluorescence. *Brain Res.* (1972). doi:10.1016/0006-8993(72)90398-8

192. Levitt, P. & Rakic, P. Immunoperoxidase localization of glial fibrillary acidic protein in radial glial cells and astrocytes of the developing rhesus monkey brain. *J. Comp. Neurol.* (1980). doi:10.1002/cne.901930316

193. Cheliout-Heraut, F., Barois, A., Urtizberea, A., Viollet, L. & Estournet-Mathiaud, B. Evoked potentials in spinal muscular atrophy. *J. Child Neurol.* **18**, 383–90 (2003).

194. Wilson, P. G. & Stice, S. S. Development and differentiation of neural rosettes derived from human embryonic stem cells. *Stem Cell Rev.* **2**, 67–77 (2006).

195. Zhang, H., Robinson, N., Wu, C., Wang, W. & Harrington, M. A. Electrophysiological properties of motor neurons in a mouse model of severe spinal muscular atrophy: In Vitro versus in Vivo development. *PLoS One* **5**, (2010).

196. Mentis, G. Z. *et al.* Early functional impairment of sensory-motor connectivity in a mouse model of spinal muscular atrophy. *Neuron* **69**, 453–67 (2011).

197. Dekkers, J. F. *et al.* A functional CFTR assay using primary cystic fibrosis intestinal organoids. *Nat. Med.* **19**, 939–45 (2013).

198. Huch, M. *et al.* Unlimited in vitro expansion of adult bi-potent pancreas progenitors through the Lgr5/R-spondin axis. *EMBO J.* **32**, 2708–21 (2013).

199. Huch, M. *et al.* Long-term culture of genome-stable bipotent stem cells from adult human liver. *Cell* (2015). doi:10.1016/j.cell.2014.11.050

200. Fordham, R. P. *et al.* Transplantation of expanded fetal intestinal progenitors contributes to colon regeneration after injury. *Cell Stem Cell* **13**, 734–744 (2013).

12. SCIENTIFIC PRODUCTS

Rinchetti P, Rizzuti M, Faravelli I, Corti S. MicroRNA Metabolism and Dysregulation in Amyotrophic Lateral Sclerosis. Mol Neurobiol. 2017 Apr 18. doi: 10.1007/s12035-017-0537-z. [Epub ahead of print] Review. PubMed PMID: 28421535.

Monfrini E, Straniero L, Bonato S, Monzio Compagnoni G, Bordoni A, Dilena R**,** **Rinchetti P**, Silipigni R, Ronchi D, Corti S, Comi GP, Bresolin N, Duga S, Di Fonzo A. Neurofascin (NFASC) gene mutation causes autosomal recessive ataxia with demyelinating neuropathy.

Corti S, Rizzuti M, Ramirez A, Rizzo F, **Rinchetti P**, Bucchia M, Bresolin N, Comi GP, Nizzardo M. Development of peptide-conjugated morpholino oligomers for SMA therapy. *Cure SMA 16-18, June 2016, Anheim*.

Ramirez A., Rizzuti M., Rizzo F., **Rinchetti P.**, Bucchia M., Bresolin N., Comi GP., Corti S., Nizzardo M. Peptide-conjugated Morpholino Oligomers for treatment of Spinal Muscular Atrophy. *XVI Congress of the Italian Association of Myology (AIM), Lecce, Italy, 2016*.

Monica Bucchia, Agnese Ramirez, Federica Rizzo, Mafalda Rizzuti, **Paola Rinchetti**, Gianna Ulzi, Giulia Bassani, Andreina Bordoni, Nereo Bresolin, Giacomo P. Comi, Stefania Corti, Monica Nizzardo. Antisense oligonucleotides approach for the development of

Amyotrophic Lateral Sclerosis therapy. *ENCALS meeting, Milan, Italy, 2016.*

I.Faravelli, **P. Rinchetti**, L. Calandriello, G. Forotti, C. Cordiglieri, N. Bresolin, G.P. Comi, Monica Nizzardo and S. Corti. Modelling Spinal Muscular Atrophy with human 3D culture systems for pathogenic studies and therapeutic development. *SIBBM 2017 Frontiers in Molecular Biology, Milan, Italy, 2017*.

V. MISHRA, V. LE VERCHE, D. B. RE, K. POLITI, **P. RINCHETTI**, M. J. ALVAREZ, A. CALIFANO, F. LOTTI, S. PRZEDBORSKI. SOD1G93A astrocytes induce toxicity in motor neurons via a DR6-mediated pathway in ALS model. *SFN 11-15 November 2017, Washington DC.*

Paola Rinchetti, Irene Faravelli, Lisa Mapelli, Silvia Tamanini, Chiara Cordiglieri, Mafalda Rizzuti, Giulia Forotti, Giacomo P. Comi, Nereo Bresolin, Monica Nizzardo, Stefania Corti. Development of central nervous system 3D in vitro models to study molecular mechanisms and develop therapeutic strategies for motor neuron diseases. *SFN 3-7 November 2018, San Diego. (**Nanosymposium**).*

I.Faravelli, **P. Rinchetti**, G. Forotti, L. Mapelli, M. Rizzuti, C. Cordiglieri, L. Calandriello, S. Tamanini, N. Bresolin, G.P.Comi, M. Nizzardo and S. Corti. Human 3D cell culture systems to model and investigate Spinal Muscular Atrophy pathology. *Cure SMA 28-30 June 2019, Anheim*.

Speaker in a Nanosymposium at “Society of Neuroscince SFN”, title: “Development of central nervous system 3D in vitro models to study molecular mechanisms and develop therapeutic strategies for motor neuron diseases”. 3 – 7 November 2018, San Diego.

This thesis was evaluated by 1 independent reviewer: Diane Re (Assistant Professor, Department of Environmental Health Sciences Center for Motor Neuron Biology and Disease, Columbia University of New York).